STRUCTURAL APPLICATIONS OF FERRITIC STAINLESS STEELS (SAFSS)

Report To: **RFCS**
Document: **Isothermal and Anisothermal Material Tests**
Version: **01**
Date: **May 2013**

Version	Date of Issue	Purpose	Author	Technical Reviewer	Approved
01	30.5.2013	Issue to RFCS and TGS8	TPM	JSk	MYl

The testing, assessment, findings and conclusions outlined in this report have been made with the intent of due diligence, care and best effort. Despite that we may not be held liable for any direct, compensatory or consequential loss or damage exceeding the amount paid for this report.

EUROPEAN COMMISSION

Research Programme of
The Research Fund for Coal and Steel - Steel RTD

Title of Research Project:	**Structural Application of Ferritic Stainless Steels (SAFSS)**
Executive Committee:	**TGS8**
Contract:	**RFSR-CT-2010-00026**
Commencement Date:	**July 01, 2010**
Completion Date:	**May 30, 2013**
Work Package No and Title:	**WP4, Structural Fire Resistance**
Final Report:	**WP4.1, Isothermal and Anisothermal Material Tests**
Beneficiary:	**Outokumpu Stainless Oy** **95490 Tornio, Finland**
Research Location:	**Outokumpu Stainless Oy** **Tornio Research Centre** **95490 Tornio, Finland**
Contact person:	**Jukka Säynäjäkangas**
Report authors:	**Timo Manninen**

Summary

This report describes the testing programme and results for isothermal (steady state) and anisothermal (transient state) material tests on commercial ferritic stainless steels at elevated temperature. The objective of this work was to derive the strength and stiffness retention factors for ferritic stainless steel grades 1.4016, 1.4509, 1.4521 and 1.4621. The elevated temperature behaviour of these steel grades has not been properly studied before.

The isothermal tests were carried out according to the elevated temperature tensile testing standard EN ISO 10002-5. Stress-strain relationships were determined for the ferritic stainless steel grades 1.4003, 1.4016, 1.4509, 1.4521 and 1.4621 in the temperature range from +20°C to +1000°C. The test materials were cold-rolled sheet metals in annealed condition.

Anisothermal tests were performed on stabilized grades 1.4509 and 1.4521 with a constant heating rate of 10°C/min. Sixteen different load levels between 10% and 90% of the room temperature yield strength were used.

The results described in this report contain information on the elevated temperature strength, ductility and stiffness characteristics of ferritic stainless steels needed for fire design of structures. The results suggest that the investigated steels grades can be divided in two groups with similar characteristics in each group. The first group contains the unstabilized grades 1.4003 and 1.4016, and the second group contains the stabilized grades 1.4509, 1.4521 and 1.4621. Fire design parameters were derived for both groups of steels based on the test results obtained in accordance with the fire design model for stainless steel in Eurocode 3.

Contents

1 Introduction

Ferritic stainless steels are low cost, price-stable, corrosion-resistant steels. In contrast to austenitic grades, ferritic grades have low thermal expansion, high thermal conductivity and they are immune for chloride-induced stress-corrosion cracking (SCC). Ferritics are widely used in the automotive and household appliance sectors. Structural applications of these materials in the construction industry are, however, scarce. Only the grade 1.4003 has been used for structural purposes e.g. in railroad carriages, buses, trucks and containers.

One major barrier to the wider use of ferritic stainless steels in construction is the lack of relevant design guidance. Only one ferritic stainless steel grade 1.4003 is currently covered by the European design code [**1**,**2**]. Moreover, the grade 1.4003 is a structural ferritic stainless steel with only 12% of chromium. The corrosion resistance of 1.4003 is not comparable to that of most common austenitic grades. Ferritic grades with higher corrosion resistance are well established, but design values for these medium and high-chromium grades are not provided by the design code.

Elevated temperature mechanical properties play an important role in the fire design of steel structures. Appropriate assessment of fire safety requires that the material response at elevated temperature can be predicted. However, past work on structural design with stainless steel has been mainly focused on the austenitic and duplex grades [**3**,**4**,**5**] . The reduction of mechanical properties of ferritic stainless steels under fire conditions is largely unknown.

In the present work, an experimental research programme was carried out to investigate the mechanical properties of various ferritic stainless steels at temperatures up to 1000°C. The objective of the work was to derive the strength retention factors for ferritic stainless steel grades 1.4016, 1.4509, 1.4521 and 1.4621 in the temperature range from +20°C to +1000°C. Material from two European producers was used when available. The test materials were cold-rolled sheet metals in annealed condition.

Isothermal (steady state) tests were carried out according to the elevated temperature tensile testing standard EN ISO 10002-5. Stress-strain relationships were determined for the ferritic stainless steel grades 1.4003, 1.4016, 1.4509, 1.4521 and 1.4621 in the temperature range from +20°C to +1000°C.

Anisothermal (transient state) tests were performed on stabilized steel grades 1.4509 and 1.4521 with a heating rate of 10°C/min. In the anisothermal test method, a constant load is applied on the specimen and the temperature is raised with a constant heating rate. The temperature and strain are measured during the test. Sixteen different load levels between 10% and 90% of the yield stress were used in the tests.

2 Test materials and experimental procedures

2.1 Materials

In total nine materials from three suppliers were studied. The test materials were cold-rolled sheets in annealed condition. The materials and their chemical compositions are given in Table 1. Material from two suppliers was studied for the grades 1.4016, 1.4509 and 1.4521. The grade 1.4621 was only available from one supplier. The steel grade 1.4003, which has been extensively studied in previous ESCS and RFCS funded projects, was included as a reference material. The room temperature mechanical properties of test materials in the rolling direction are summarized in Table 2. The room temperature properties were measured according to the standard EN ISO 6892-1 A224.

Table 1. Chemical composition of test materials (wt%).

Identifier	Grade	Supplier	Type	C	Si	Mn	Cr	Ni	Mo	Ti	Nb	Cu	Al	N	KFF
4003-1	1.4003	B	2B	0.015	0.26	1.45	11.4	0.4	0.0	0.00	0.01	0.1	0.00	0.013	7.4
4016-1	1.4016	C	2B	0.023	0.36	0.46	16.3	0.2	0.0	0.01	0.01	0.1	0.01	0.028	14.8
4016-2	1.4016	B	2B	0.046	0.30	0.48	16.1	0.2	0.2	0.00	0.02	0.1	0.00	0.027	14.1
4509-1	1.4509	C	2B	0.017	0.55	0.45	17.8	0.2	0.0	0.14	0.49	0.0	0.05	0.018	19.3
4509-2	1.4509	B	2B	0.020	0.55	0.48	17.9	0.3	0.0	0.12	0.40	0.1	0.01	0.030	18.4
4521-1	1.4521	C	2B	0.011	0.48	0.44	17.7	0.3	2.0	0.17	0.43	0.1	0.00	0.016	26.6
4521-2	1.4521	B	2B	0.015	0.52	0.49	18.0	0.1	2.0	0.13	0.40	0.2	0.01	0.019	27.3
4521-3	1.4521	B	2B	0.012	0.48	0.49	17.9	0.2	2.0	0.13	0.39	0.2	0.01	0.023	27.0
4621-1	1.4621	A	2R	0.014	0.21	0.23	20.6	0.2	0.0	0.01	0.45	0.4	0.00	0.014	19.7

KFF = Kaltenhauser Ferrite Factor

Table 2. Room-temperature mechanical properties of test materials.

Identifier	Thickness (mm)	Rp0,01 (N/mm²)	Rp0,1 N/mm²	Rp0,2 N/mm²	Rp1,0 N/mm²	Rt2,0 N/mm²	Rm N/mm²	Ag %	A80 %	A5 %
4003-1	2.0	234	318	330	357	389	493	16.2	31	51
4016-1	2.0	225	299	311	338	358	478	16.8	26	38
4016-2	2.0	237	305	315	333	349	458	17.4	33	53
4509-1	2.0	250	321	331	353	369	479	17.6	29	43
4509-2	2.0	287	358	367	384	400	488	15.9	33	54
4521-1	2.0	291	367	375	396	416	542	16.2	29	45
4521-2	2.0	309	382	394	419	438	564	15.6	28	44
4521-3	2.0	337	379	391	411	427	532	17.3	28	42
4621-1	1.5	279	351	359	373	406	469	15.9	32	56

The grades 1.4509, 1.4521 and 1.4621 are modern stabilized ferritic stainless steels. In these alloys, the interstitial carbon and nitrogen is bound by stabilizing elements such as Nb and Ti. The precipitated nitrides and carbides act as barriers to dislocation motion, and inhibit grain boundary sliding and grain growth [**6**]. This improves the elevated temperature strength and creep resistance of these alloys. Consequently, stabilized ferritic stainless steels are commonly used for elevated temperature applications such as exhaust pipes.

2.2 Testing equipment

The isothermal and anisothermal material testing was performed using a Zwick Z250/SW5A tensile testing machine with the capacity of 250kN, Figure 1. The tensile testing machine is equipped with a low temperature environmental chamber and a high temperature furnace shown in Figure 2. The environmental chamber was used for temperatures in the range from 25ºC to 550ºC. For temperatures in the range of 550ºC to 1000ºC, the high temperature oven was used.

The environmental chamber used for testing at lower temperatures below 600ºC is a convection oven with an automatic temperature control in the convector unit. The high temperature furnace is heated with three resistor zones. The oven temperature in each zone is controlled with a thermocouple connected to a PID controller unit (Eurotherm 2416).

The tensile testing machine is equipped with GTM load cell and Maytec side-entry extensometer, Figure 3. The specimen is held by shouldered holders. The sensor arms of the extensometer are made of ceramic material as shown in Figures 2 and 3. The equipment is regularly calibrated according to the standards SFS-EN ISO 7500-1:2004 and SFS-EN ISO 9513:2002.

Figure 1. Zwick Z250 tensile test machine.

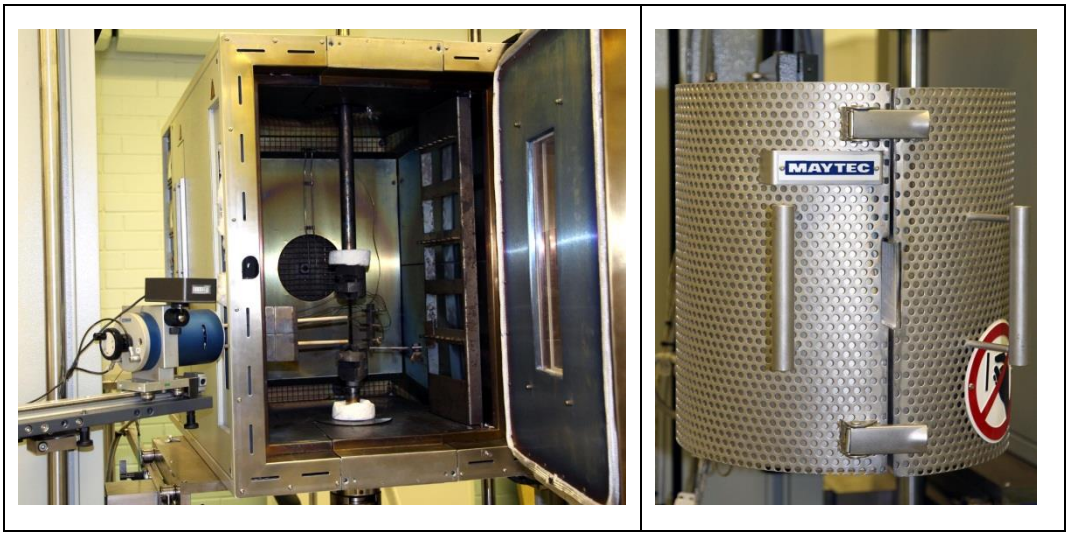

Figure 2. Environmental chamber (left) and the high temperature furnace (right).

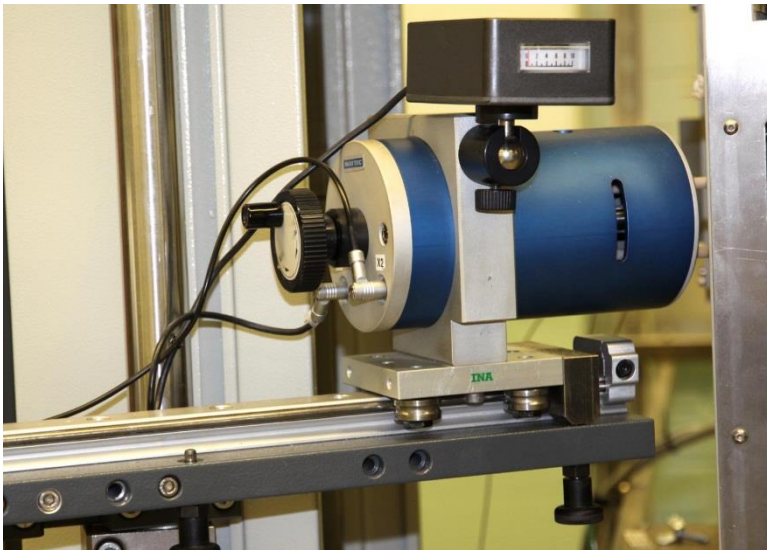

Figure 3. Maytec extensometer with ceramic sensor arms.

According to EN ISO 7500-1:2004, the tensile testing machine belongs to accuracy class 1. It follows that

- The relative error of the original gauge length is less than 1.0%.
- The error on the movement of one arm of the extensometer is 3µm or 1% depending on which measure is larger.
- The error on the force value is less than 1.0%.
- The resolution of extensometer arm movement is 1.0µm.
- The resolution of the force sensor is 1N.

2.3 Test piece geometry

The piece geometry is shown in Figure 4. The test pieces were obtained by machining. The manufacturing tolerances depend on the sample thickness according to the standard specification. The test piece geometry corresponds to specifications given for non-proportional test pieces in the annex A of standard ISO EN 10002-5. The original gauge length used for this test piece type is $L_0 = 50mm$.

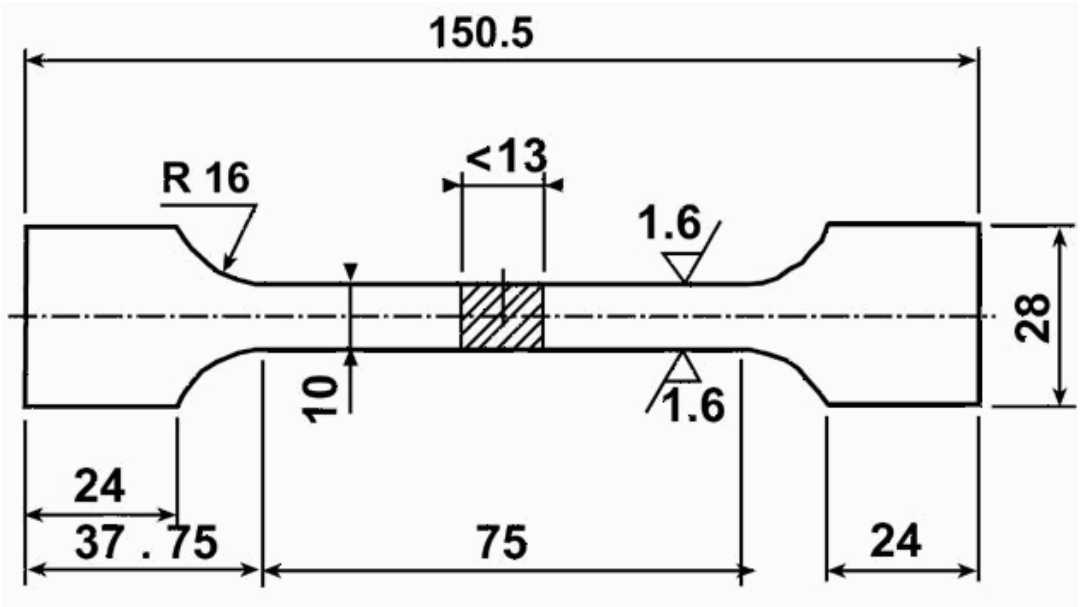

Figure 4. Test piece geometry.

2.4 Isothermal test procedure

Isothermal (steady state) tests were performed at temperature intervals of 100°C between room temperature and 500°C and at temperature intervals of 50°C between 500°C and 1000°C. Two identical tests were carried out at each temperature. If there was a significant disparity between the results, a third test was performed. The environmental chamber was used for temperatures in the range of 25ºC and 550ºC. For temperatures in the range of 550ºC and 1000ºC, the high temperature furnace was used.

The test piece temperature in the oven was measured by means of three K-type thermocouples pressed to the surface of the test piece. The temperature of the test piece was controlled within the limits given in Table 3. In the beginning of the test, the test piece was heated to the specified temperature and maintained at that temperature for 10 minutes before loading. The sample elongation was measured using the Maytec side-entry extensometer shown in Figure 3.The extensometer was reset to zero immediately before the onset of loading.

Table 3. Maximum allowed temperature deviation.

Range	Maximum allowed deviation (°C)
T ≤ 600°C	±3°C
600°C ≤ T ≤ 800°C	±4°C
800°C ≤ T ≤ 1000°C	±5°C

The tensile test standard SFS-EN ISO 10002-5 specifies different limits for the machine rate in different parts of the testing. The maximum values permitted by the standard were used in the present testing programme, Table 4.

Table 4. Loading rates used in steady state testing.

Range	Straining rate (min^{-1})
Proof strength	$\dot{\varepsilon}$ = 0.005
Tensile strength	$\dot{\varepsilon}$ = 0.2

2.5 Anisothermal test procedure

In the anisothermal tests, the load applied on the specimen is kept constant and the temperature is increased with a constant heating rate. The temperature and the elongation of the specimen are measured continuously during the test. The test is continued until the specimen fails or the target temperature is reached.

The anisothermal tests were carried out using the high temperature furnace shown on the right in Figure 2. The sample elongation was measured using the Maytec side-entry extensometer shown in Figure 3. The sample temperature was measured using three K-type thermocouples attached to the surface of the test piece. The median of all valid temperature values was used as the sample temperature.

The anisothermal tests were conducted using sixteen evenly spaced stress levels between 10% and 90% of the yield stress. Two equal tests were performed at each stress level. If there was a significant disparity between the results, a third test was performed. The heating rate was 10°C/min and the target temperature 1000°C. The thermal expansion of the sample was measured using a small stress level of 3 MPa.

3 Results of isothermal tests

Stress-strain curves determined for all studied test materials are shown in the appendices. The proof stress values corresponding to the 0.1%, 0.2% and 1% plastic strains, the ultimate tensile strength values, maximum elongation and elastic modulus values are also summarized in the appendices.

Grade 1.4003

The grade 1.4003 has been extensively studied in earlier ECSC and RFCS funded research projects. Therefore, this grade was included in the test programme as a reference material.

Figure 5 shows the stress-strain curves measured for the steel grade 1.4003. The following three stages can be identified in the curves:

- In the range 200°C $\leq T \leq$ 400°C, the strength of the material remains roughly constant despite of the increasing temperature. This behaviour can be attributed to dynamic strain aging (DSA) which is typical of materials with ferritic structure containing free interstitials [**7**,**8**]. Further evidence of DSA in the form of serrations and a negative strain-rate dependency are also visible in the curves. The latter can be observed as a drop in the flow stress when the loading rate is increased. The increase of strength by DSA is associated with a decrease in ductility. In the present case, the tensile strain A50 has a global minimum of A50 = 16% at T = 400°C.

- In the temperature range 600°C $\leq T \leq$ 750°C, the material exhibits no strain hardening during plastic deformation and the strength decreases rapidly with increasing temperature. In this stage, the material is deforming under steady state creep condition. The strength is essentially constant and depends mainly on temperature and on the rate of loading. The small difference between the measured proof stress values and the ultimate tensile strength value is caused by the increase of loading rate during the test.

- Between 750°C and 800°C, the material undergoes a phase transition from ferritic to austenitic state. Consequently, the strength of the material increases, and the work hardening capability is restored. The phase transition is associated with a volume decrease of approximately 1% and with a change in the physical properties such as thermal conductivity and the coefficient of thermal expansion. The critical temperature for the phase transformation depends on the chemical composition of the steel and is therefore slightly different for steels from different suppliers [**9**,**10**].

The proof stress values corresponding to the 0.1%, 0.2% and 1% plastic strains and the ultimate tensile strength values for this material are shown in Figure 6. The reduction factors corresponding to proof stress and ultimate tensile strength values are shown in Figure 7. The three stages discussed above are clearly visible in both figures 6 and 7.

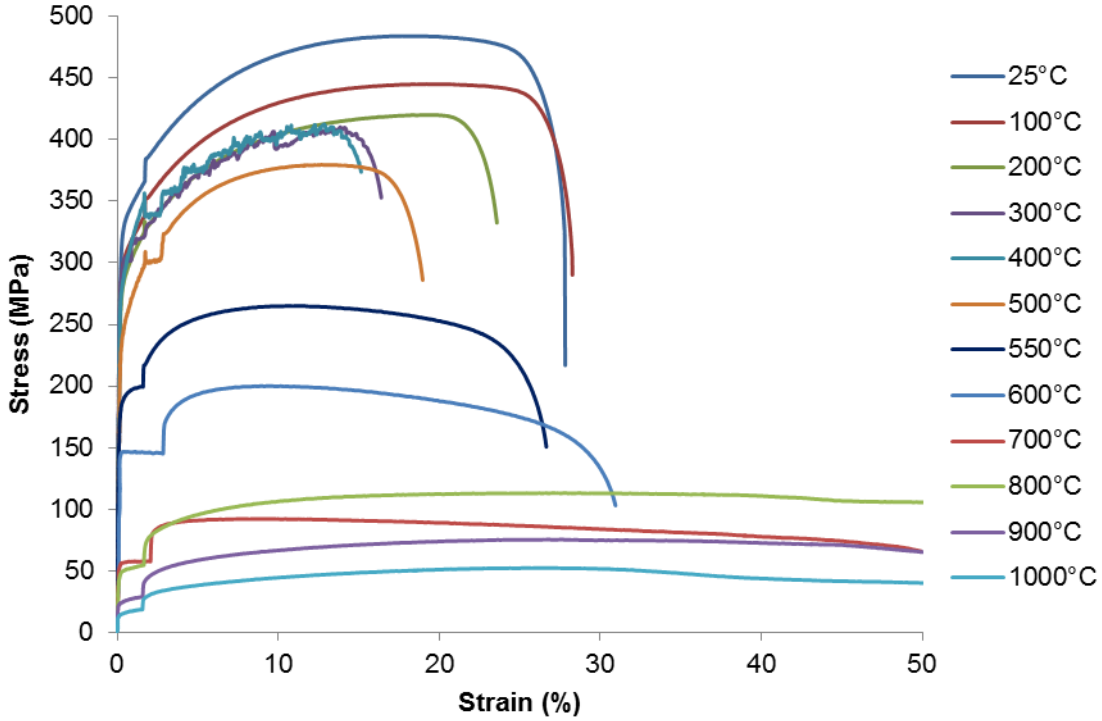

Figure 5. Stress-strain curves at elevated temperatures for the grade 1.4003. Some curves have been omitted for clarity.

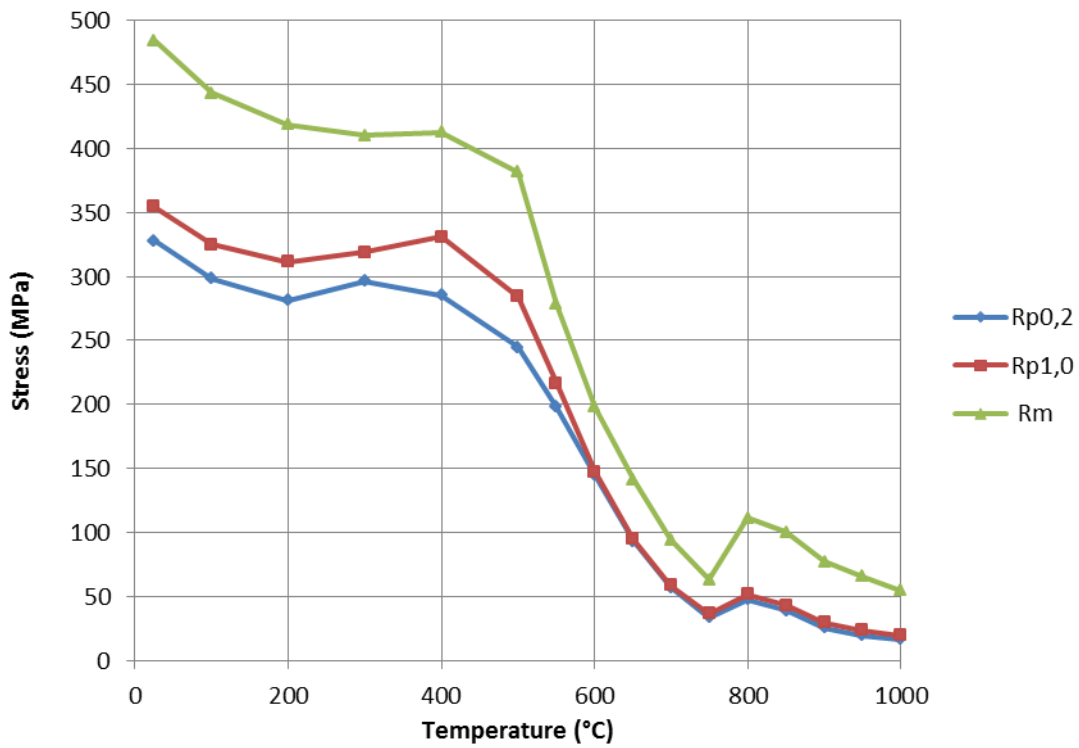

Figure 6. Stress values corresponding to 0.2% and 1% plastic strain and the ultimate tensile stress for the grade 1.4003.

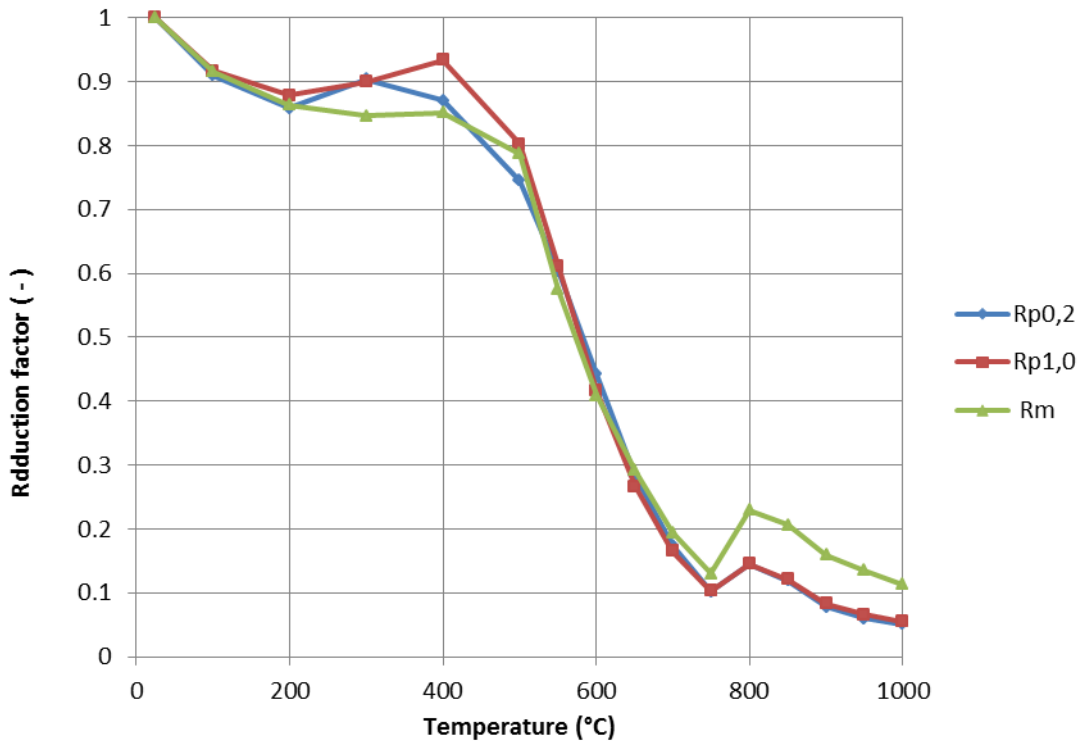

Figure 7. Reduction factors for the 0.2% and 1% proof stress and for the ultimate tensile strength for the grade 1.4003.

Grade 1.4016

Figure 8 shows the stress-strain curves for the steel 4016-2. The grade 1.4016 has similar characteristics as the grade 1.4003. In particular, the dynamic strain aging stage and the non-strain hardening stage can be observed:

- In the range 100°C $\leq T \leq$ 400°C, the strength of the material remains roughly constant despite of the increasing temperature. As mentioned before in the case of 1.4003, this behaviour can be attributed to dynamic strain aging (DSA). Further evidence of DSA in the form of serrations in the curves and in the form of decrease in ductility can be observed. In the present case, the A50 tensile strain value has a global minimum of A50 = 16% at T = 500°C.

- In temperatures above 600°C, the material exhibits no strain hardening during plastic deformation and the strength decreases rapidly with increasing temperature. In this stage, the material is deforming under steady state creep. The strength depends mainly on temperature and the rate of loading. The small difference between the measured proof stress values and the ultimate tensile strength value is caused by the increase of loading.

The proof stress values corresponding to the 0.2% and 1% plastic strains and the ultimate tensile strength values for this material are shown in Figure 9. The reduction factors corresponding to proof stress and ultimate tensile strength values are shown in Figure 10. The two stages discussed above are clearly visible in the Figures 9 and 10. The third stage observed with the grade 1.4003, the austenitic stage, does not show in the curves even

though the starting temperature for the phase transition is typically between 850°C and 950°C for 1.4016. The absence of a clearly defined austenitic stage is related to the fact that only a part of ferrite in 1.4016 will transform to austenite when the critical temperature is exceeded [**9**,**10**].

There were no significant differences between the test materials supplied by the two steel producers B and C. The reduction factors corresponding to the 0.2% proof stress and the ultimate tensile strength for both materials are shown for comparison in Figure 11. Apart from the visible difference in the DSA stage, the reduction factors of these two materials are similar. The stronger dynamic strain aging in the steel 4016-2 is most likely caused by the higher carbon content in this material.

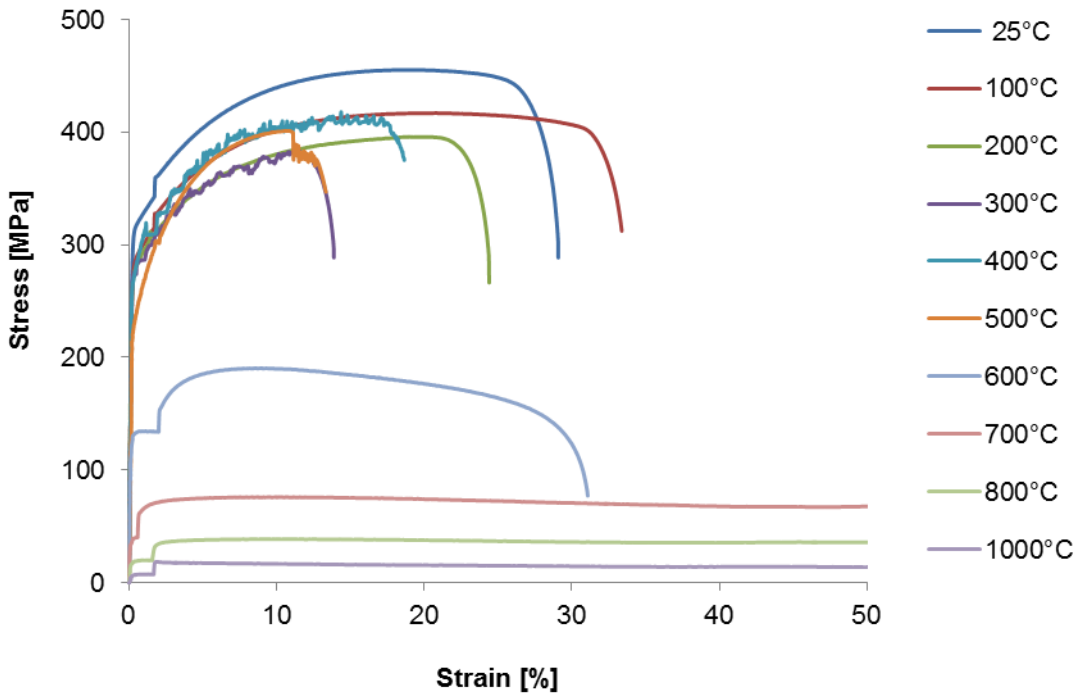

Figure 8. Stress-strain curves at elevated temperatures for steel 4016-2. Some curves have been omitted for clarity.

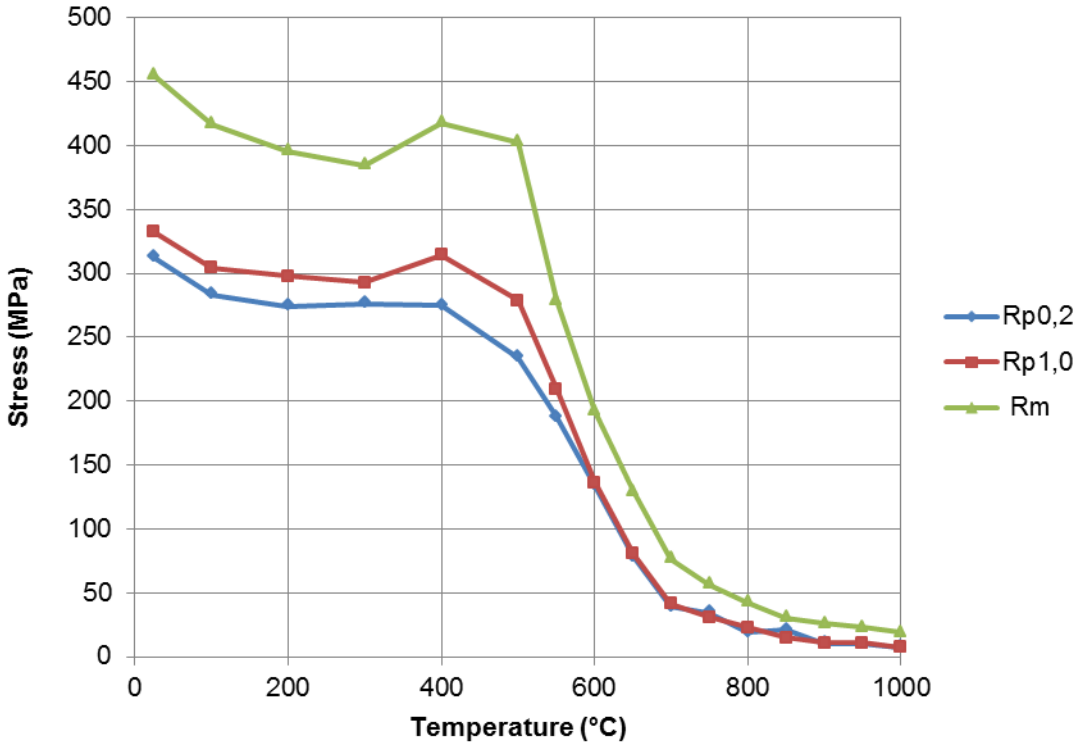

Figure 9. Proof stress values corresponding to 0.2% and 1% plastic strain and the ultimate tensile strength for the steel 4016-2.

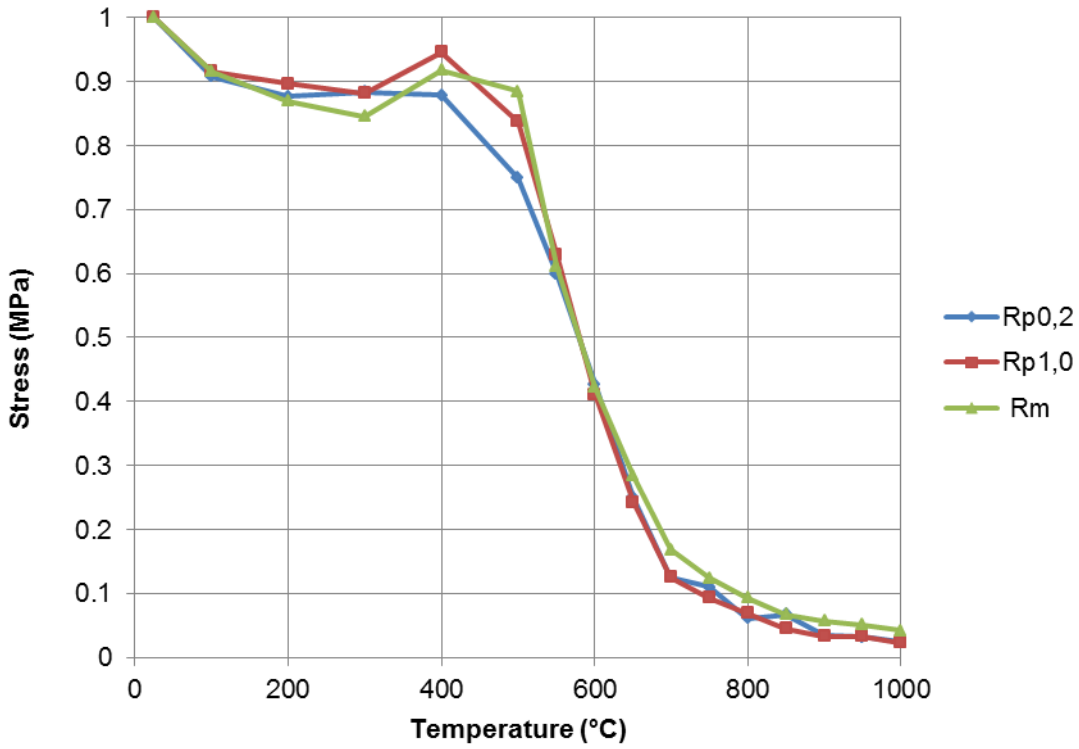

Figure 10. Reduction factors corresponding to the 0.2% and 1% proof stress and the ultimate tensile strength for the steel 4016-2.

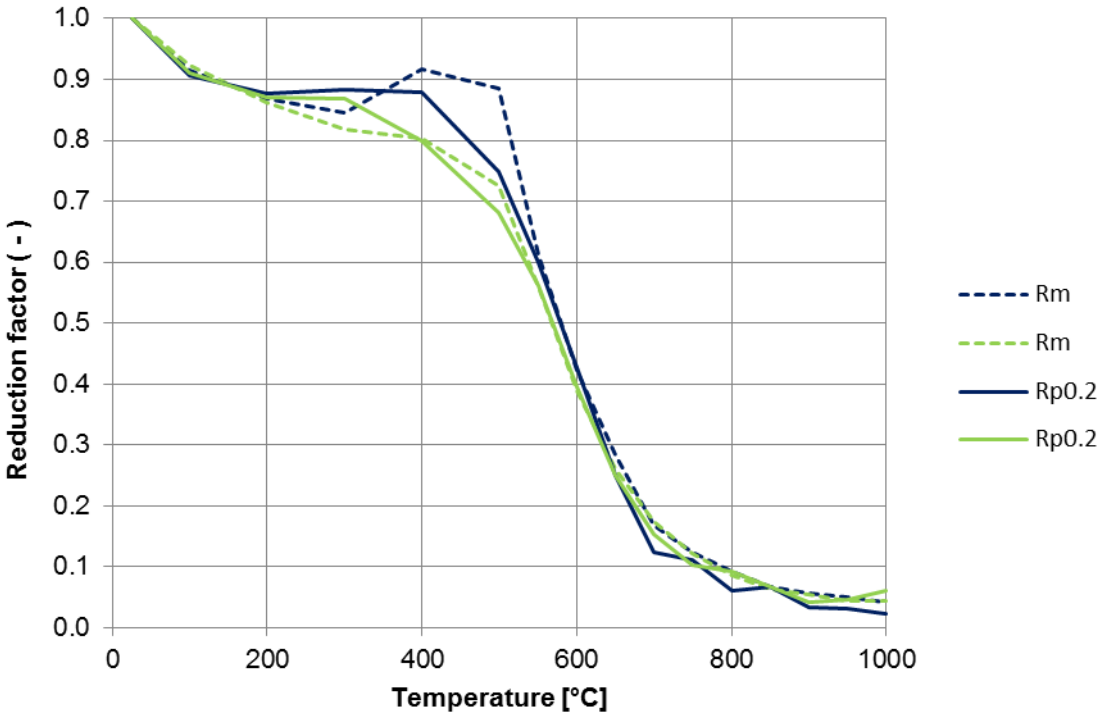

Figure 11. Reduction factors for the 0.2% proof stress and ultimate tensile strength for grade 1.4016 materials by two producers. The green curves correspond to the steel 4016-1 and the blue curves to the steel 4016-2.

Grade 1.4509

The high temperature behaviour of stabilized grades 1.4509, 1.4521 and 1.4621 differs from that of the unstabilized grades discussed above. In stabilized grades, the free interstitial elements are bound to stable nitrides/carbides by the stabilizing elements such as Nb and Ti. Therefore, the stabilized grades are less susceptible to dynamic and static strain aging. Furthermore, the nitrides and carbides formed act as barriers to dislocation motion and inhibit grain boundary sliding and grain growth. Hence, stabilization improves the elevated temperature mechanical properties of ferritic stainless steels. The stabilized grades are largely used for elevated temperature applications such as exhaust pipes in the automotive industry.

The stress-strain curves for the steel 4509-2 are shown in the Figure 12. It can be observed, that the effect of DSA is almost negligible, and the region of steady state creep deformation, being translated to higher temperatures, starts at T = 750°C. The corresponding proof stress values and the reduction factors are shown in the Figures 13 and 14. The differences between materials obtained from different suppliers are minimal for the grade 1.4509, Figure 15.

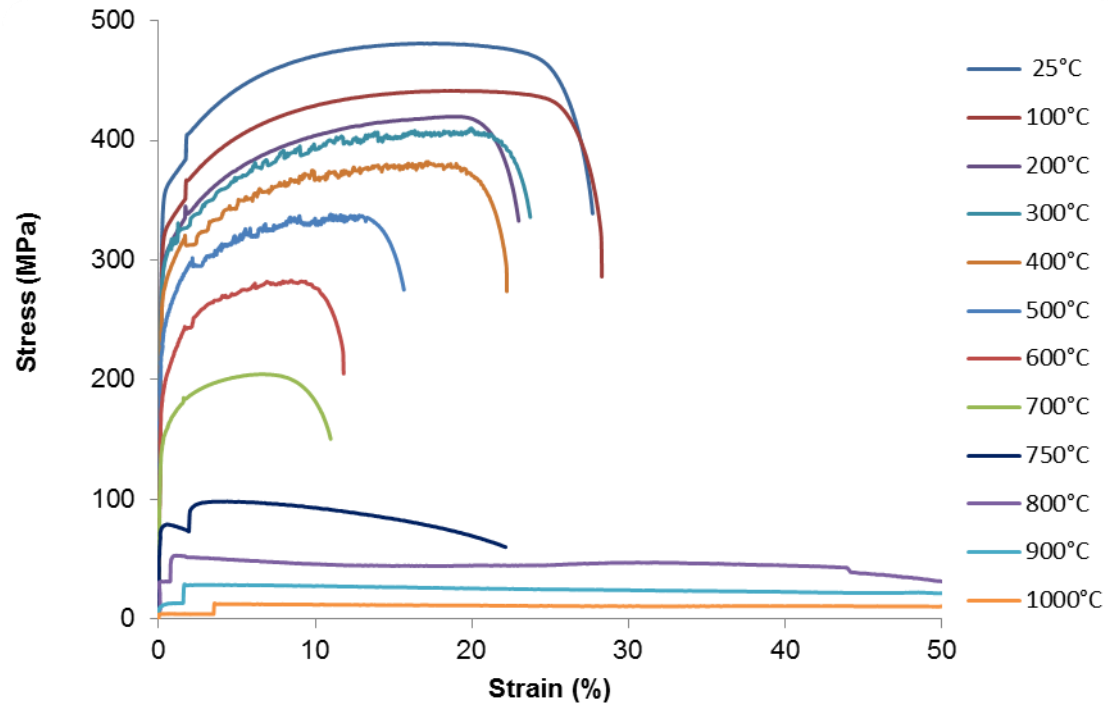

Figure 12. Stress-strain curves at elevated temperatures for the steel 4509-2.

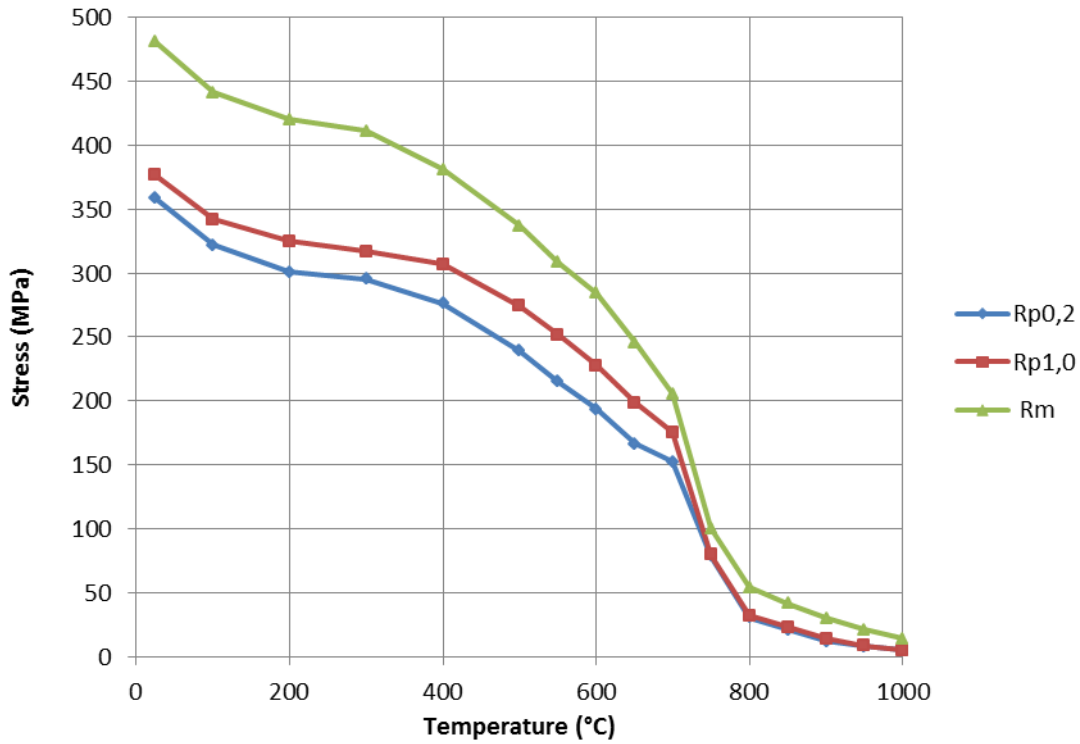

Figure 13. Proof stress values corresponding to 0.2% and 1% plastic strain and the ultimate tensile strength for the steel 4509-2.

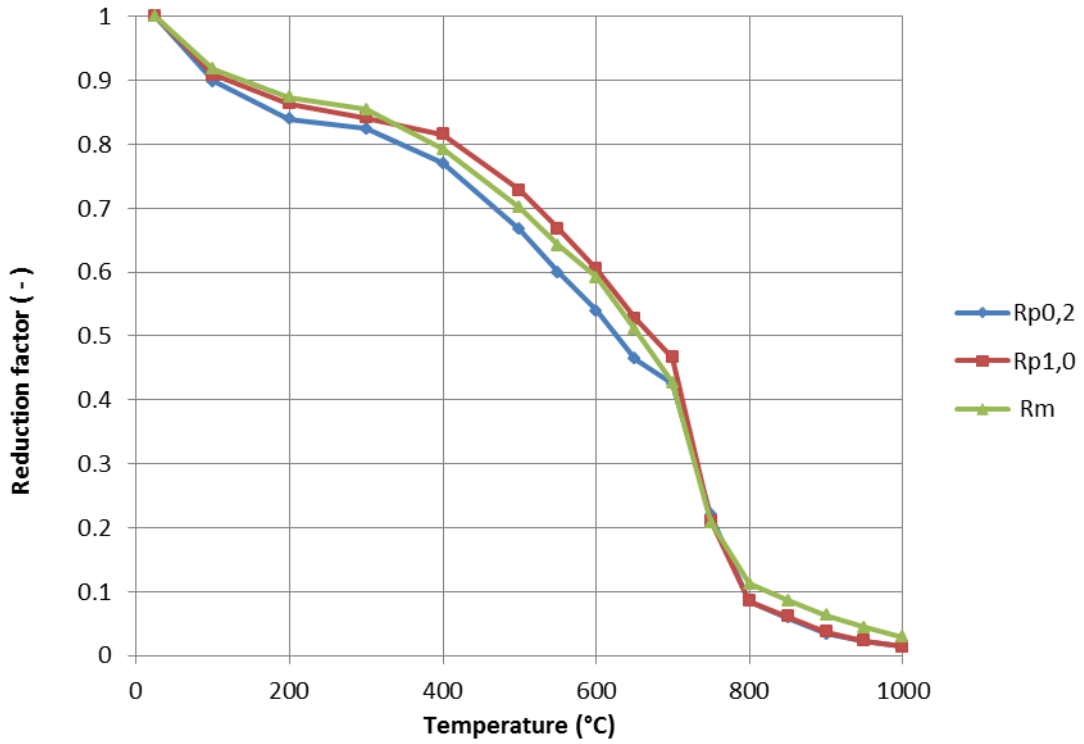

Figure 14. Reduction factors corresponding to the 0.2% and 1% proof stress and the ultimate tensile strength for the steel 4509-2.

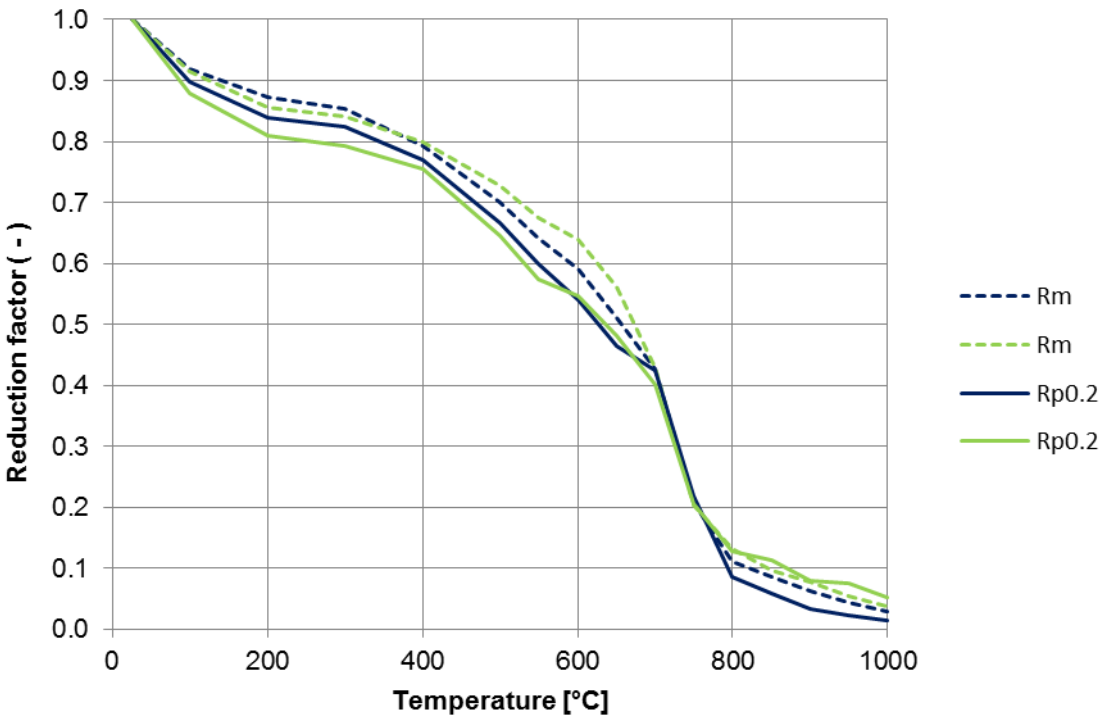

Figure 15. Reduction factors for the 0.2% proof stress and ultimate tensile strength for grade 1.4016 materials by two producers. The green curves correspond to the steel 4509-1 and the blue curves to the steel 4509-2.

Grade 1.4521

Figure 16 shows the stress-strain curves for 4521-2. It can be seen from the curves, that the grade 1.4521 has similar characteristics as the grade 1.4509. The influence of DSA is small, and the region of steady state creep deformation starts at T = 750°C.

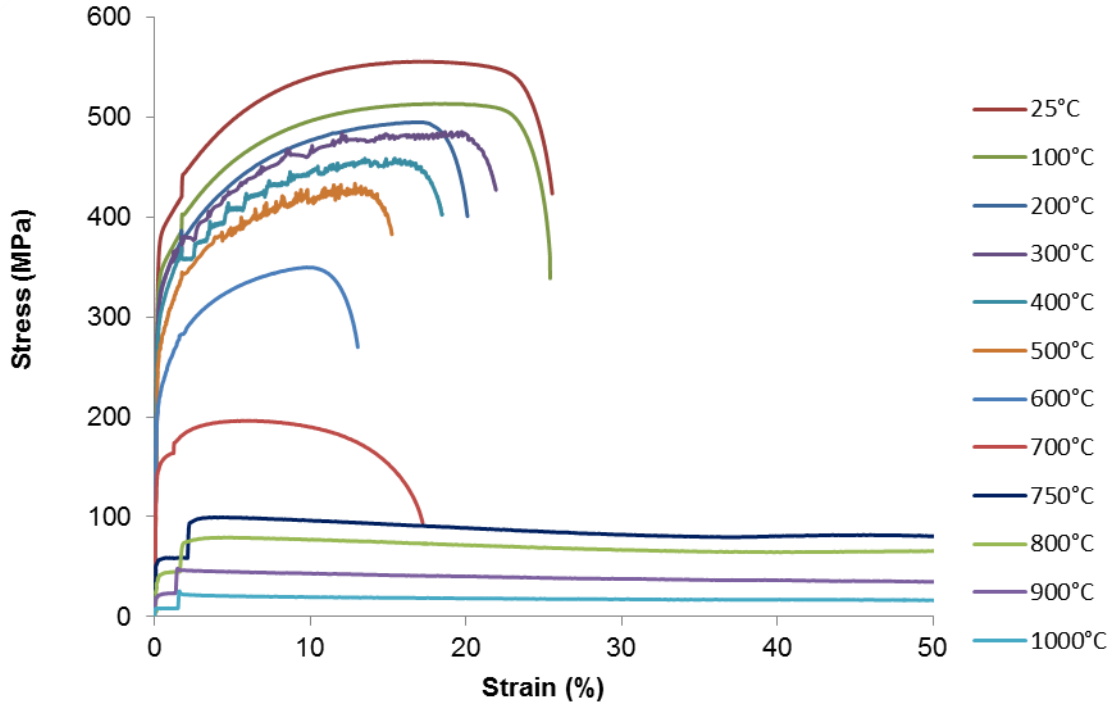

Figure 16. Stress-strain curves at elevated temperatures for the steel 4521-2.

The proof stress values and the reduction factors for the steel 4521-2 are shown in Figures 17 and 18. The shapes of the curves resemble closely to the ones obtained for 1.4509. The differences between materials from two producers B and C are small, Figure 19.

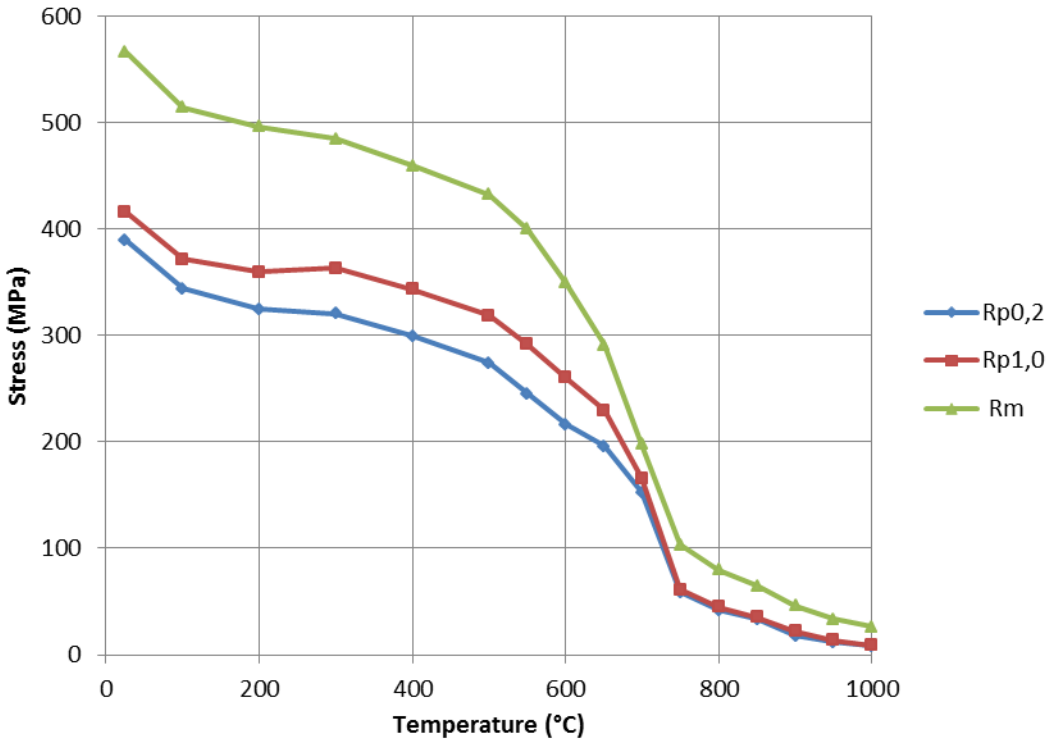

Figure 17. Proof stress values corresponding to 0.2% and 1% plastic strain and the ultimate tensile strength for the steel 4521-2.

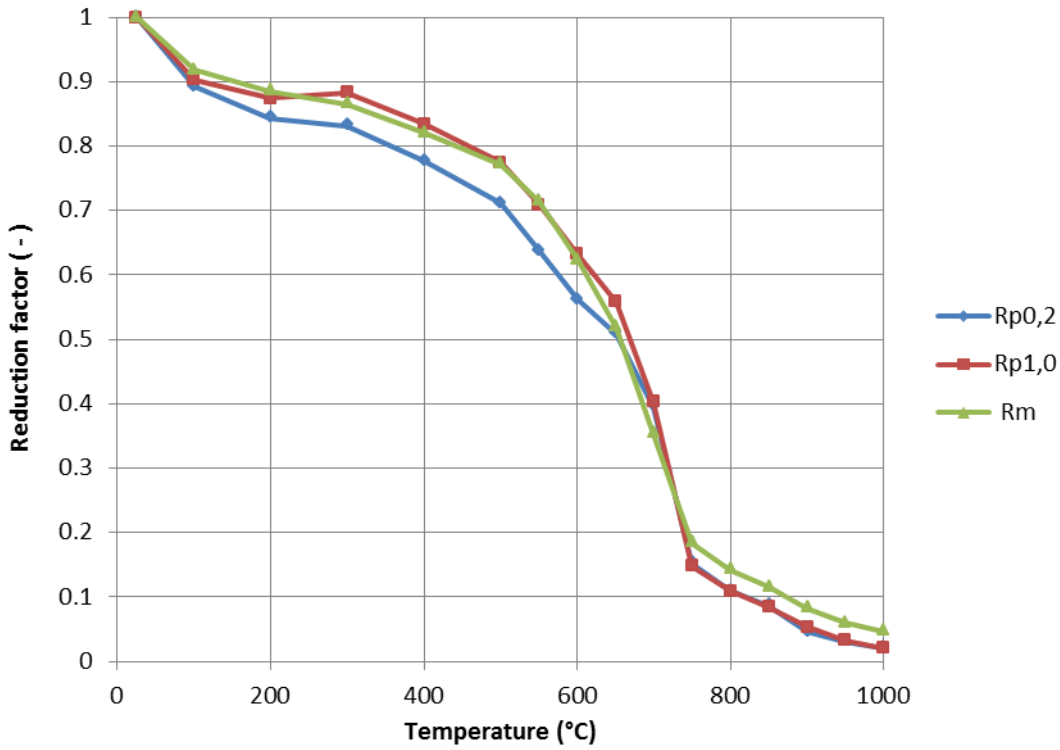

Figure 18. Reduction factors corresponding to the 0.2% and 1% proof stress and the ultimate tensile strength for the steel 4521-2.

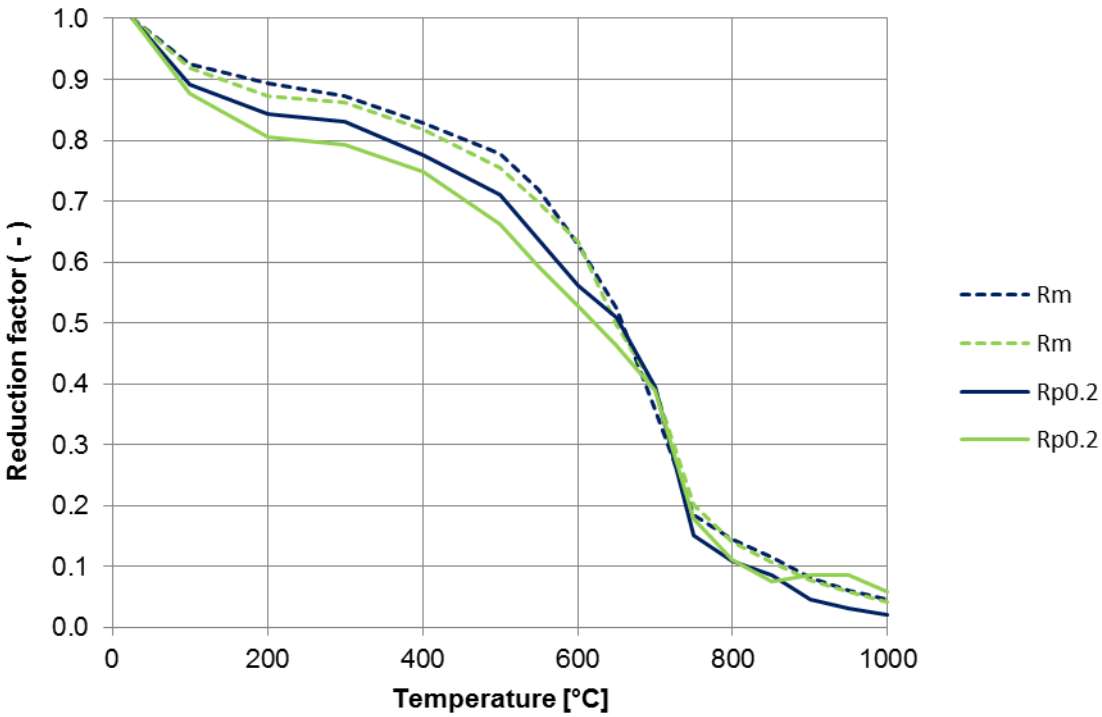

Figure 19. Reduction factors for the 0.2% proof strength and ultimate tensile strength for two grade 1.4521 materials by producers B and C. The green lines correspond to the steel 4521-1 and the blue lines to the steel 4521-2.

Grade 1.4621

Figure 20 shows the stress-strain curves for steel grade 1.4621. The proof stress values and the reduction factors for this steel are shown in the Figures 21 and 22. The shapes of the proof stress and the reduction factor curves resemble to those of the other stabilized grades 1.4509 and 1.4521. In addition, the steady state creep region starts approximately at the same temperature, T = 750°C, for all stabilized grades.

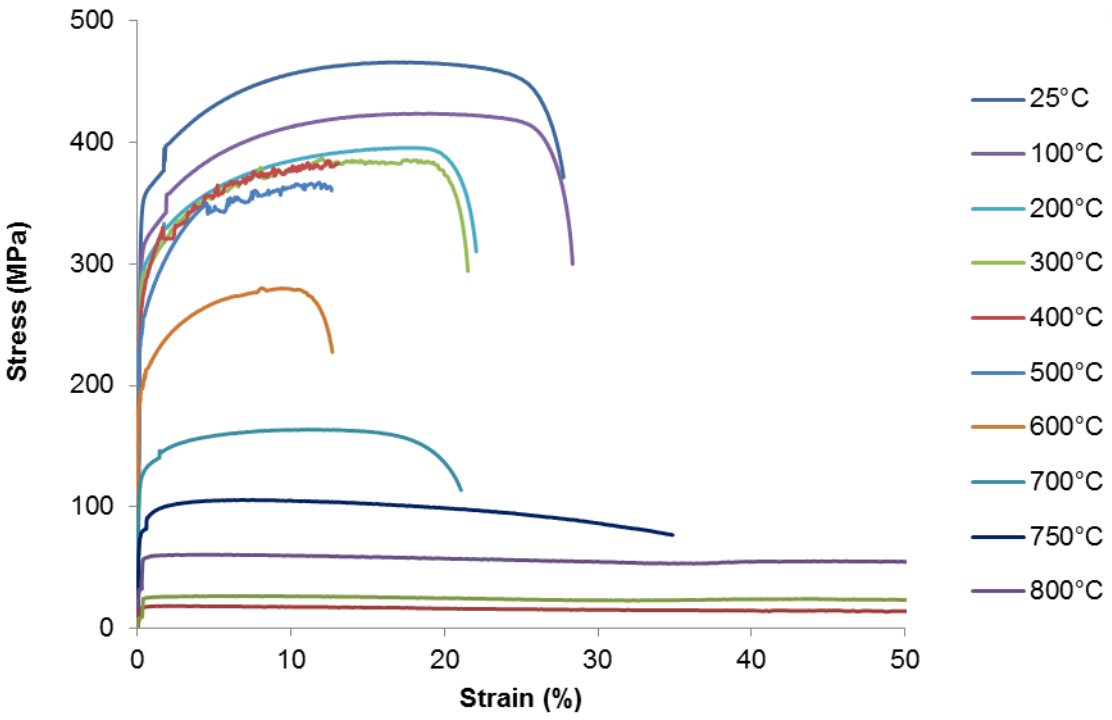

Figure 20. Stress-strain curves for the grade 1.4621.

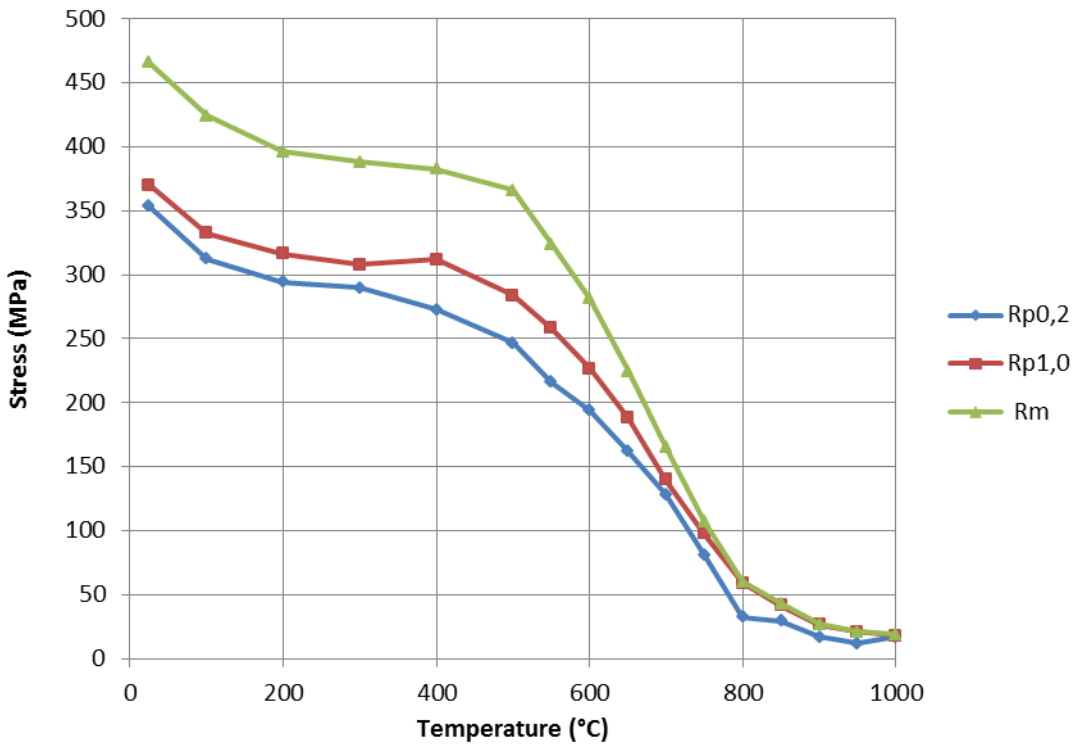

Figure 21. Proof stress values corresponding to 0.2% and 1% plastic strain and the ultimate tensile strength for the grade 1.4621.

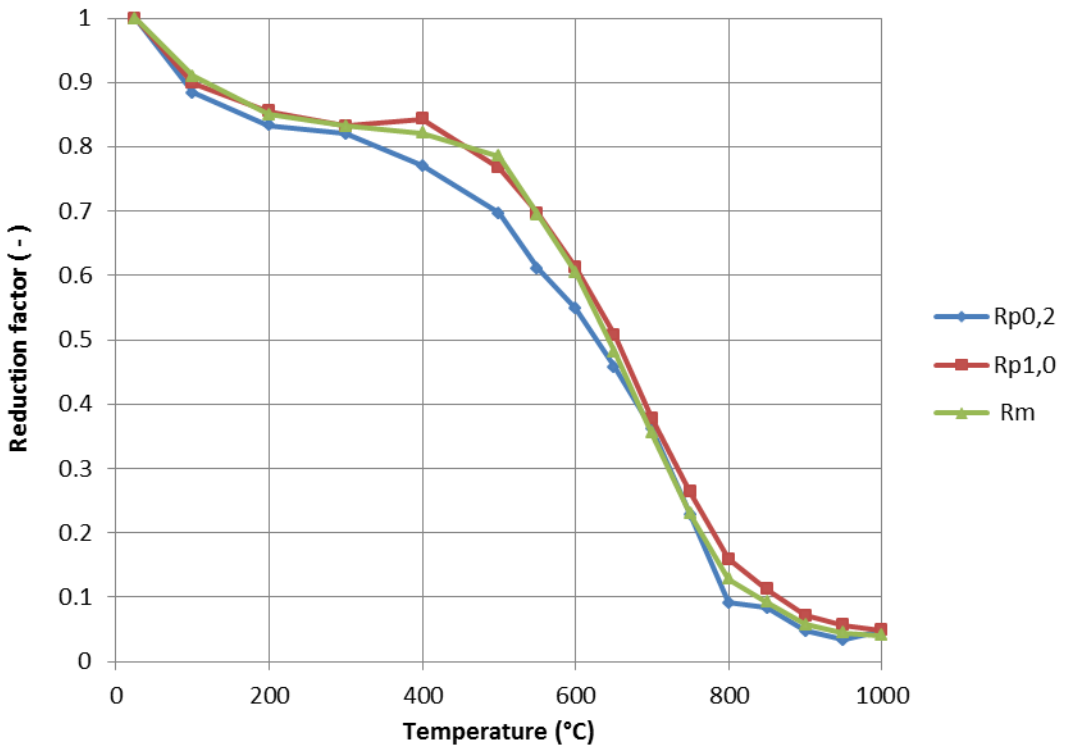

Figure 22. Reduction factors corresponding to the 0.2% and 1% proof stress and the ultimate tensile strength for the grade 1.4621.

Degradation of elastic stiffness

The modulus of elasticity was determined based on the slope of the initial part of the stress-strain curve. Accurate determination of the modulus of elasticity based tensile test results is very difficult for a number of reasons [**11**]. On one hand, the linear-elastic part of the stress-strain curve is short for materials, which do not exhibit a clearly defined yield point. Therefore, inelastic effects such as creep and early yielding are influencing the test results. The systematic error caused by the inelastic behaviour on the elastic modulus is always negative; creep and plasticity tend to decrease the slope of the curve rather than to increase it. On the other hand, a small error in the test setup such as a small initial curvature of the test piece or a small misalignment of the specimen may have a significant influence on the obtained Young's modulus. Consequently, the dispersion in values of the elastic modulus determined from tensile test results is usually large.

The elastic modulus values determined using the steady state test results for all studied steel are shown in Figure 23. The dispersion in the elastic modulus values is remarkable. Due to the large dispersion, no systematic trends could be observed between different steel grades Therefore, all measurements were treated as one set of data and a common reduction factor curve was derived for all studied grades. The data was fitted with a piecewise linear function. The result is shown in Figure 24. The end-points of the line segments are given in Table 5. The standard error of the model equals to $\sigma = 0.14$.

The degradation of elastic stiffness in the present work is somewhat high compared to the values published by steel producers [**12**,**13**]. The discrepancy becomes pronounced in the steady state creep domain, above $T = 600°C$.

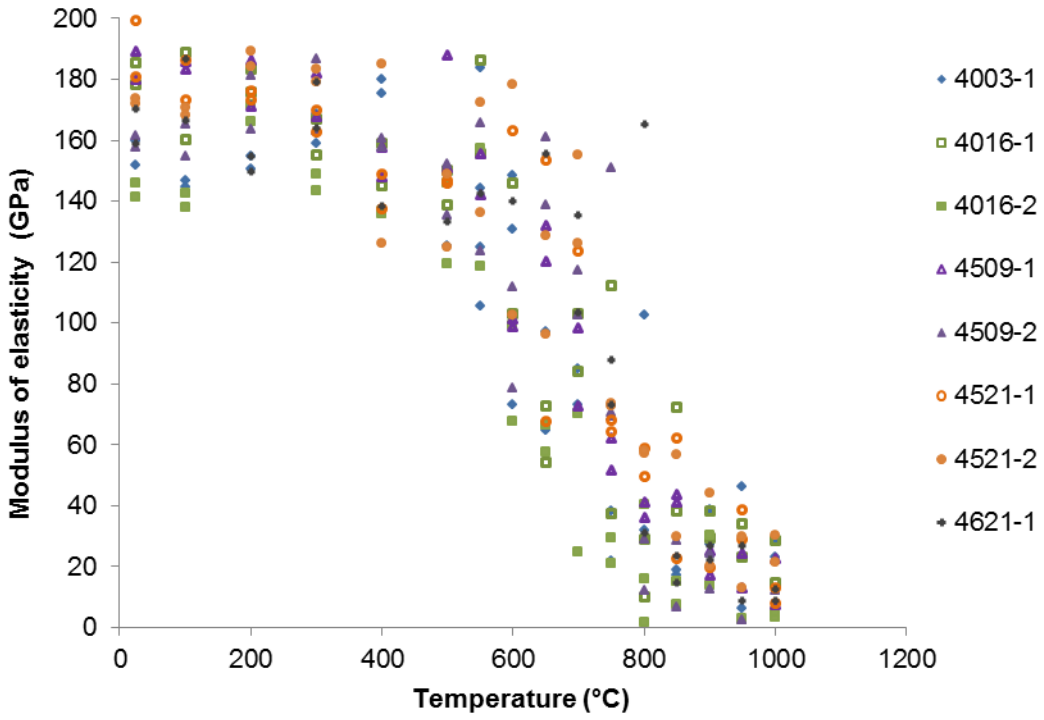

Figure 23. Modulus of elasticity values for all test materials. A small number of obvious outliers were removed from the figure.

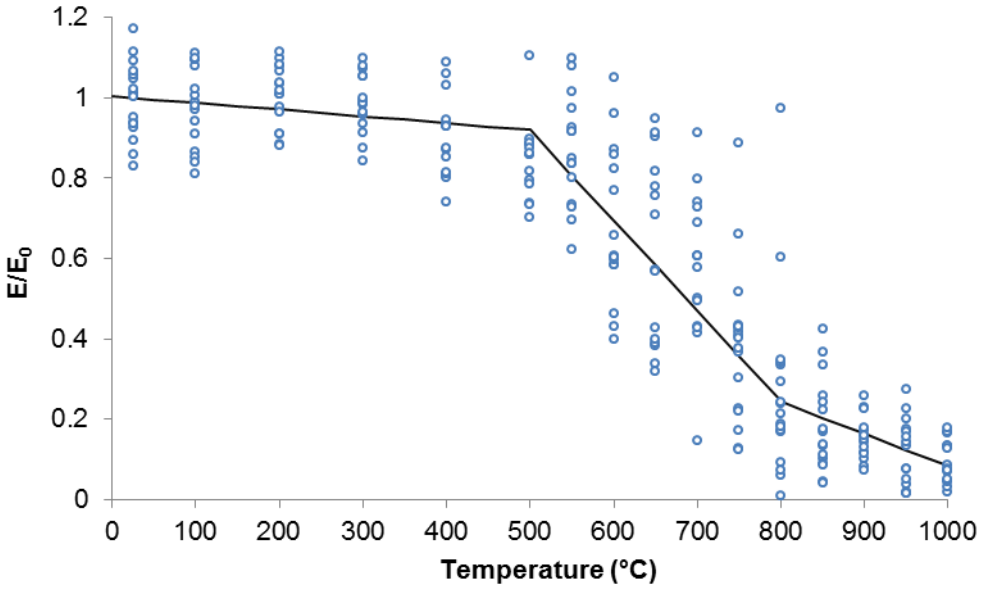

Figure 24. Reduction factor for the elastic stiffness from isothermal tensile tests.

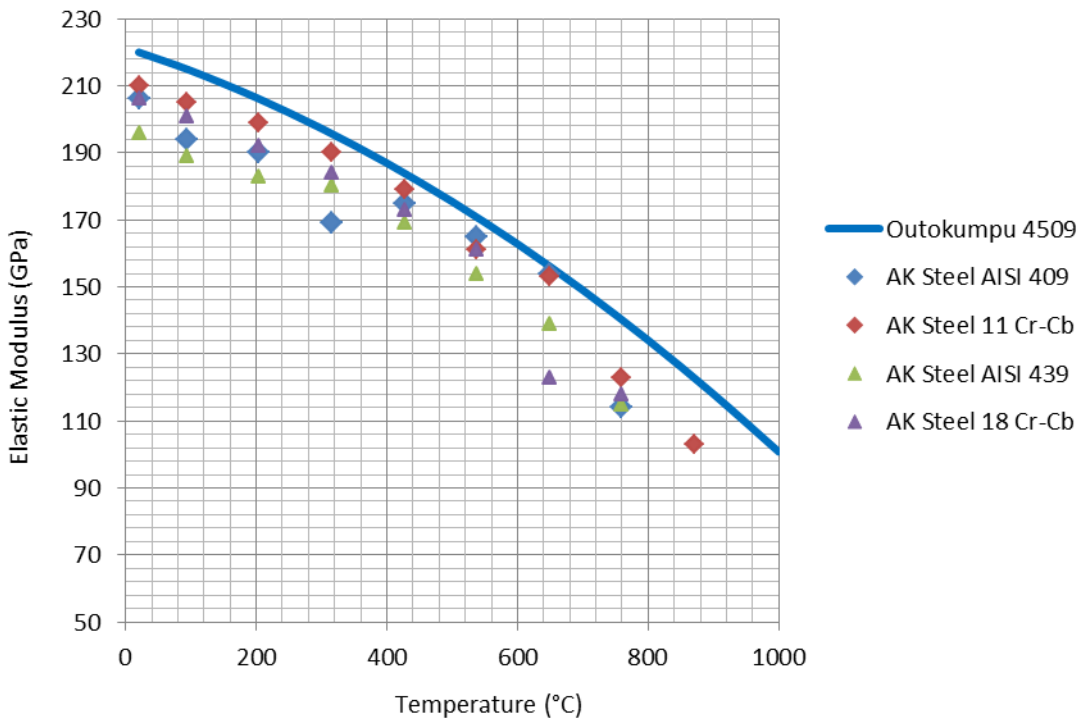

Figure 25. The elastic modulus of ferritic stainless steels at elevated temperature according to steel producers' publications.

Table 5. Line segment end-points for the reduction factor of elastic stiffness.

Temperature (°C)	Reduction factor value
25	1.00
500	0.92
800	0.24
1100	0.00

4 Anisothermal tests

Based on isothermal test results, the ferritic stainless steel studied could be divided in two groups with similar characteristics in each group. The first group contains the unstabilized grades 1.4003 and 1.4016, and the second group contains the stabilized grades 1.4509, 1.4521 and 1.4621.

The steel grade 1.4003 has been extensively studied previously. The strength and stiffness reduction factors for this grade are already included in the EN 1993-1-2. Therefore, the fire design parameters for the first group can be considered known. Consequently, two steels 4509-2 and 4521-3 from the second group were selected for anisothermal tests.

In the anisothermal tests, the elastic strain was calculated using the elevated temperature elastic modulus values published by Outokumpu for steel grades 1.4509 and 1.4521. These values have been measured by the Katholieke Universiteit Leuven using the impulse excitation technique [**13**,**14**]. The experimental Young's modulus values are accurately described by the second order polynomial

$$E = E_0[-2.61 \times 10^{-7}\,\theta^2 - 2.87 \times 10^{-4}\,\theta + 1.0] \qquad (1)$$

where θ (°C) is the steel temperature and E_0=*220 GPa*.

4.1 Anisothermal test results for 1.4509

In the anisothermal test procedure, the parasitic strain caused by thermal expansion was measured using the load level of 3 MPa. The thermal expansion is shown in Figure 26. The downward deflection in the curve at T = 900°C is an artefact caused by bending of the test piece in the furnace. The figure also shows a second order polynomial fit to the measured thermal expansion. Based on the experimental results, the linear coefficient thermal expansion between room temperature and 100°C was $\alpha = 12.0 \cdot 10^{-6}$ 1/°C for this steel.

Figure 27 shows transient test results for the steel grade 1.4509. The step-like features on curves is can be attributed to dynamic strain aging. The strength values corresponding to 0.2% plastic strain, 2.0% total strain and the ultimate tensile strength for both steels are shown in Figure 28. It can be seen that the strength starts to degrade rapidly as the temperature approaches T = 800°C.

Figures 29 and 30 compare the strength reduction factors obtained using the isothermal and the transient test methods. There is a good agreement between the two sets of reduction factors. The transient method gave slightly lower reduction factor values below T = 700°C. Above this limit, i.e., in the steady state creep domain, the transient test method gave slightly higher values for the reduction factors.

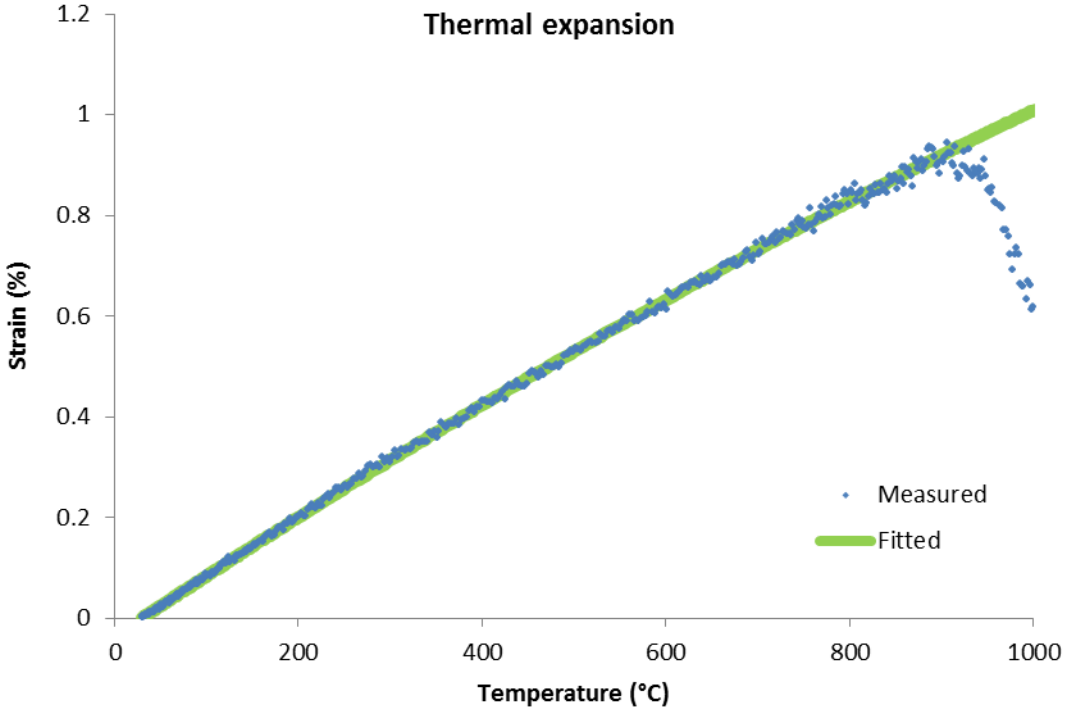

Figure 26. Measured parasitic strain for the steel 4509-2.

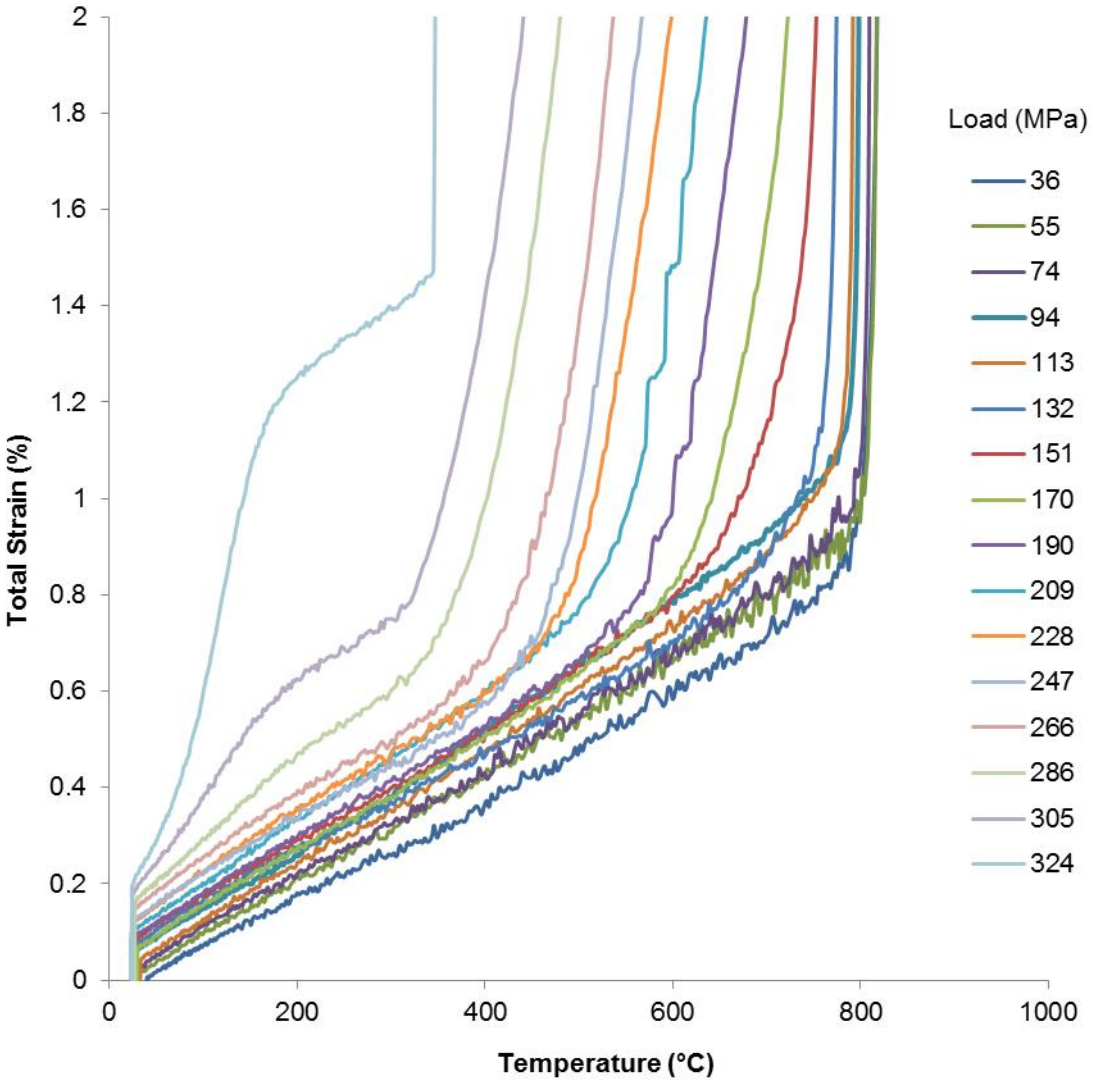

Figure 27. The transient test results for 4509-2. The strain includes the thermal expansion. The room-temperature 0.2% proof stress value was Rp0.2 = 367 MPa for the steel 4509-2.

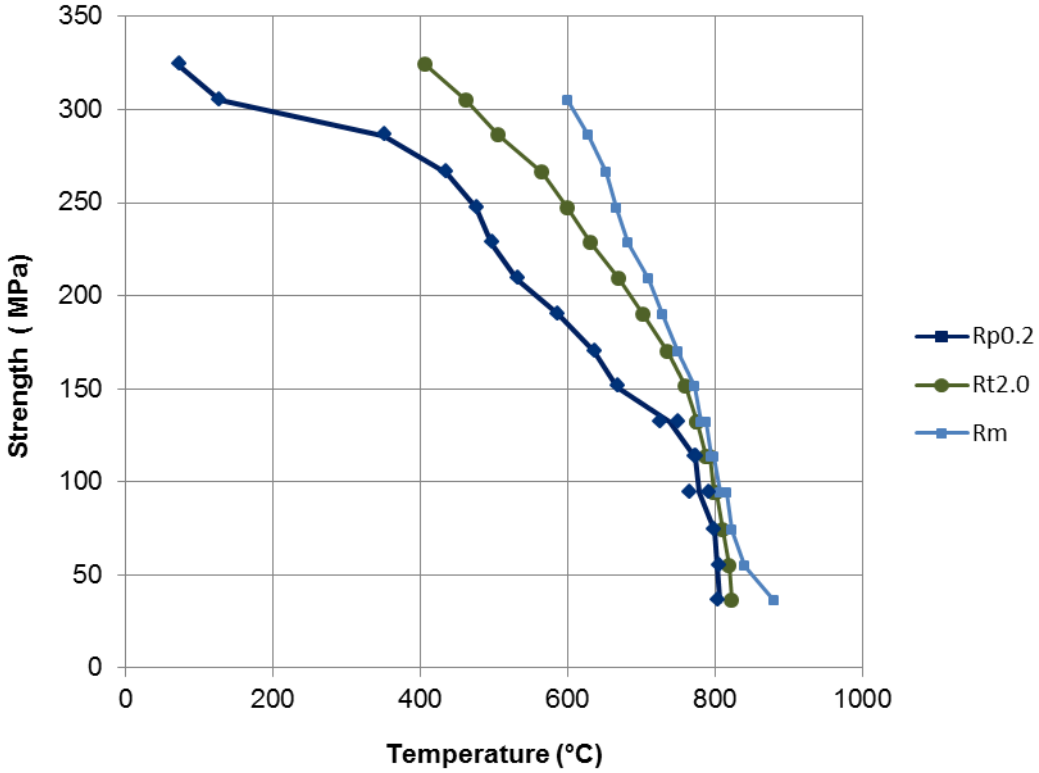

Figure 28. The stress values corresponding to 0.2% plastic strain, 2% total strain and the ultimate tensile strength obtained for the steel 4509-2 using the transient test method.

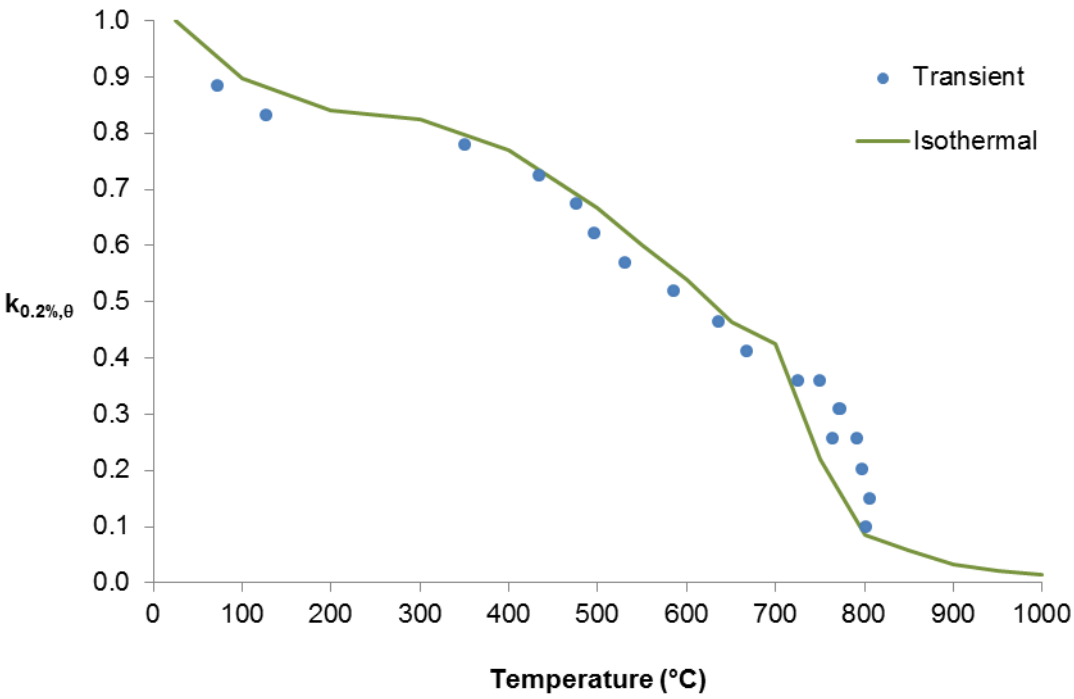

Figure 29. Reduction factor corresponding to the 0.2% proof stress obtained for the steel 4509-2 using the isothermal and the transient test methods.

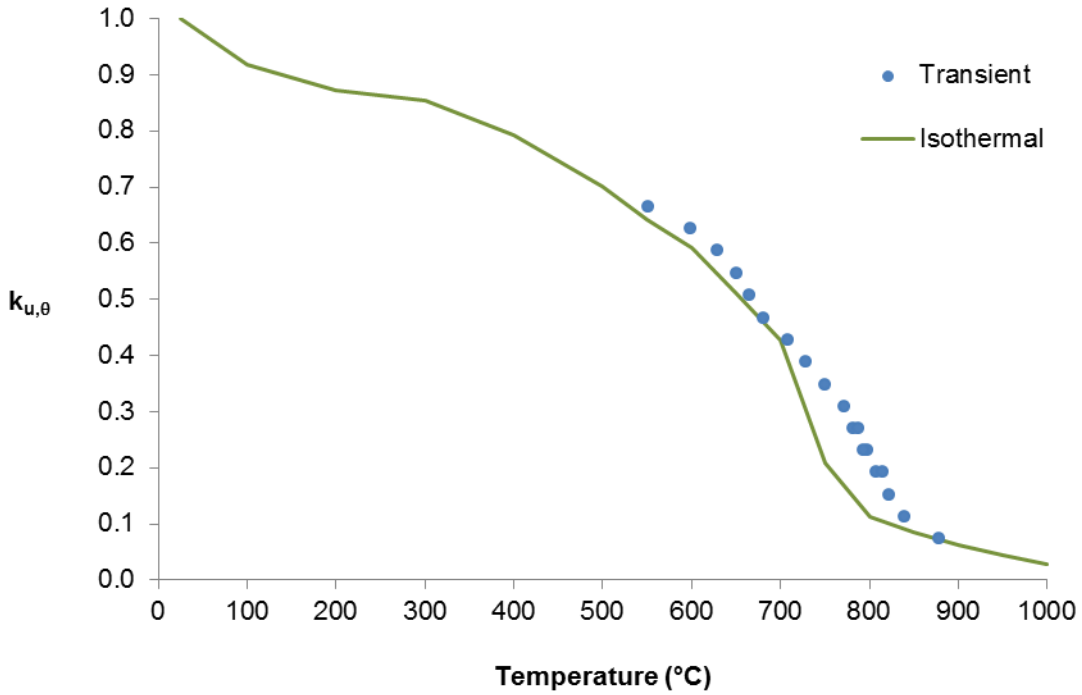

Figure 30. Reduction factor corresponding to the ultimate tensile strength obtained for the steel 4509-2 using the isothermal and the transient test method.

4.2 Anisothermal test results for 1.4521

The thermal expansion of 1.4521 is shown in Figure 31. For this grade, the thermal expansion was calculated as the average of two tests shown in the figure. The results were fitted with a third order polynomial shown in the figure. Based on the experimental results, the linear coefficient thermal expansion between room temperature and 100°C was $\alpha = 11.2 \cdot 10^{-6}$ 1/°C for this grade.

Figure 32 shows transient test results for the grade 1.4521. The step-like features in the curves are repeatable and can be attributed to dynamic strain aging, Figure 33. The strength values corresponding to 0.2% plastic strain, 2.0% total strain and the ultimate tensile strength are shown in Figure 34. It can be seen that the strength starts to degrade rapidly as the temperature approaches T = 800°C.

Figures 35 and 36 compare the strength reduction factors obtained using the isothermal and the transient test methods. There is a good agreement between the two sets of reduction factors. The transient method gave slightly lower reduction factor values below T = 700°C. Above this limit, i.e., in the steady state creep domain, the transient test method gave slightly higher values for the reduction factors.

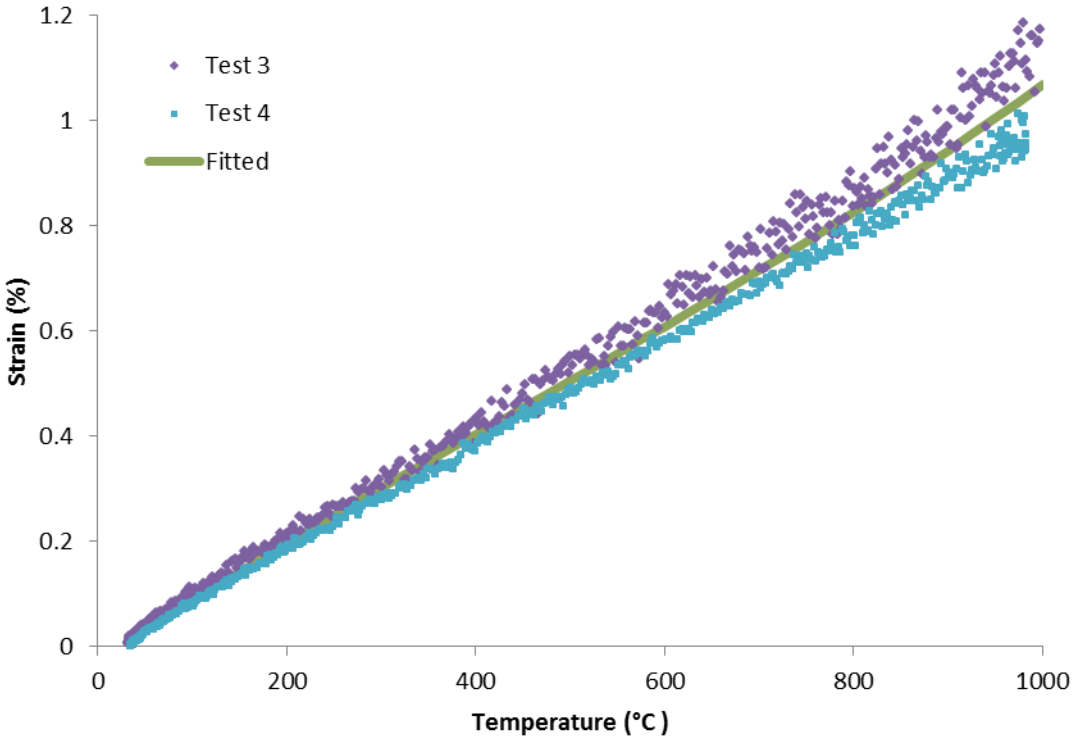

Figure 31. Measured parasitic strain for the steel 4521-3.

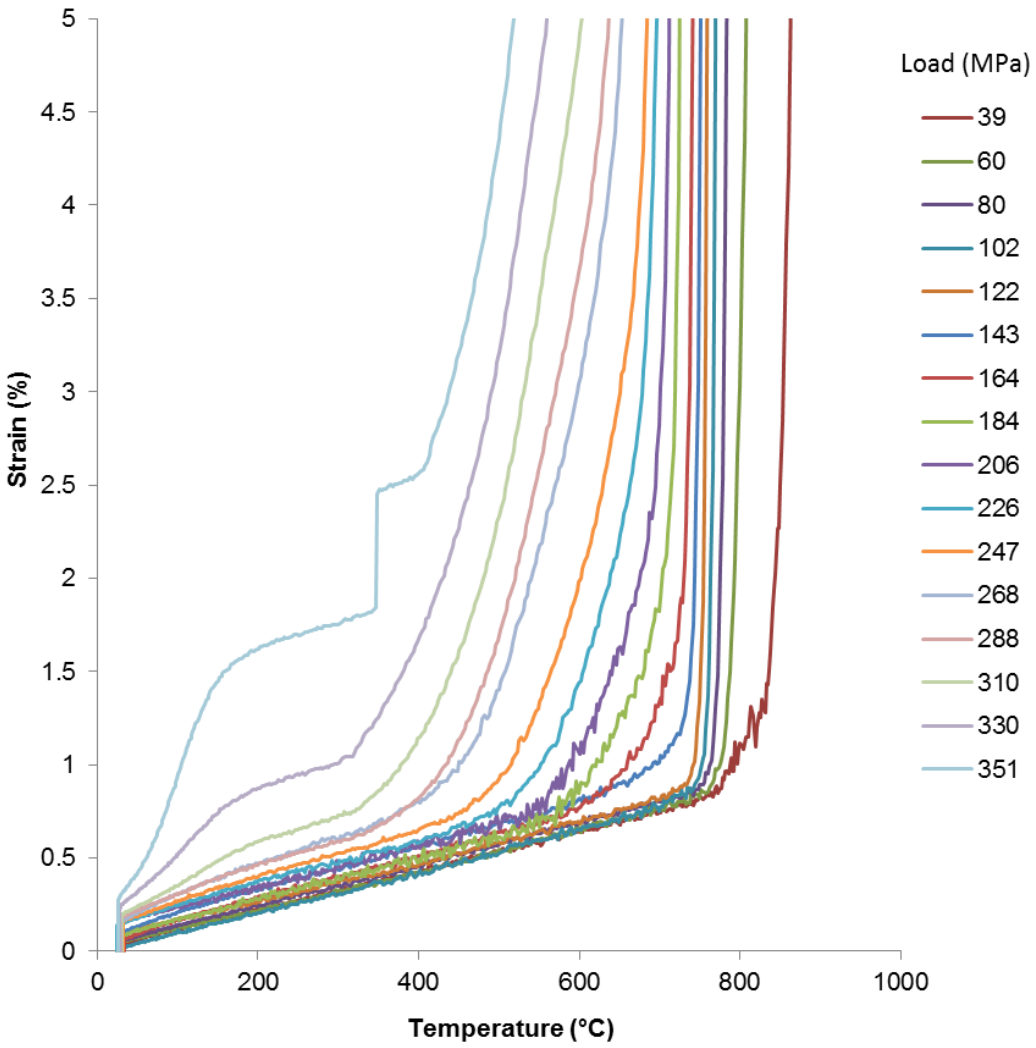

Figure 32. The transient test results for 4521-3. The strain includes the thermal expansion. The room-temperature 0.2% proof stress value is Rp0.2 = 391 MPa for the steel 4521-3.

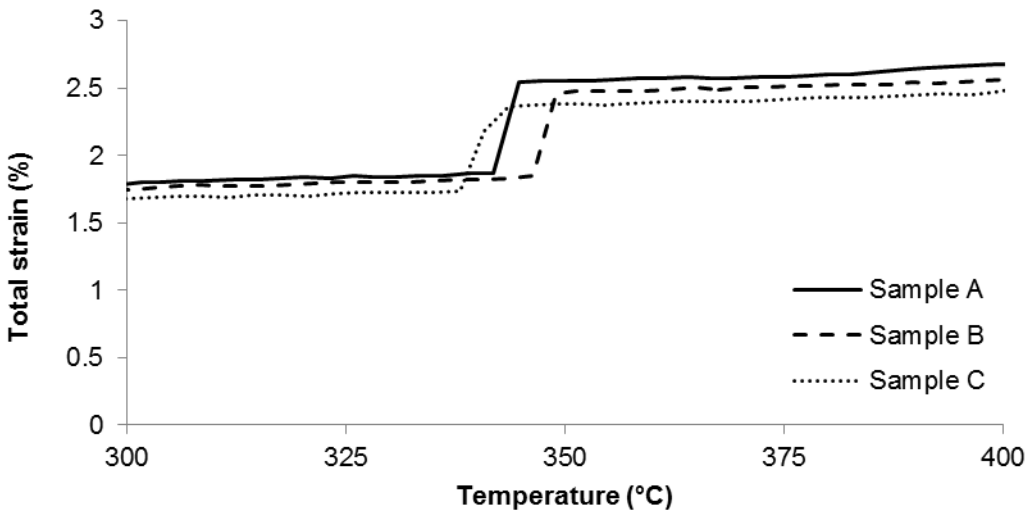

Figure 33. Three repeats with the load level of 351 MPa.

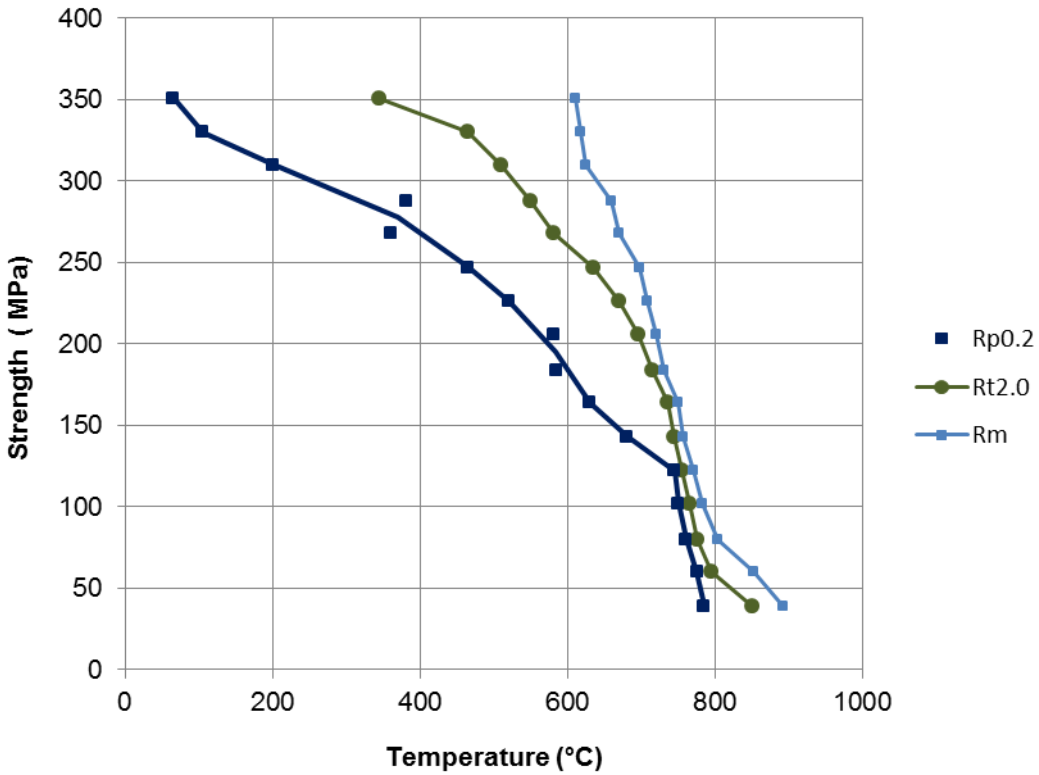

Figure 34. The stress values corresponding to 0.2% plastic strain, 2% total strain and the ultimate tensile strength obtained for the steel 4521-3 using the transient test method.

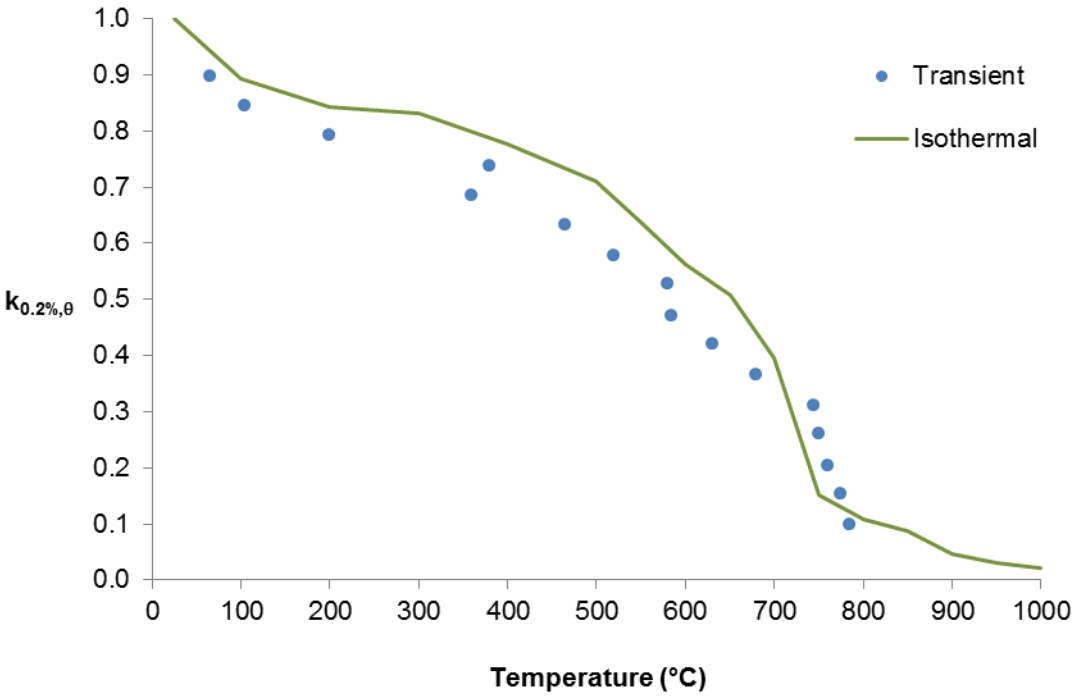

Figure 35. Reduction factor corresponding to the 0.2% proof stress obtained for two similar steels 4521-2 and 4521-3 using the isothermal and the transient test method.

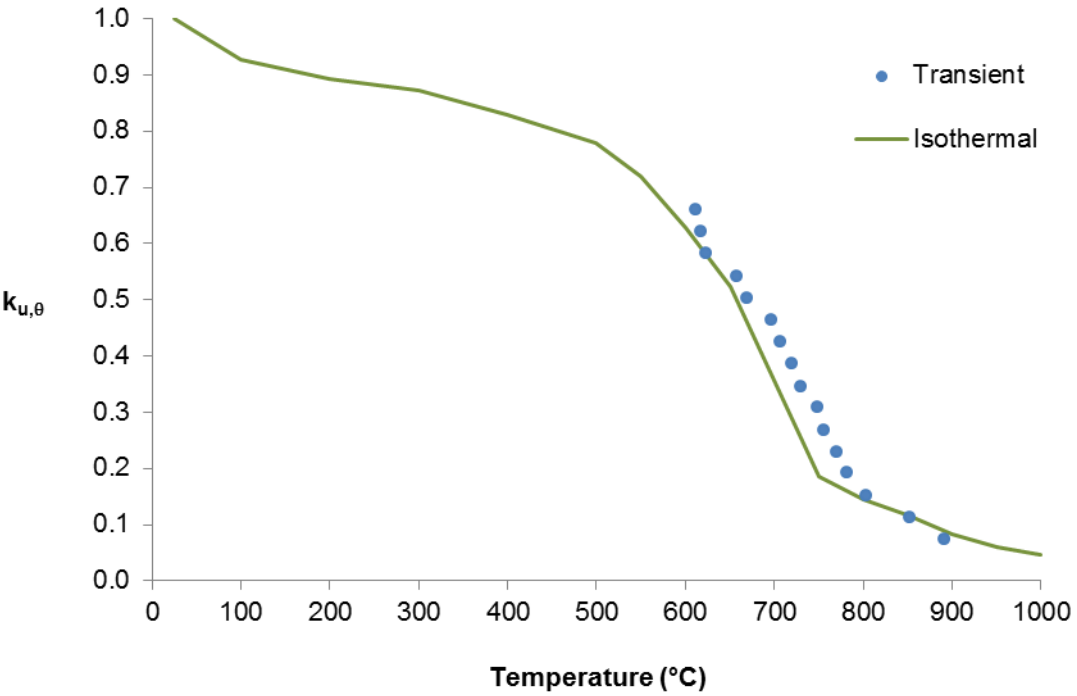

Figure 36. Reduction factor corresponding to the ultimate tensile strength obtained for two similar steels 4521-2 and 4521-3 using the isothermal and the transient test method.

5 Discussion

The experimental results suggest that the investigated ferritic stainless steels grades can be divided in two groups with similar characteristics in each group. The first group contains the unstabilized grades 1.4003 and 1.4016. The second group contains the stabilized grades 1.4509, 1.4521 and 1.4621.

Three design curves are needed for fire design of stainless steel structures:

- Reduction factor for the 0.2% proof strength $k_{0.2,\theta}$.
- Reduction factor for the ultimate tensile strength $k_{u,\theta}$.
- Factor $k_{2\%,\theta.}$ which determines the elevated temperature strength at 2% total strain by means of the 0.2% proof strength and the ultimate tensile strength.

The factor $k_{2\%,\theta}$ is formally defined by the equation

$$\sigma_{t2.0,\theta} = \sigma_{0.2,\theta} + k_{2\%.\theta}\left(\sigma_{u,\theta} - \sigma_{0.2,\theta}\right), \qquad (2)$$

where $\sigma_{0.2,\theta}$ is the 0.2% proof strength, $\sigma_{0.2,\theta}$ is the strength at 2% total strain and $\sigma_{u,\theta}$ is the ultimate tensile strength.

The reduction factors obtained for the first group steels, the unstabilized ferritic grades 1.4003 and 1.4016, are summarized in Figures 37, 38 and 39. The values provided in EN 1993-1-2 for the grade 1.4003 are shown for comparison. It can observed that there is a small difference between the present experimental values and the design values of EN 1993-1-2 between the room temperature and T = 300°C. This discrepancy is most likely caused by industrial dispersion in the steels and by differences in the testing procedures.

One important factor influencing the yield strength in isothermal testing is the soaking time, i.e. the time, which the specimen is maintained in the testing temperature before loading. In the present work, the soaking time of 10 minutes was used. Soaking times between 10 to 30 minutes are commonly used. Since unstabilized ferritic stainless steels are susceptible to static strain aging [**15**], the yield strength of the steel may increase during the soaking period. The increase of strength is caused by diffusion of interstitial atoms to dislocations. Hence, the strength of the material increases with soaking time and with temperature.

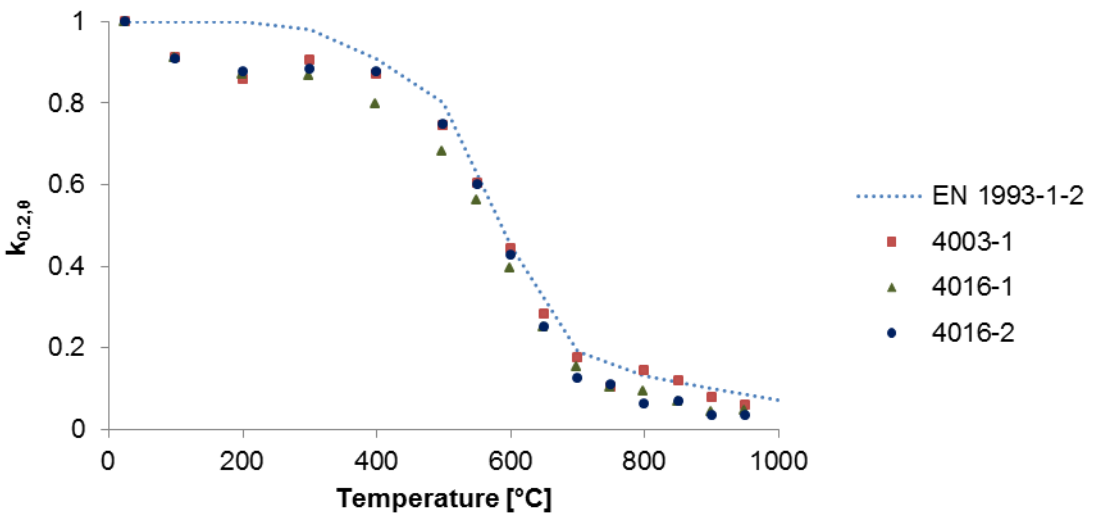

Figure 37. Strength reduction factors $k_{0.2,\theta}$ measured in the present work for unstabilized grades 1.4003 and 1.4016 and the values provided by EN 1993-1-2 for 1.4003.

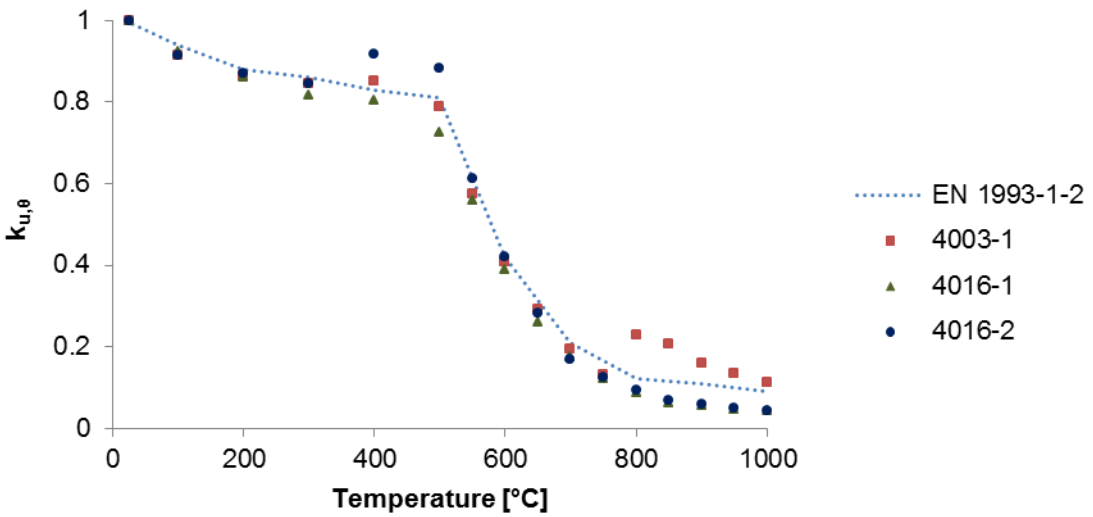

Figure 38. Strength reduction factors $k_{u,\theta}$ measured in the present work for unstabilized grades 1.4003 and 1.4016 and the values provided by EN 1993-1-2 for 1.4003.

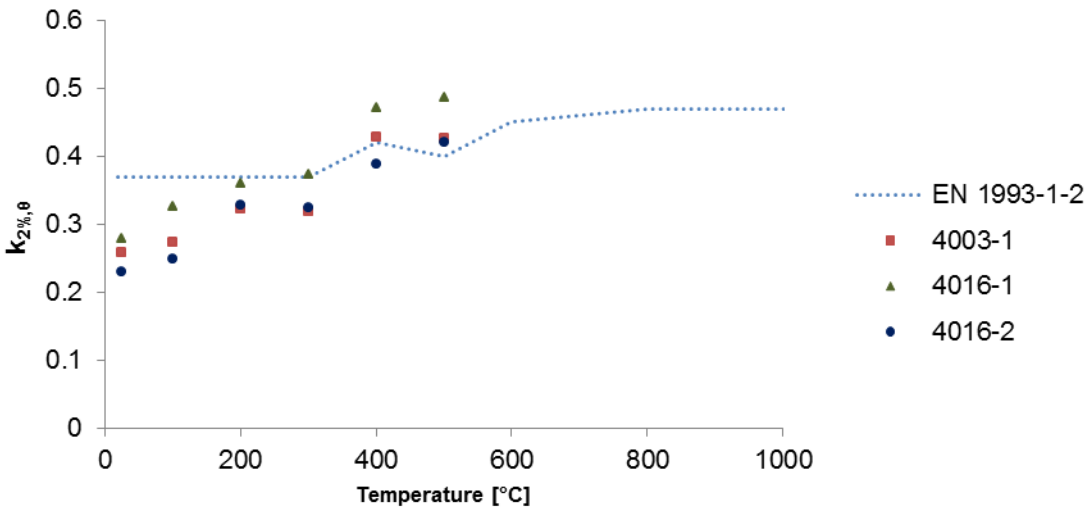

Figure 39. Factor $k_{2\%,\theta}$ measured in the present work for unstabilized steel grades 1.4003 and 1.4016 and the values provided by EN 1993-1-2 for 1.4003.

The reduction factors obtained for the second group of materials, the stabilized grades 1.4509, 1.4521 and 1.4621, are summarized in Figures 40 and 41. It can be seen that the dispersion between different grades and different steel producers is small. Figures 42 and 43 show the values of factor $k_{2\%,\theta}$ determined in the present work for the stabilized grades. The $k_{2\%,\theta}$ factors obtained for the stabilized grades follow a similar trend as the ones derived for the unstabilized grades, Figure 39.

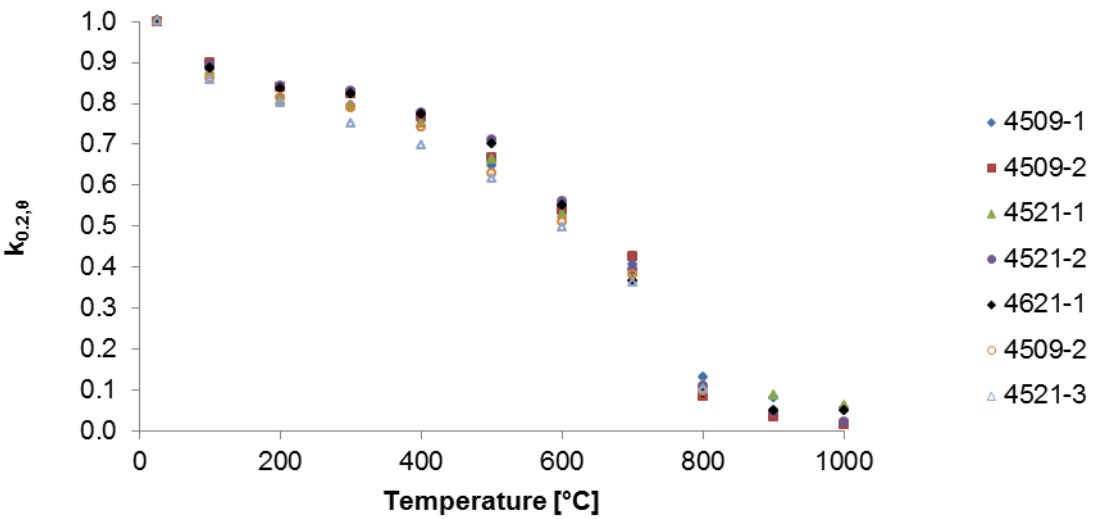

Figure 40. Strength reduction factors $k_{0.2,\theta}$ obtained in the present work for the stabilized grades. The steady state test results are marked with filled symbols.

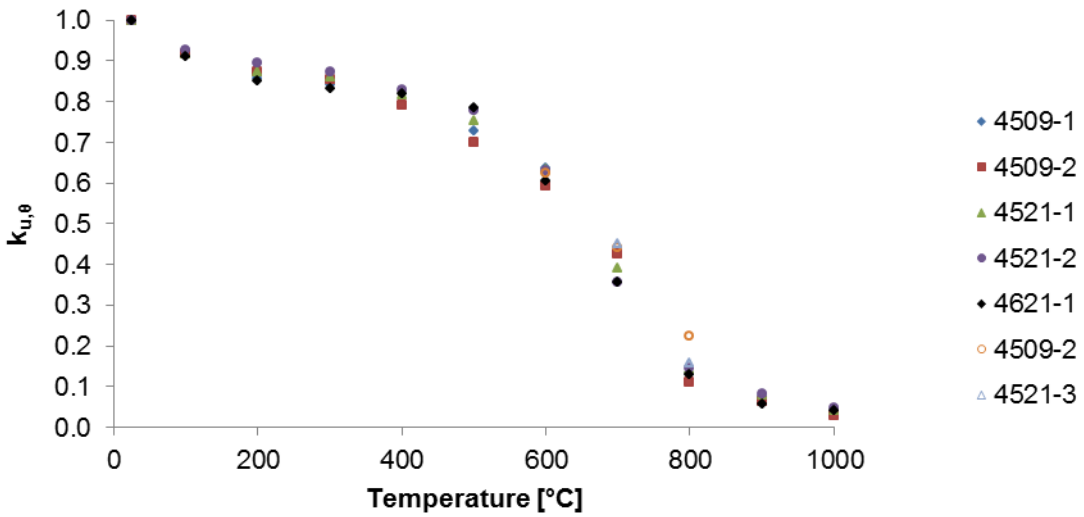

Figure 41. Strength reduction factors $k_{u,\theta}$ obtained in the present work for the stabilized grades. The steady state test results are marked with filled symbols.

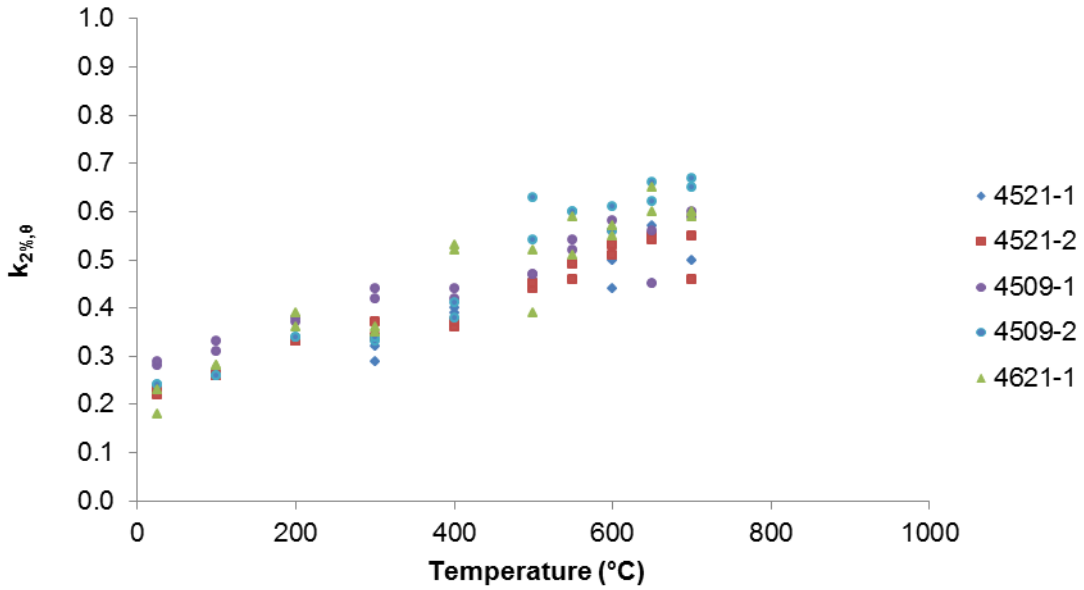

Figure 42. The factor $k_{2\%,\theta}$ for the stabilized grades obtained using the isothermal test method.

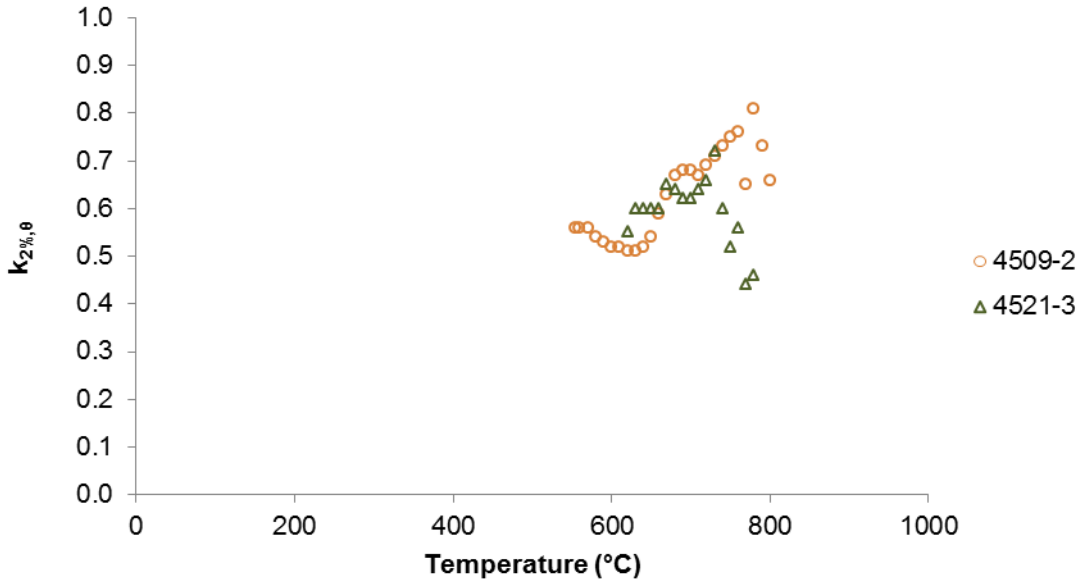

Figure 43. The factor $k_{2\%,\theta}$ for the stabilized grades obtained using the anisothermal test method.

6 Design parameters

The isothermal and anisothermal test results presented above have been used to derive fire design parameters for both groups of steels.

The fire design parameters proposed for the first group of materials, the unstabilized grades, are shown in Figures 44, 45 and 46. The proposed values were derived by averaging the steady state test results shown in the Figures 37, 38 and 39. The design values provided by EN 1995-1-2 for the grade 1.4003 are shown for reference. The difference between the current design values for 1.4003 and the values proposed here are insignificant. Therefore, the design values provided by EN 1995-1-2 for 1.4003 could be used for both unstabilized grades 1.4003 and 1.4016.

In the range 600°C ≤ T ≤ 1000°C, the unstabilized grades are deforming under steady state creep condition. In this stage, the material exhibits no strain hardening. Consequently, the stress strain curve becomes flat, and the factor $k_{2\%,\theta}$ becomes indeterminate. In the proposed design curve, the last value of factor $k_{2\%,\theta}$ obtained before the onset of steady state creep deformation has been extended to the higher temperatures.

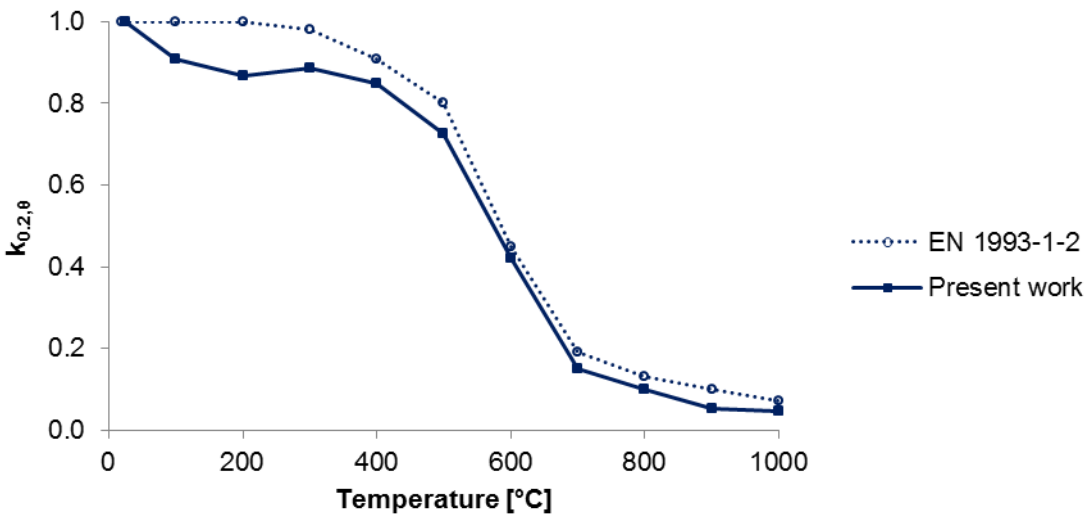

Figure 44. Proposed reduction factor $k_{0.2,\theta}$ for unstabilized ferritic stainless steels. The design curve provided by EN 1993-1-2 is shown for reference.

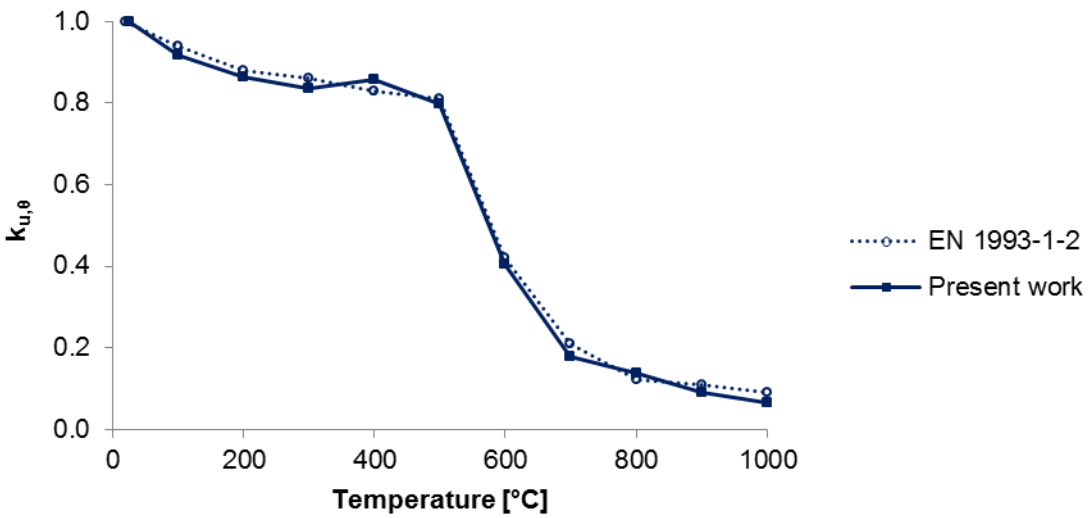

Figure 45. Proposed reduction factor $k_{u,\theta}$ for unstabilized ferritic stainless steels. The design curve provided by EN 1993-1-2 is shown for reference.

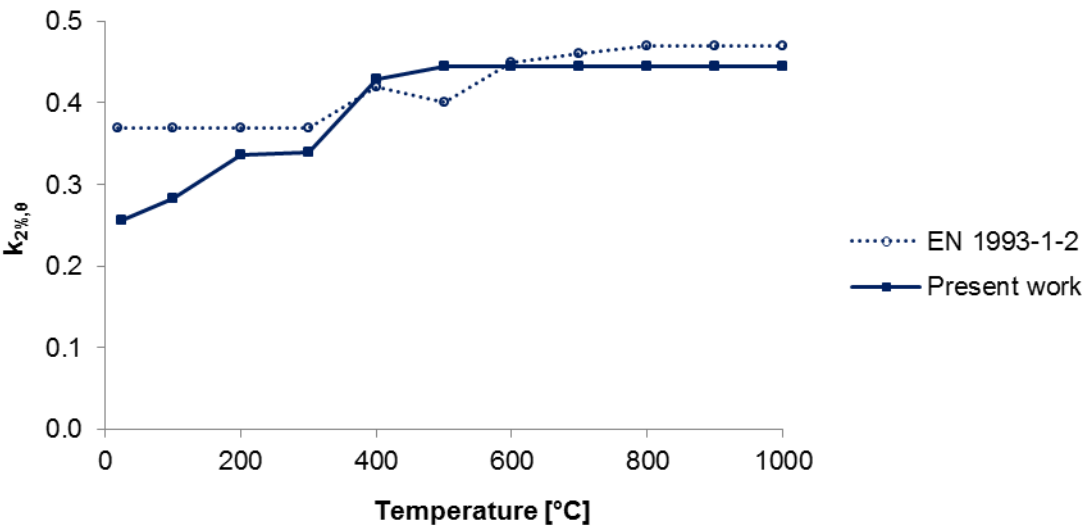

Figure 46. Proposed design factor $k_{2\%,\theta}$ for unstabilized ferritic stainless steels. The design curve provided by EN 1993-1-2 is shown for reference.

The fire design parameters for the second group of materials, the stabilized grades 1.4509, 1.4521 and 1.4621 were derived by combining the steady state and transient state test results. The average of transient test results was used when available. The steady state results were used to supplement the transient test results in the regions where the transient test results were not available. The derived values are shown in Figures 47, 48 and 49.

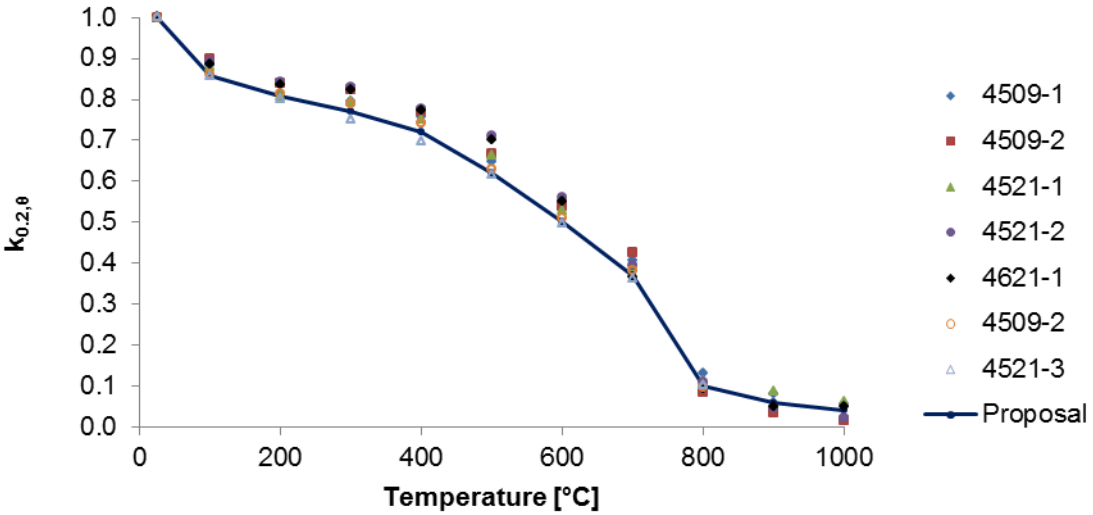

Figure 47. Proposed reduction factor $k_{0.2,\theta}$ for stabilized ferritic stainless steels. The experimental data is shown for reference. The steady state test results are marked with filled symbols.

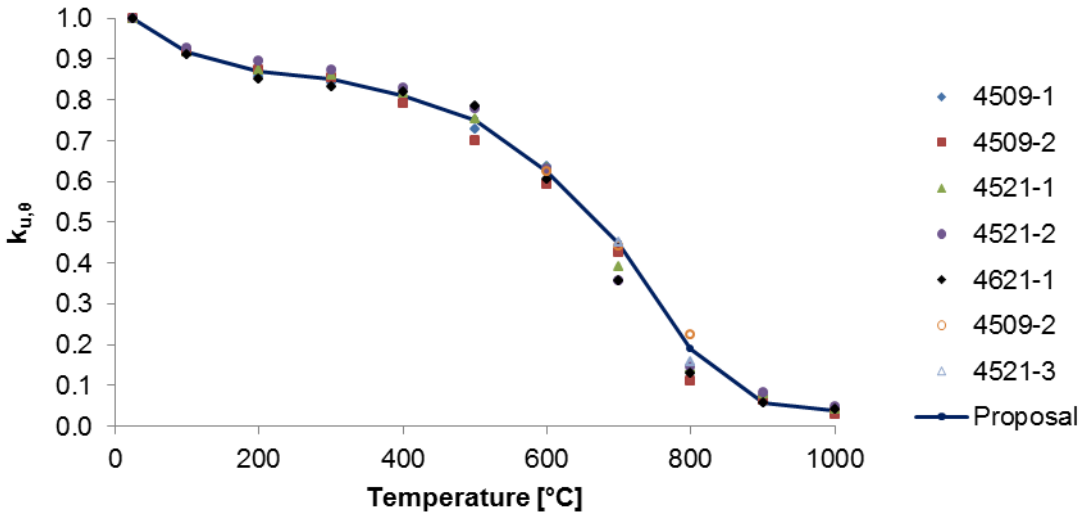

Figure 48. Proposed reduction factor $k_{u,\theta}$ for stabilized ferritic stainless steels. The experimental data is shown for reference. The steady state test results are marked with filled symbols.

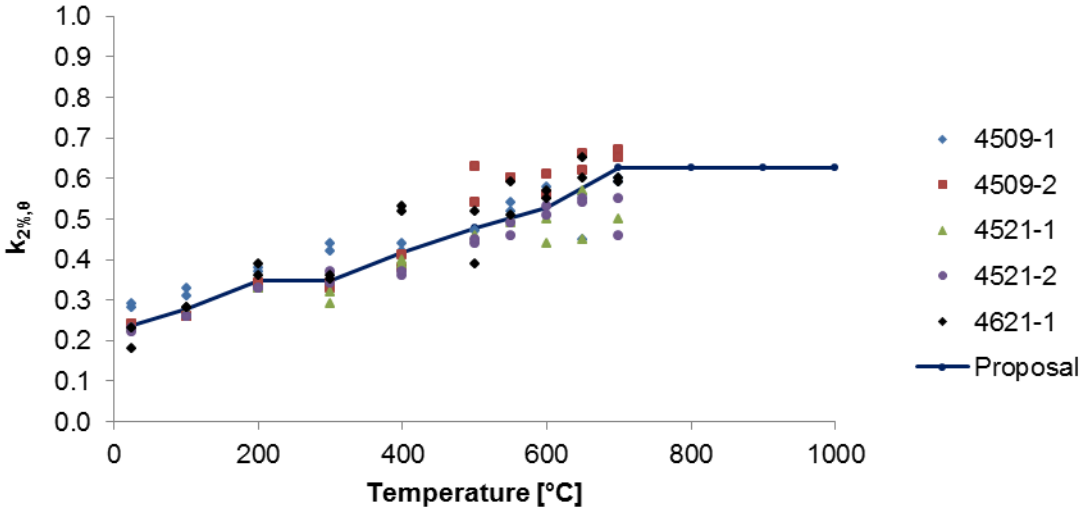

Figure 49. Proposed design factor $k_{2\%,\theta}$ for stabilized ferritic stainless steels. The experimental data obtained using the steady state test method is shown for reference.

The design parameters proposed in the present work for the two groups of ferritic stainless steels are summarized in Tables 6 and 7. As discussed above, the factor $k_{2\%,\theta}$ could not be reliably determined throughout the whole temperature range. The steady state test results were used up to the beginning of the steady state creep deformation. The transient test results, on the other hand, were used up to the point in which the 0.2% strength curve becomes almost vertical.

Table 6. Proposed fire design parameters for unstabilized ferritic grades.

Temperature (°C)	$k_{0.2,\theta}$	$k_{u,\theta}$	$k_{2\%,\theta}$
20	1.00	1.00	0.26
100	0.91	0.92	0.28
200	0.87	0.87	0.34
300	0.89	0.84	0.34
400	0.85	0.86	0.43
500	0.73	0.80	0.44
600	0.42	0.41	0.44
700	0.15	0.18	0.44
800	0.10	0.14	0.44
900	0.05	0.09	0.44
1000	0.05	0.07	0.44

Table 7. Proposed fire design parameters for the stabilized ferritic grades.

Temperature (°C)	$k_{0.2,\theta}$	$k_{u,\theta}$	$k_{2\%,\theta}$
20	1.00	1.00	0.24
100	0.86	0.92	0.28
200	0.81	0.87	0.35
300	0.77	0.85	0.35
400	0.72	0.81	0.42
500	0.62	0.75	0.48
600	0.50	0.62	0.53
700	0.37	0.45	0.63
800	0.10	0.19	0.63
900	0.06	0.06	0.63
1000	0.04	0.04	0.63

7 Conclusions

- An experimental research programme was carried out to investigate the mechanical properties of ferritic stainless steels at elevated temperature. Both isothermal (steady state) and anisothermal (transient state) tests were used for investigating the elevated temperature material behaviour. The test materials were cold-rolled sheet metals in annealed condition. Material from two European producers was used when available

- The experimental results show that the investigated ferritic stainless steels grades can be divided in two groups with similar characteristics in each group. The first group contains the unstabilized grades 1.4003 and 1.4016. The second group contains the stabilized grades 1.4509, 1.4521 and 1.4621. The experimental test results were used to derive fire design parameters for both groups.

- Elevated temperature elastic modulus values were determined using the isothermal stress-strain curves. The dispersion in the elastic modulus values obtained was large. No systematic trends could be observed between different steel grades. Consequently, one stiffness reduction factor was proposed for all studied grades.

- In the temperature range from 200°C to 400°C, the strength of unstabilized steels remained roughly constant despite of the increasing temperature. This behaviour can be attributed to dynamic strain aging, which is typical of materials with ferritic structure containing free interstitials. The increase of strength was associated with a slight decrease of ductility.

- In the range 600°C $\leq T \leq$ 1000°C, the unstabilized grades were deforming under steady state creep condition. In this stage, the material exhibits no strain hardening and the strength decreases rapidly with increasing temperature. The critical temperature for the onset of steady state creep deformation of stabilized grades was T = 750°C, i.e. 150°C higher than that of the unstabilized grades.

- The high temperature behaviour of stabilized grades 1.4509, 1.4521 and 1.4621 differs from that of the unstabilized grades. In stabilized grades, the free interstitial elements are bound to stable nitrides and carbides by the stabilizing elements such as Nb and Ti. The nitrides and carbides act as barriers to dislocation motion and inhibit grain boundary sliding and grain growth. This improves the elevated temperature strength and creep resistance of these alloys.

References

1 *EN 1993-1-2. Eurocode 3: Design of steel structuresPart 1.2: General rules - Structural fire design.* CEN, Brussels, 2005.

2 *EN 1993-1-4. Eurocode 3. Design of steel structures: Part 1.4: General rules - Supplementary rules for stainless steels*. CEN, Brussels, 2006.

3 Gardner, L. and Baddoo, N.R. Fire testing and design of stainless steel structures. *Journal of Constructional Steel Research*, 62 (2006), 532-543.

4 Chen, J. and Young, B. Stress–strain curves for stainless steel at elevated temperatures. *Engineering Structures*, 28 (2006), 229–239.

5 Gardner, L., Insausti, A., Ng, K.T., and Ashraf, M. Elevated temperature material properties of stainless steel alloys. *Journal of Constructional Steel Research*, 66 (2010), 634-647.

6 Baroux, B. The 17% Cr Ferritic Stainless Steels. In Lacombe, P. et al., eds., *Stainless Steels*. Les Editions de Physique Les Ulis, 1993.

7 Bishop, R.J. and Smallman, R.E. *Modern Physical Metallurgy*. Butterworth-Heinemann, Oxford, 1999.

8 Abbaschian, R., Abbaschian, L., and Reed-Hill, R.E. *Physical Metallurgy Principles*. Cengage Learning, Stamford, 2008.

9 Demo, J. J. Structure and Constitution of Wrought Ferritic Stainless Steels. In Peckner, I.M.Bernstein and D., ed., *Handbook of Stainless Steels*. McGraw-Hill, New York, 1977.

10 Pistorius, P.G.H. *The Transformation Kinetics of Austenite to Ferrite in Dual Phase 12% Chromium Steels*. University of Pretoria, 1992.

11 Lord, J.D. and Morrell, R. M. Elastic modulus measurement - obtaining reliable data from the tensile test. *Metrologia*, 47 (2010), S41–S49.

12 AK STEEL. *Product Data Bulletin for 11Cr-Cb Stainless Steel*. West Chester, 2007.

13 OUTOKUMPU. *Outokumpu Ferritic Stainless Steel Grades*. Avesta, 2012.

14 Roebben, G., Bollen, B., Brebels, Van Humbeeck J., and Van der Biest, O. Impulse excitation apparatus to measure resonant frequencies, elastic moduli, and internal friction at room and high temperature. *Review of Scientific Instruments*, 68 (1997), 4511–4515.

15 Buono, V.T.M., Gonzales, B.M., and Andrade, M.S. Strain aging of AISI 430 ferritic stainless steel. *Scripta Materialia*, 38 (1998), 185-190.

Appendices

A. Isothermal stress-strain curves for 4003-1.

B. Isothermal stress-strain curves for 4016-1 and 4016-2.

C. Isothermal stress-strain curves for 4509-1 and 4509-2.

D. Isothermal stress-strain curves for 4521-1 and 4521-2.

E. Isothermal stress-strain curves for 4621-1.

F. Summary of isothermal test results.

G. Factor $k_{2\%,\theta}$ determined using the steady state test results.

H. Transient state test results for 4509-2.

I. Transient state test results for 4521-3.

Isothermal stress-strain curves for the steel 4003-1

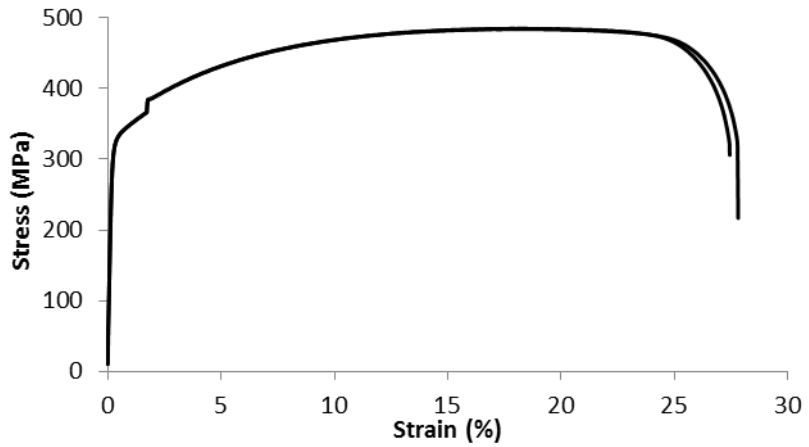

4003-1
T = 25°C

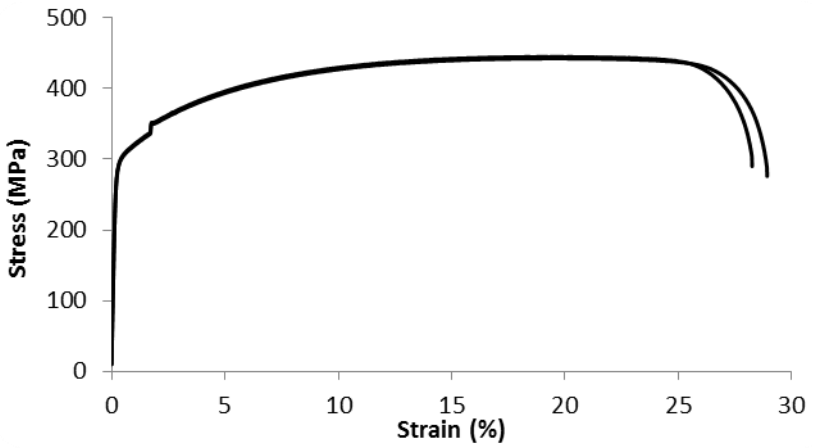

4003-1
T = 100°C

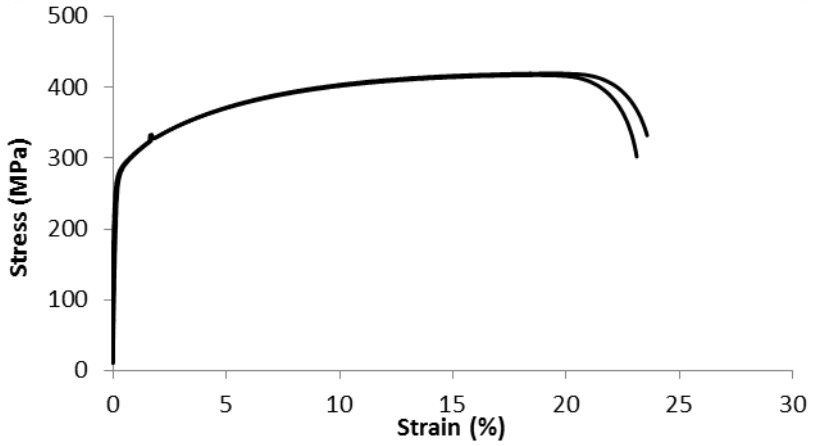

4003-1
T = 200°C

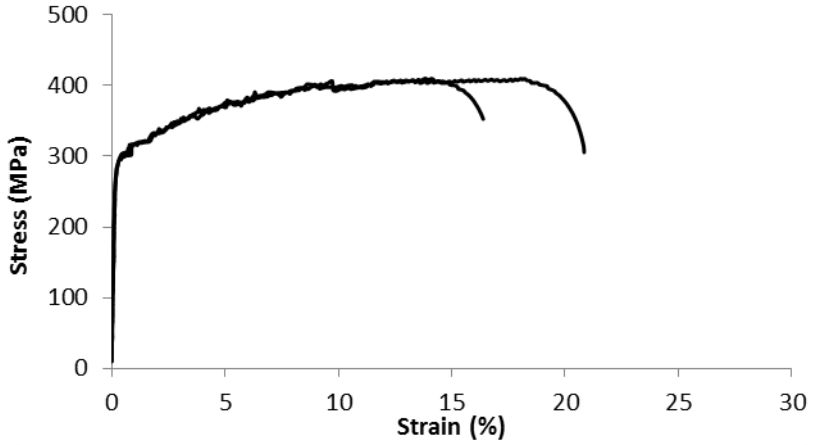

4003-1
T = 300°C

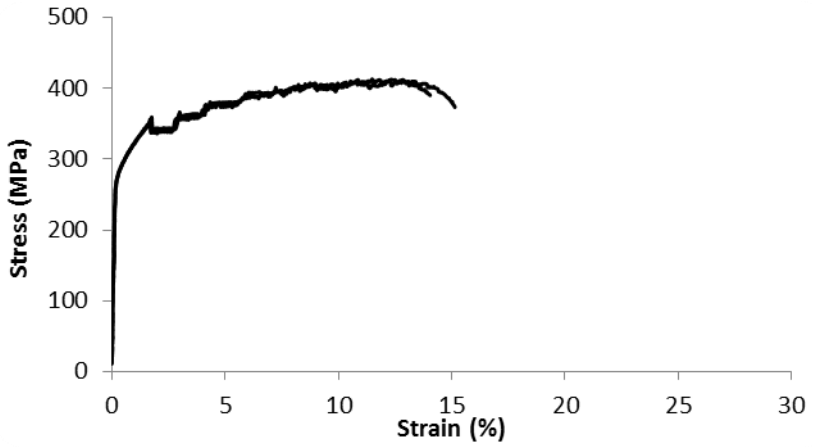

4003-1
T = 400°C

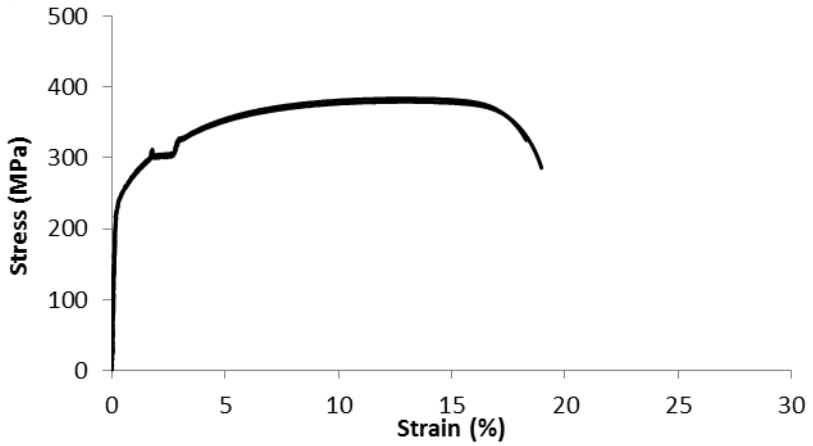

4003-1
T = 500°C

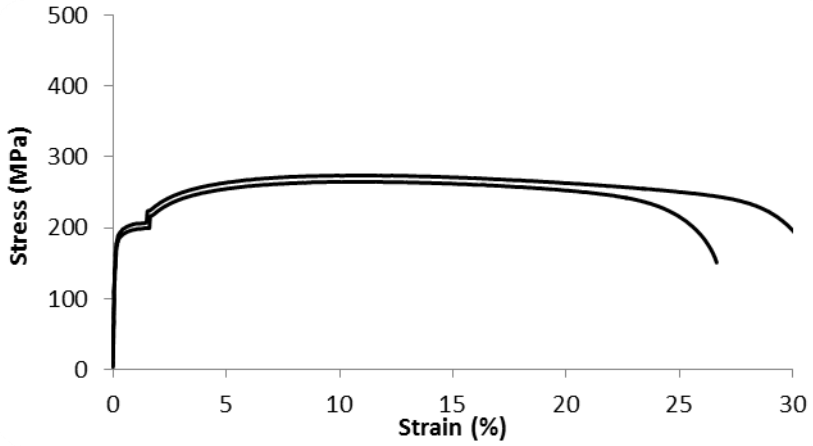

4003-1
T = 550°C

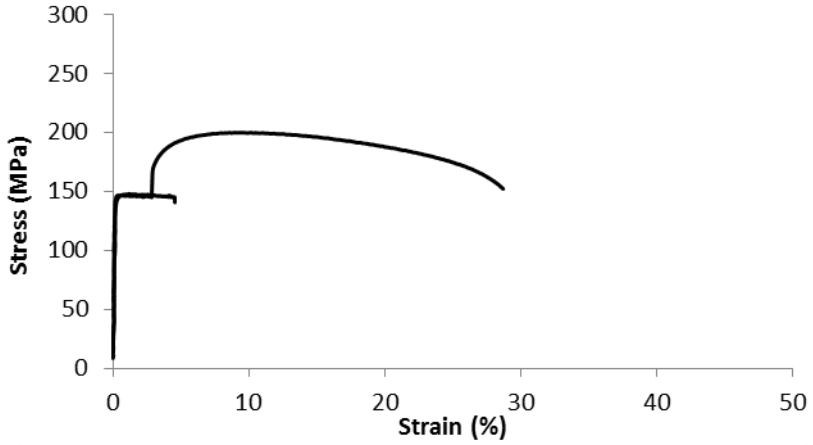

4003-1
T = 600°C

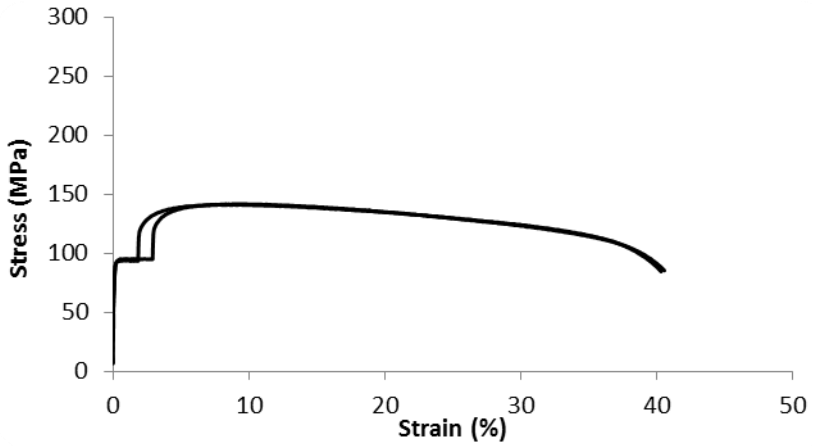

4003-1
T = 650°C

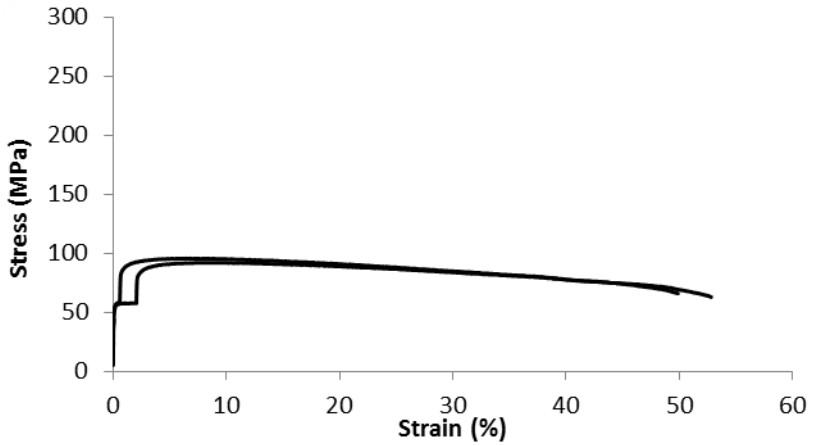

4003-1
T = 700°C

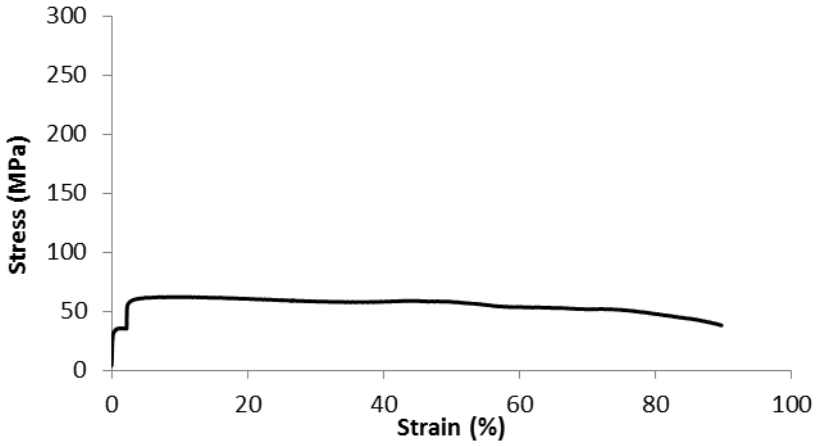

4003-1
T = 750°C

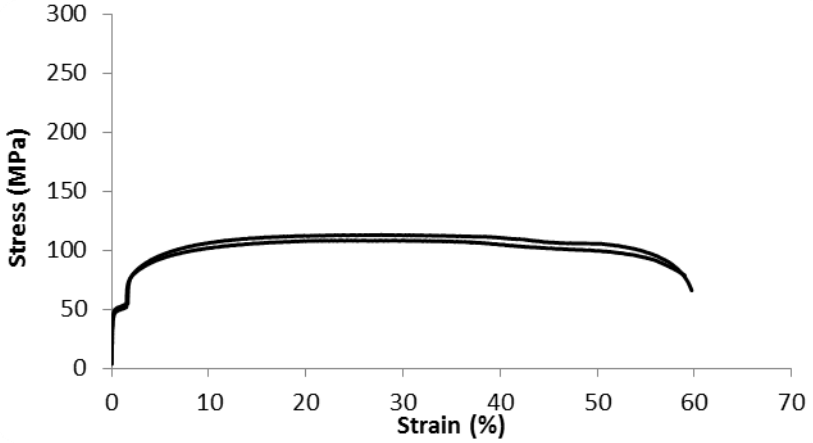

4003-1
T = 800°C

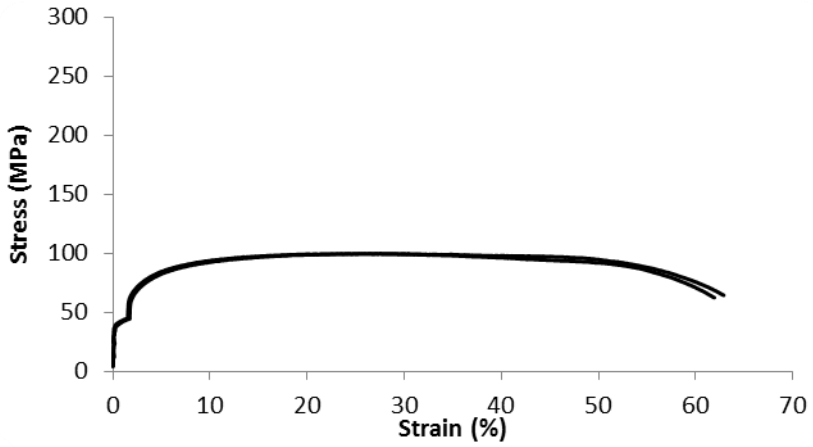

4003-1
T = 850°C

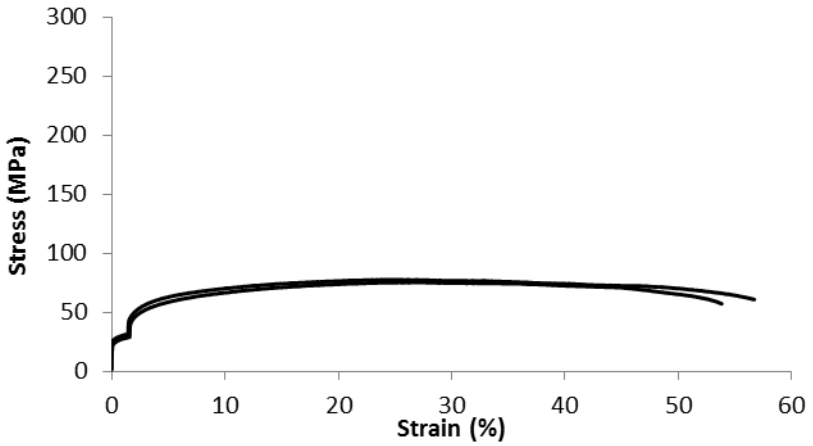

4003-1
T = 900°C

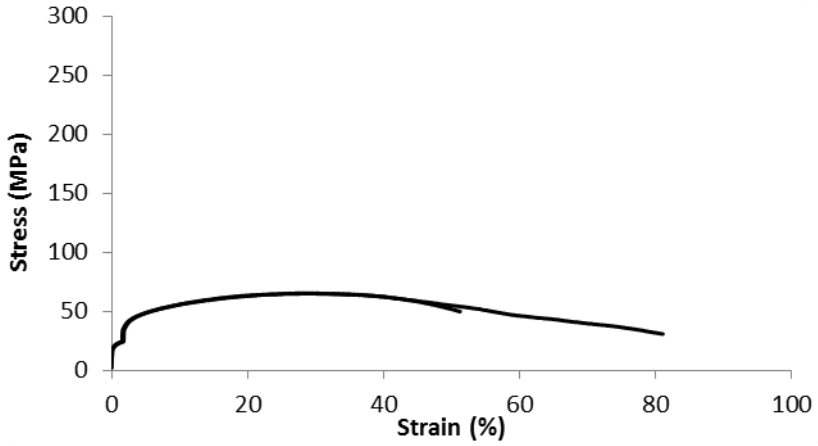

4003-1
T = 950°C

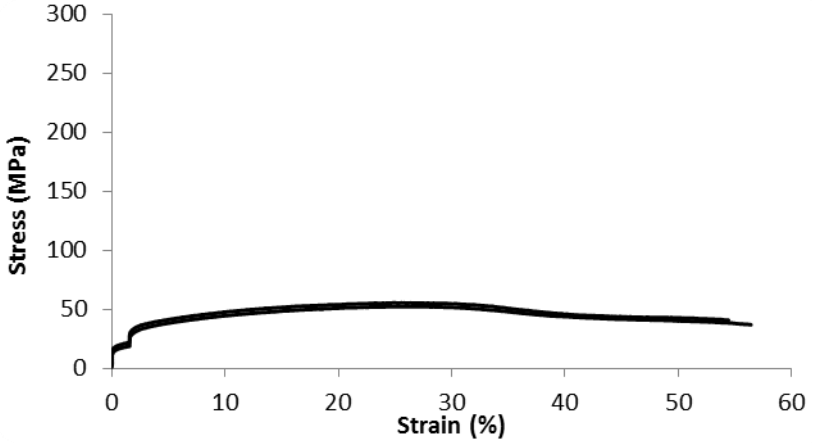

4003-1
T = 1000°C

Isothermal stress-strain curves for the steels 4016-1 and 4016-2.

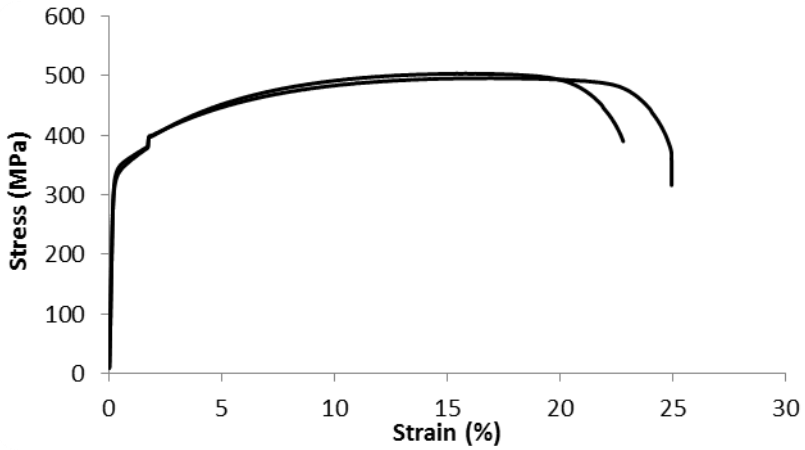

4016-1
T = 25°C

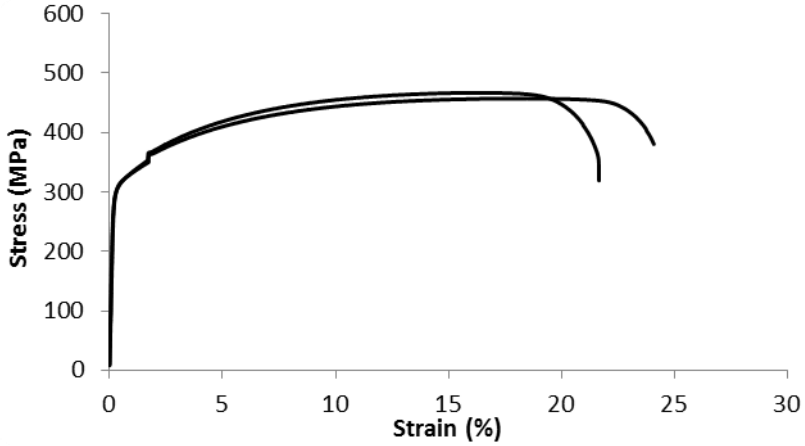

4016-1
T = 100°C

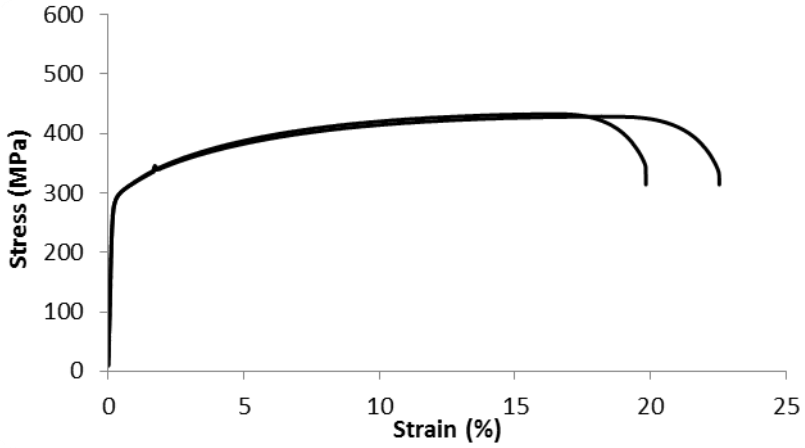

4016-1
T = 200°C

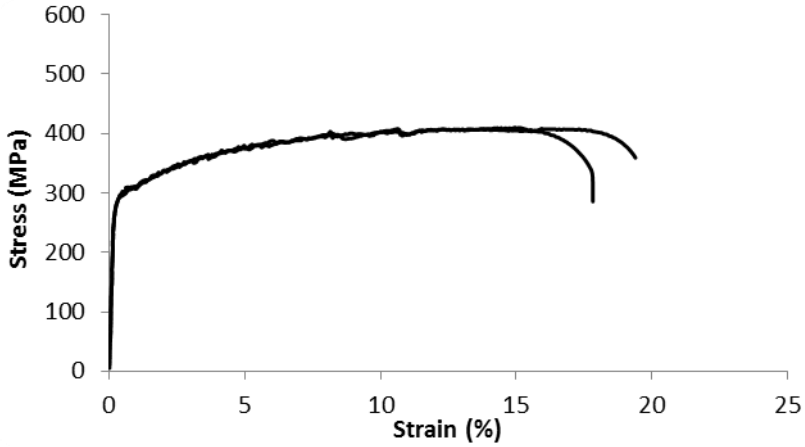

4016-1
T = 300°C

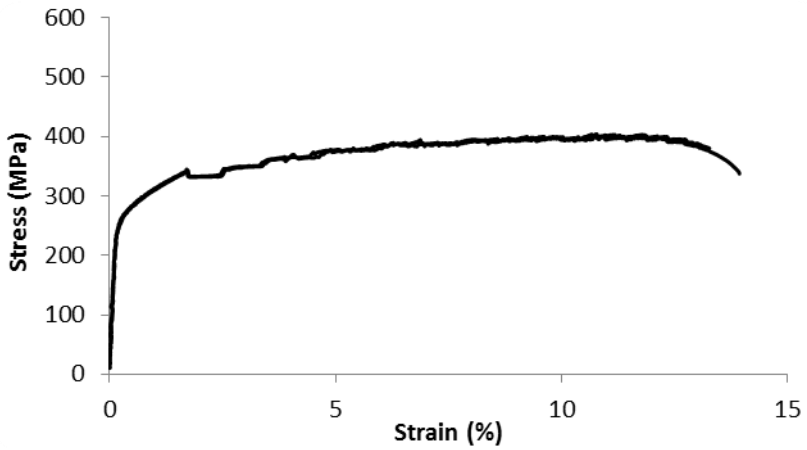

4016-1
T = 400°C

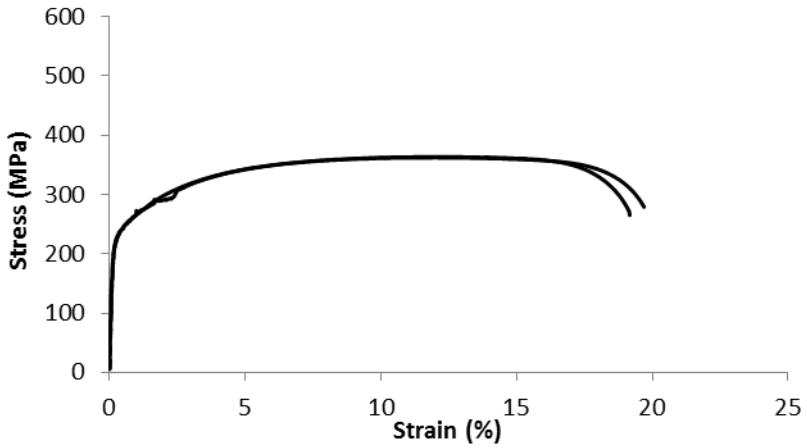

4016-1
T = 500°C

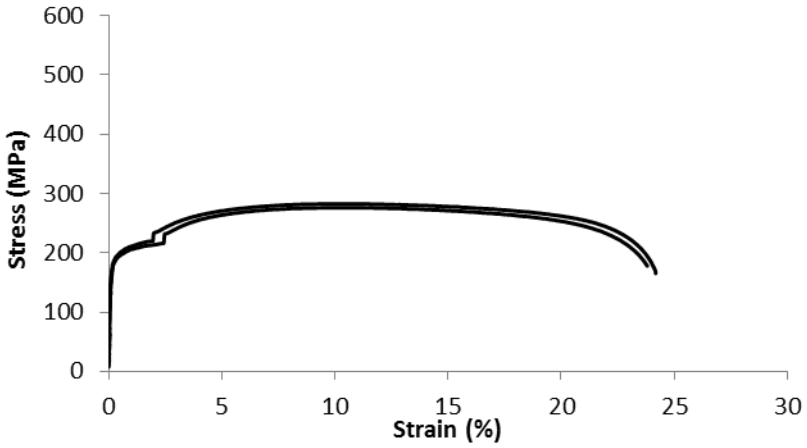

4016-1
T = 550°C

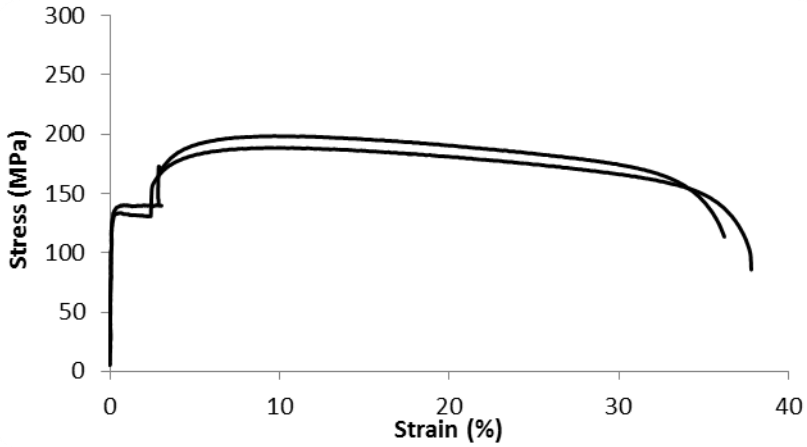

4016-1
T = 600°C

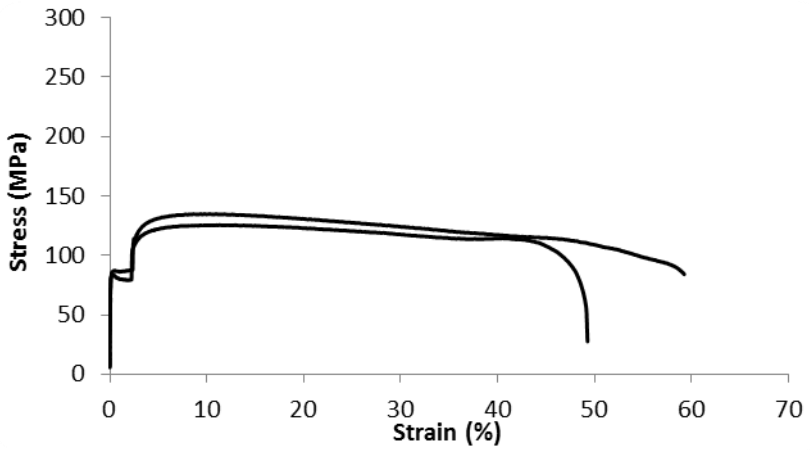

4016-1
T = 650°C

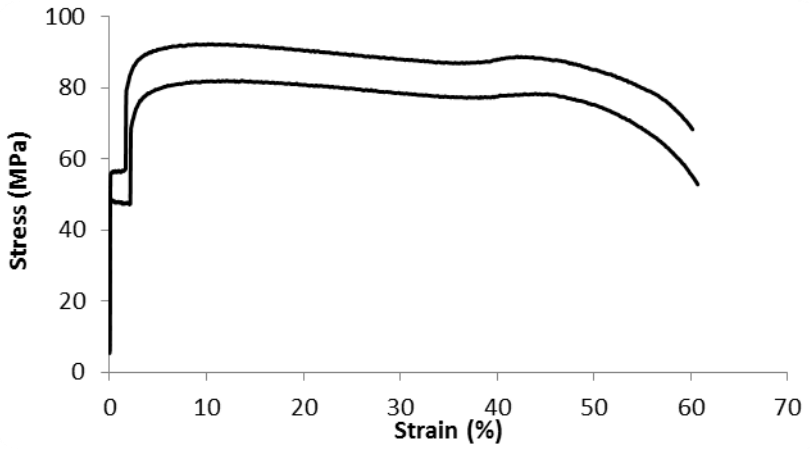

4016-1
T = 700°C

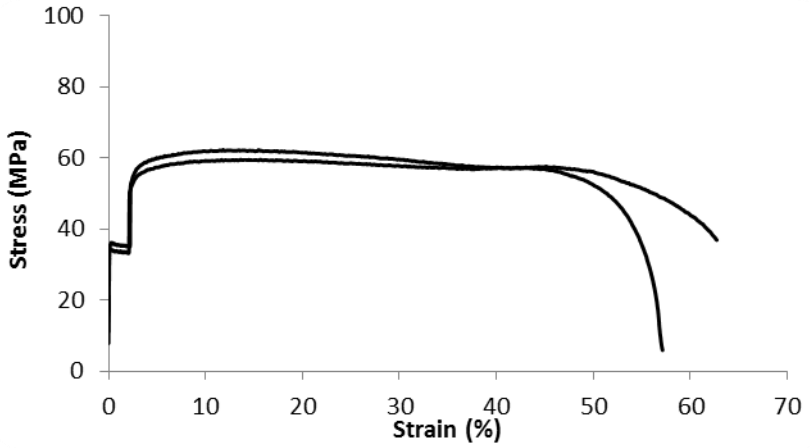

4016-1
T = 750°C

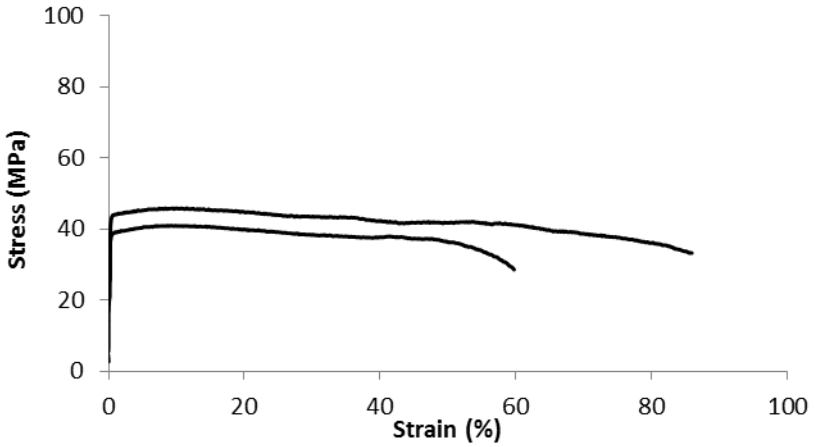

4016-1
T = 800°C

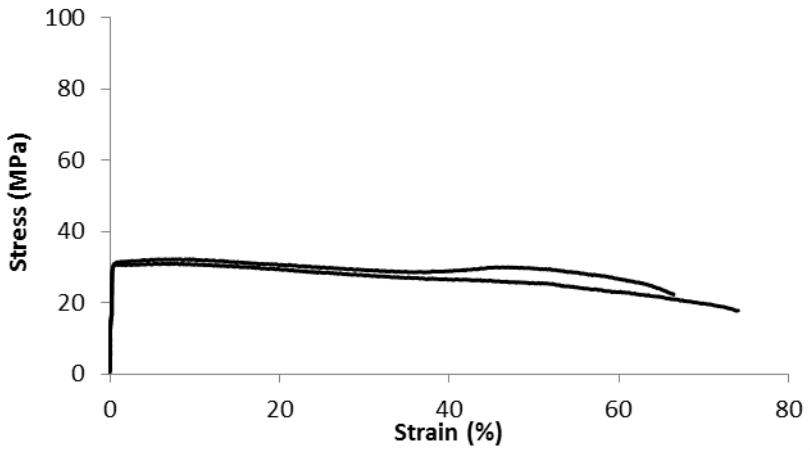

4016-1
T = 850°C

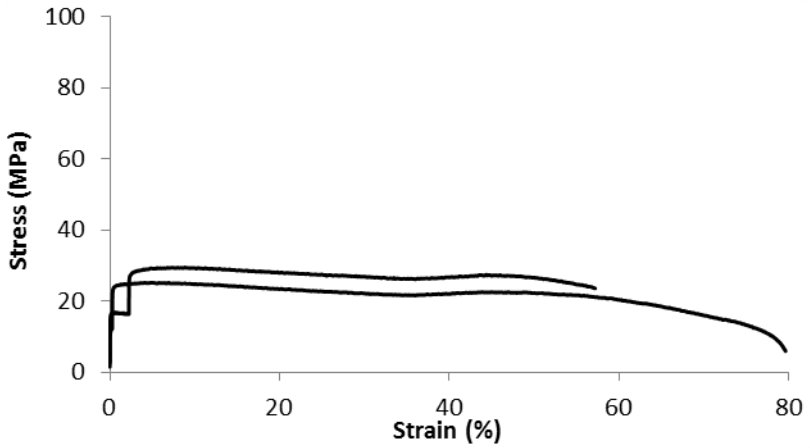

4016-1
T = 900°C

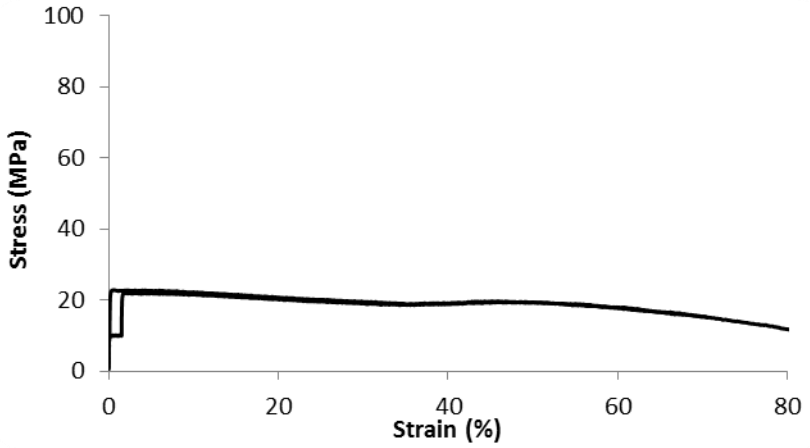

4016-1
T = 950°C

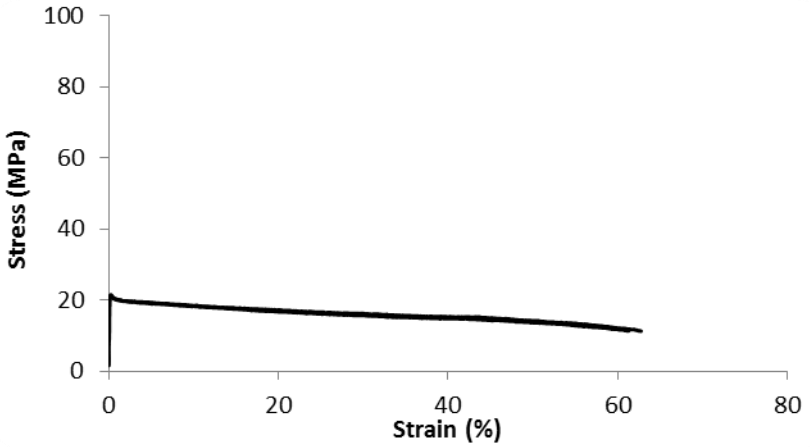

4016-1
T = 1000°C

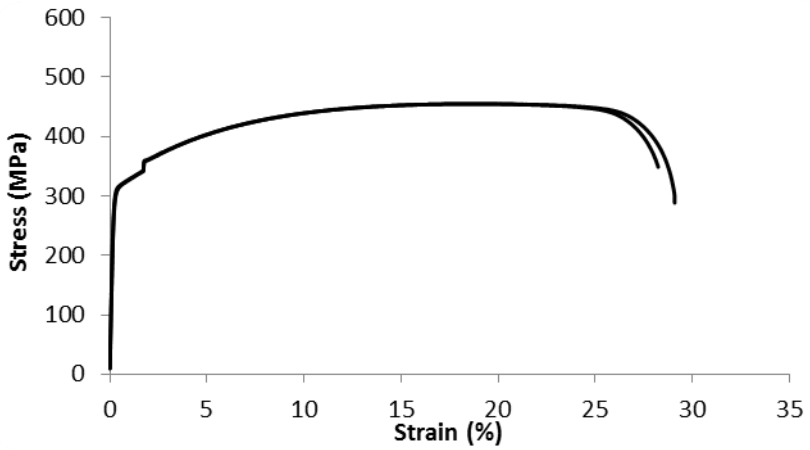

4016-2
T = 25°C

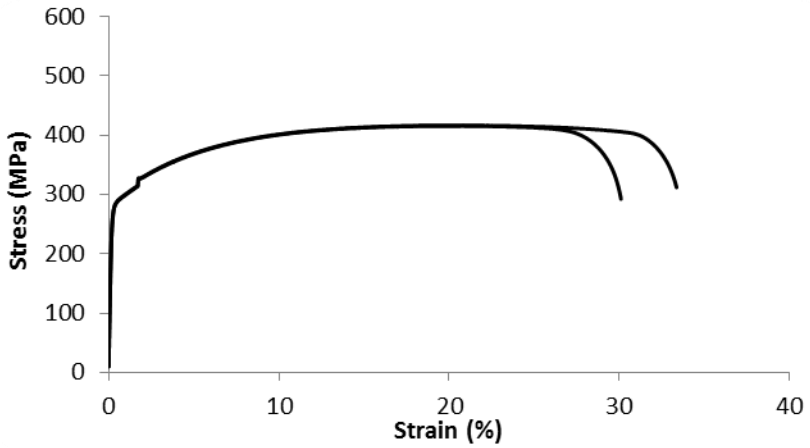

4016-2
T = 100°C

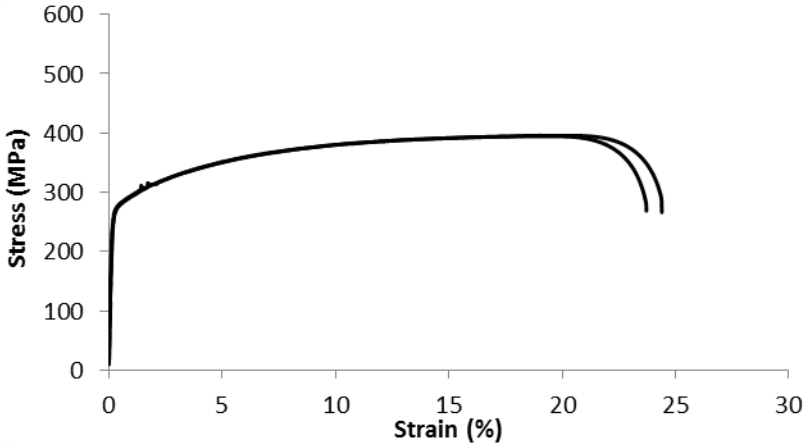

4016-2
T = 200°C

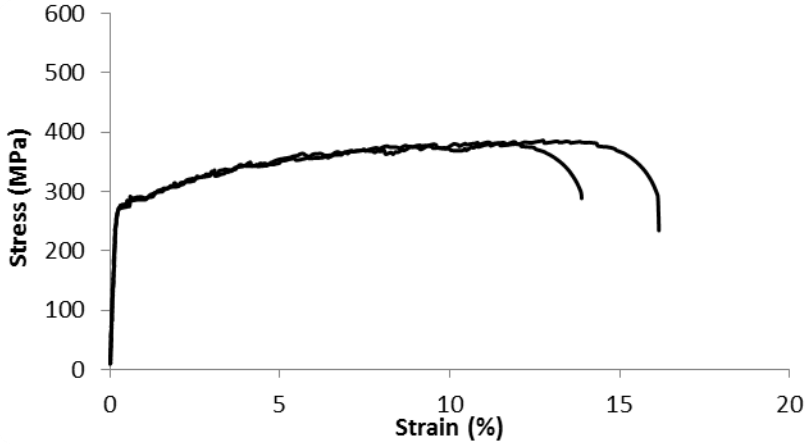

4016-2
T = 300°C

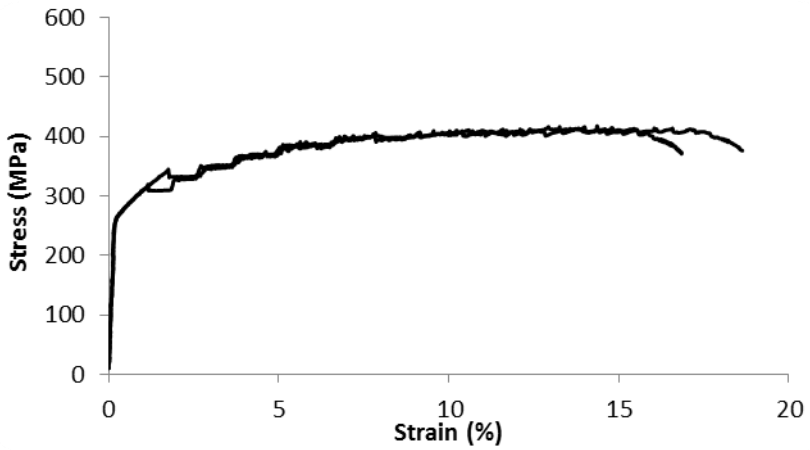

4016-2
T = 400°C

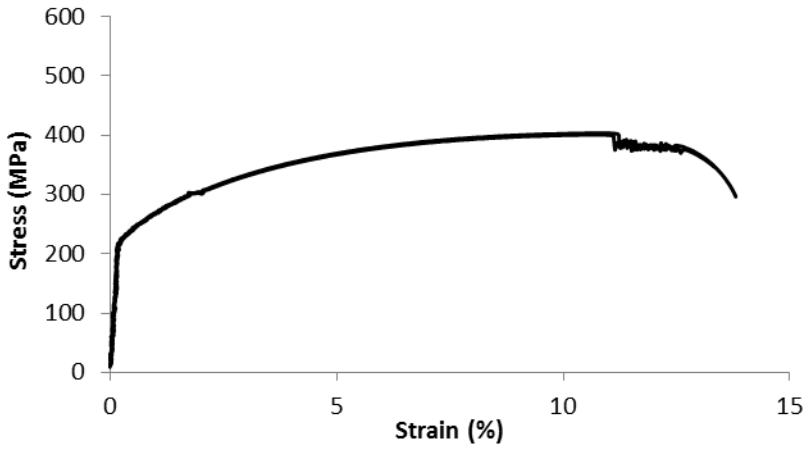

4016-2
T = 500°C

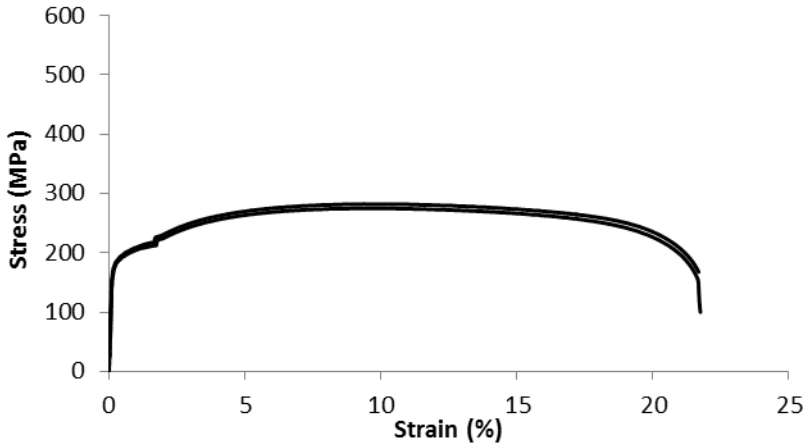

4016-2
T = 550°C

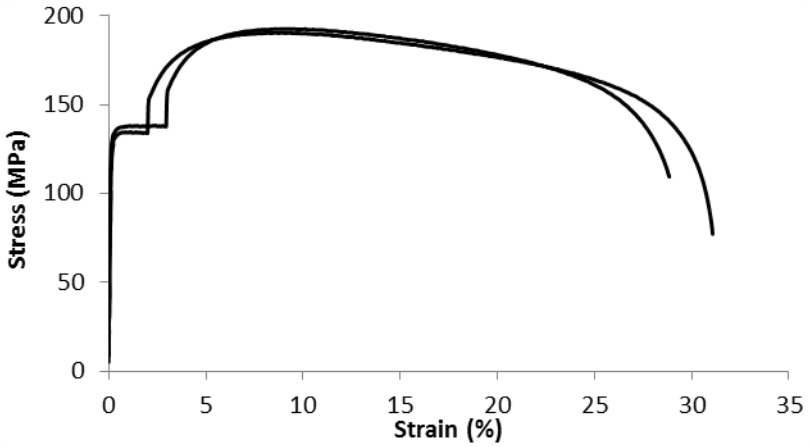

4016-2
T = 600°C

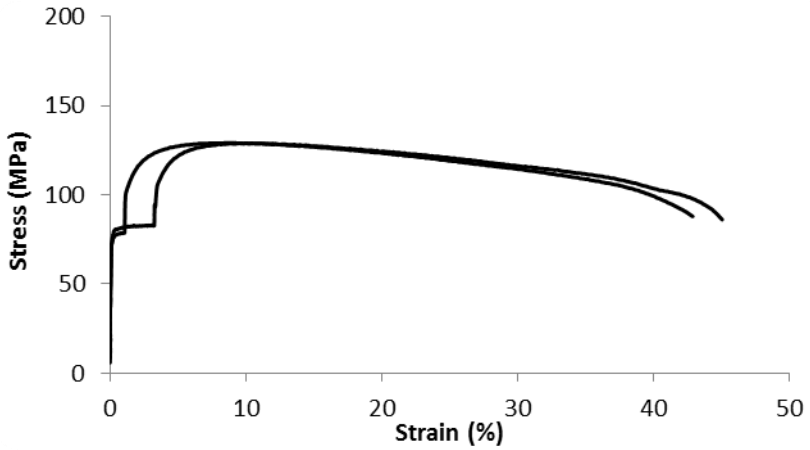

4016-2
T = 650°C

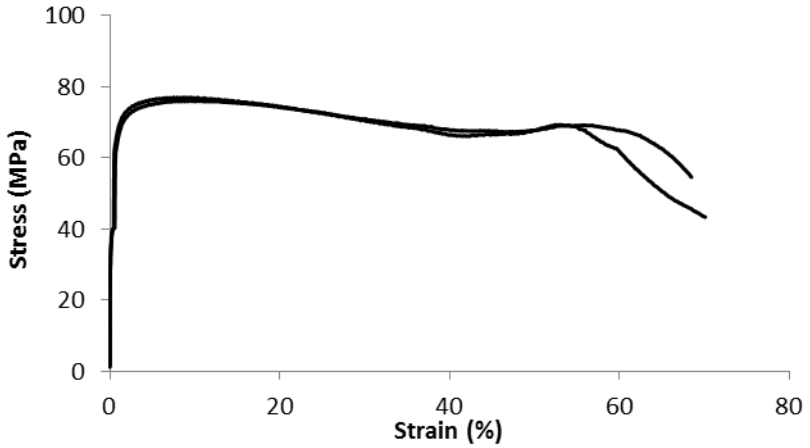

4016-2
T = 700°C

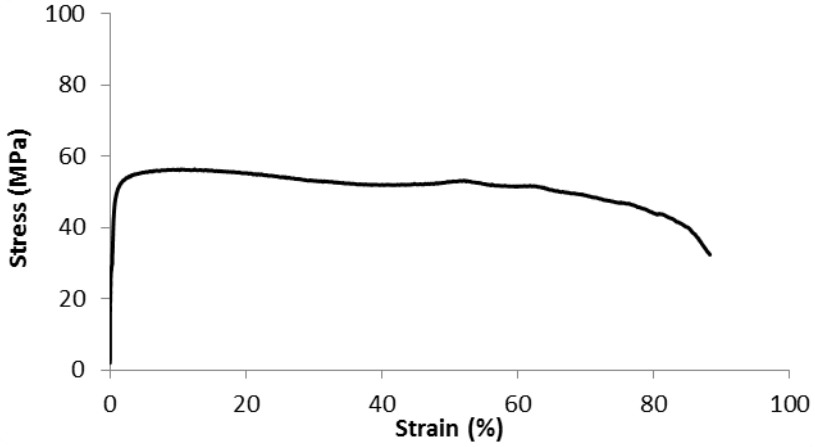

4016-2
T = 750°C

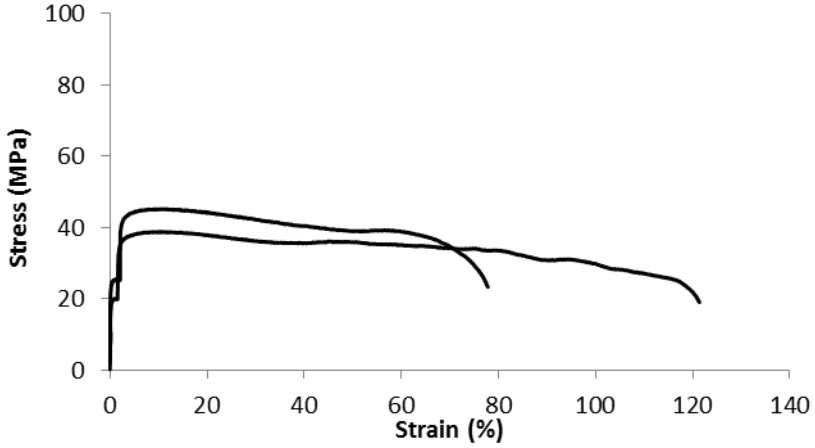

4016-2
T = 800°C

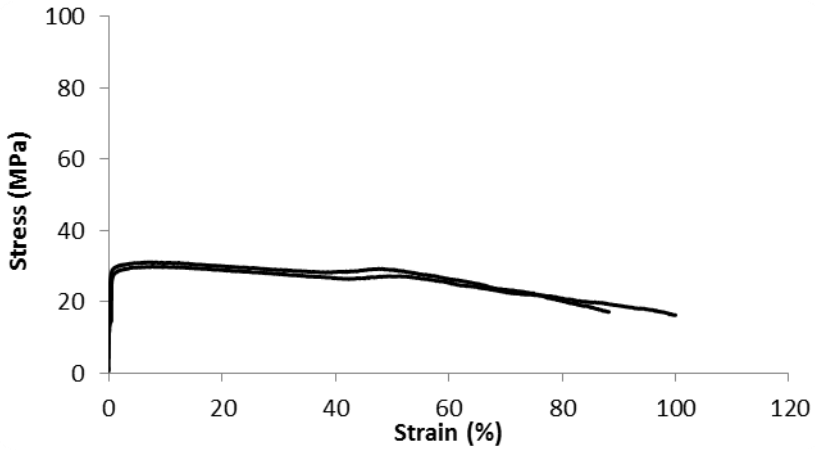

4016-2
T = 850°C

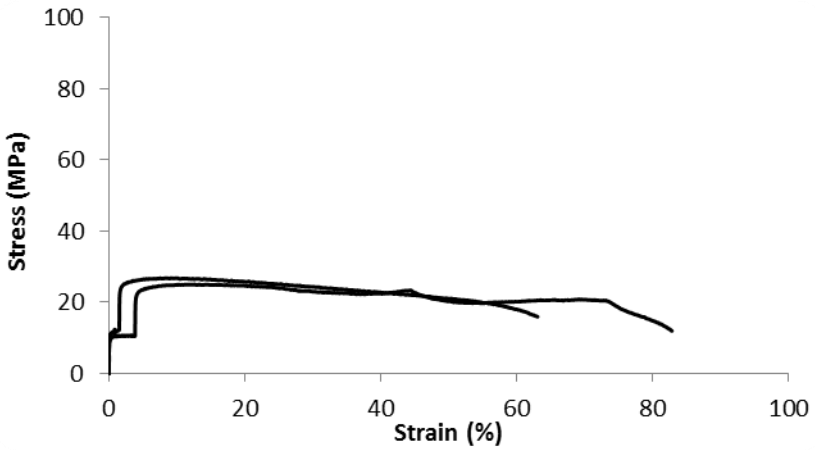

4016-2
T = 900°C

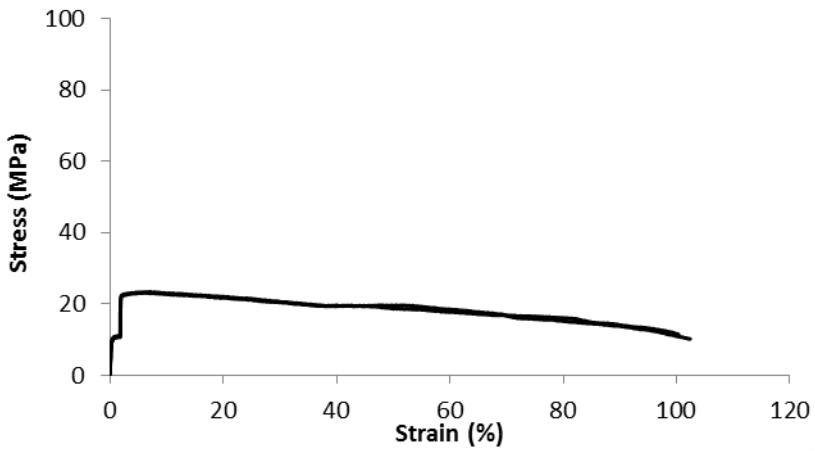

4016-2
T = 950°C

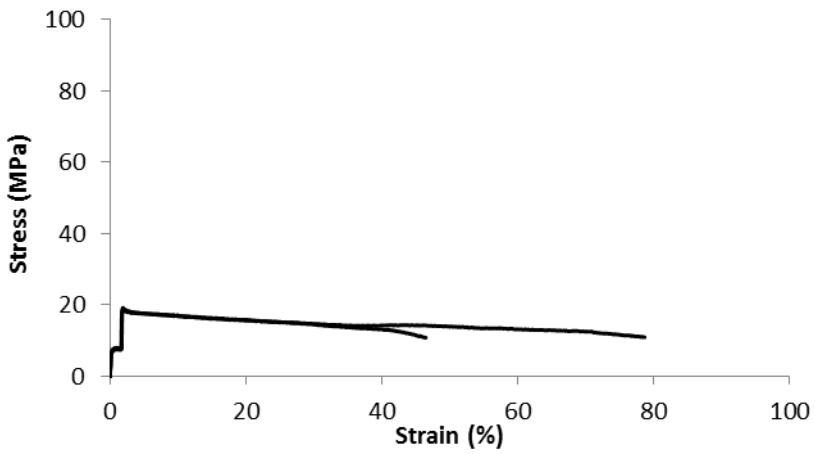

4016-2
T = 1000°C

Isothermal stress-strain curves for the steels 4509-1 and 4509-2.

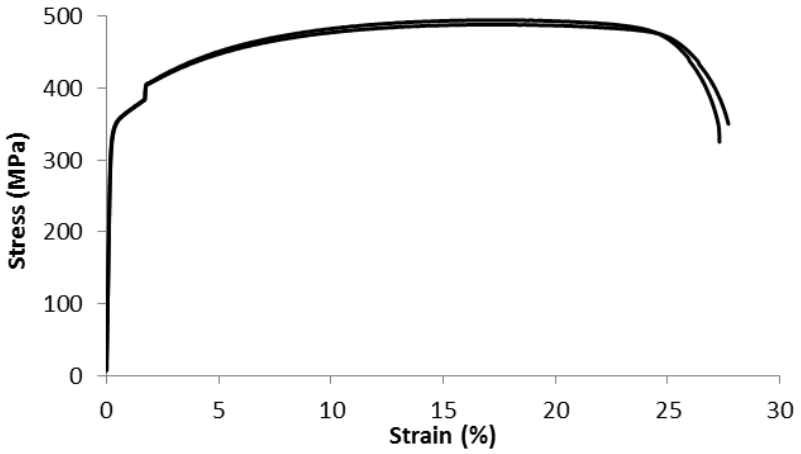

4509-1
T = 25°C

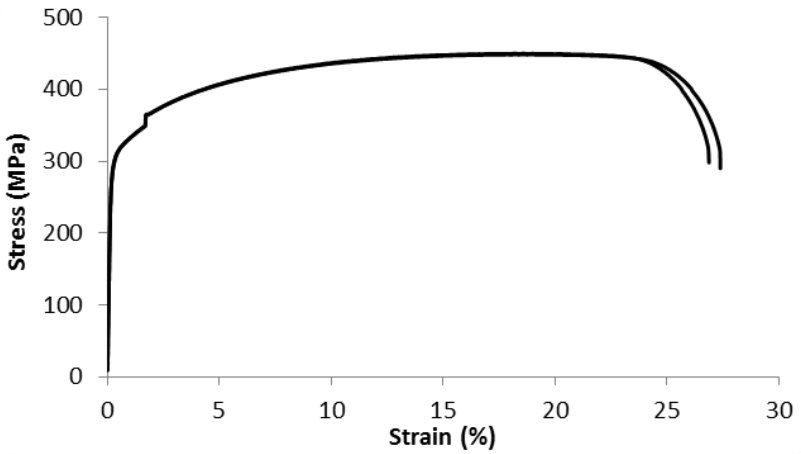

4509-1
T = 100°C

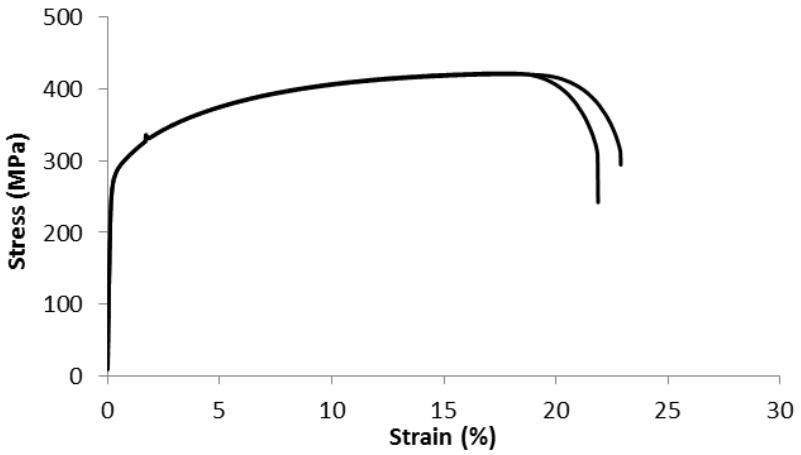

4509-1
T = 200°C

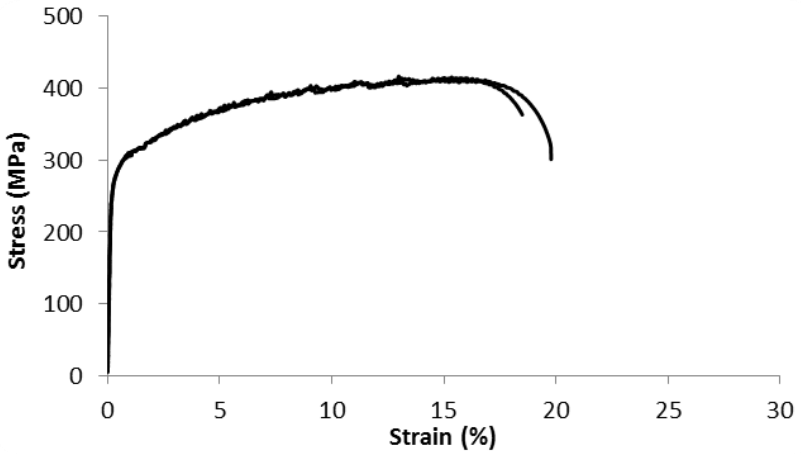

4509-1
T = 300°C

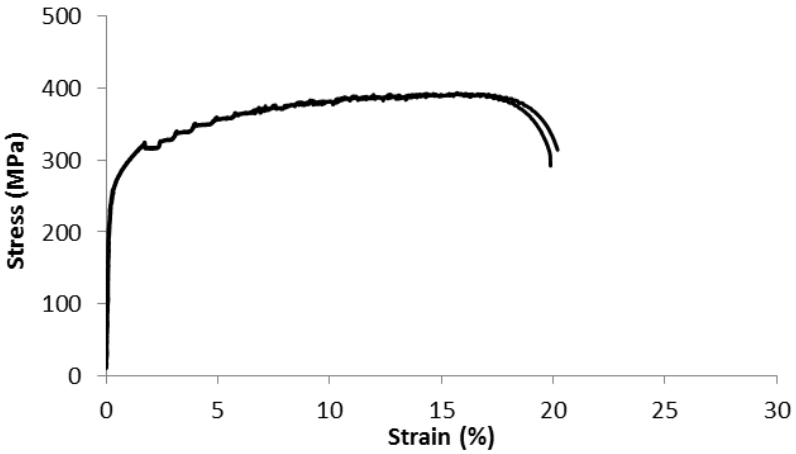

4509-1
T = 400°C

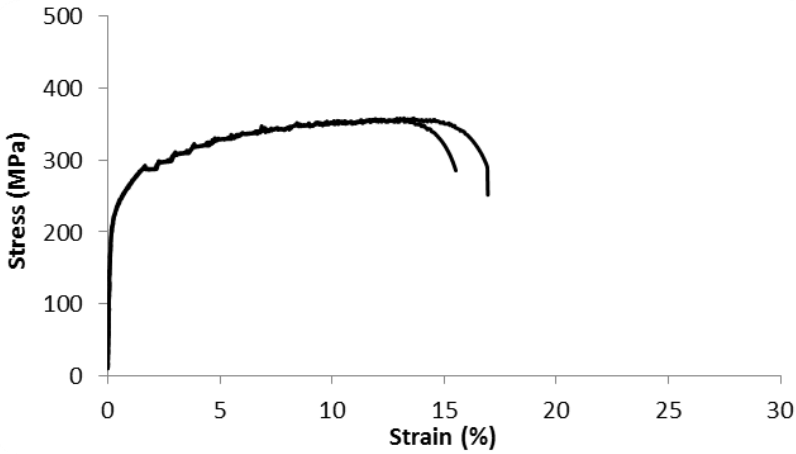

4509-1
T = 500°C

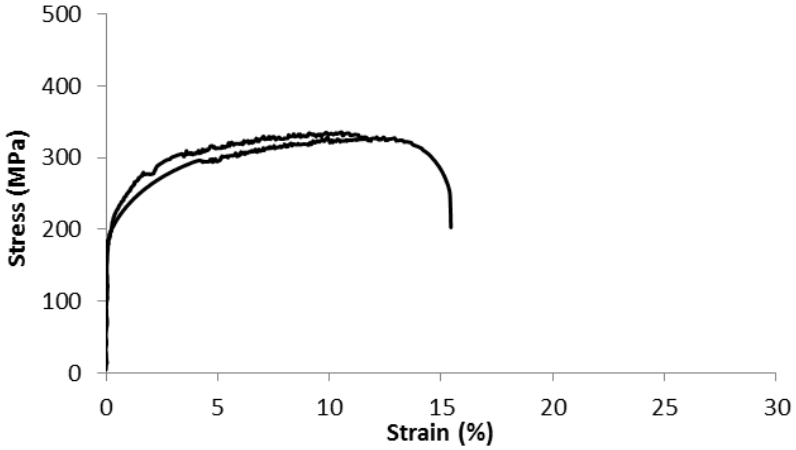

4509-1
T = 550°C

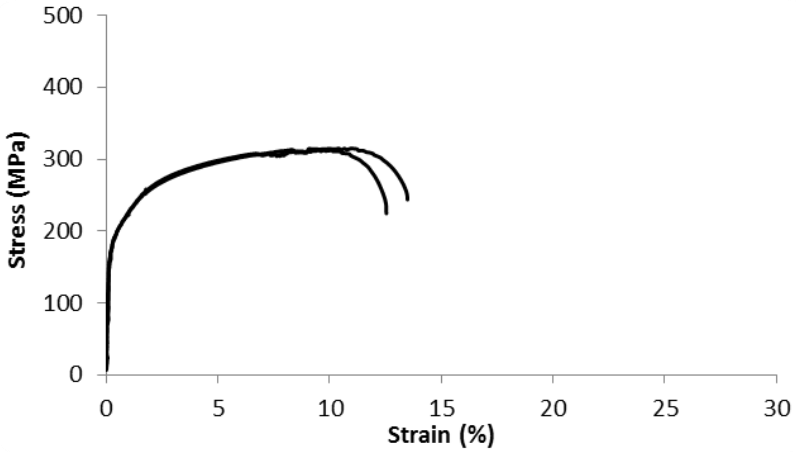

4509-1
T = 600°C

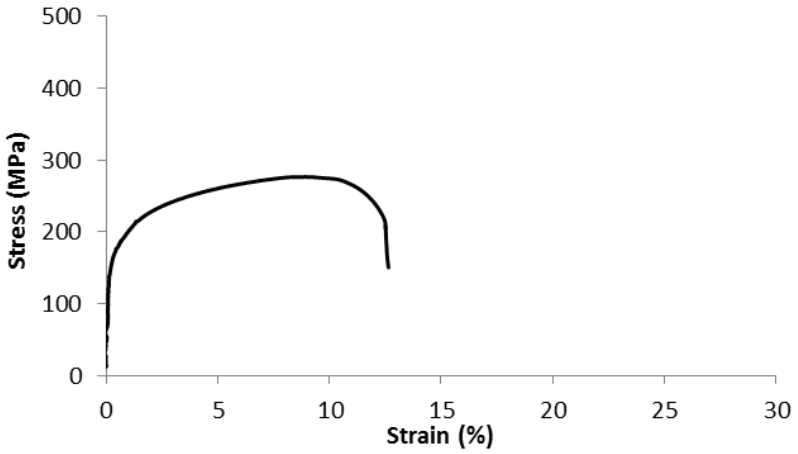

4509-1
T = 650°C

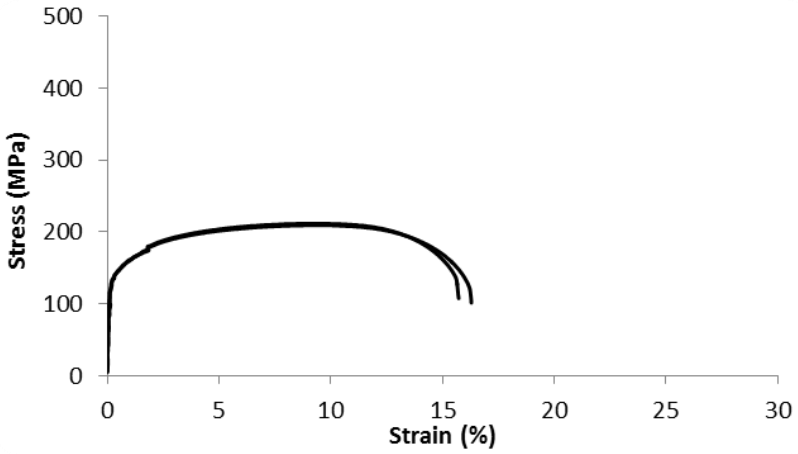

4509-1
T = 700°C

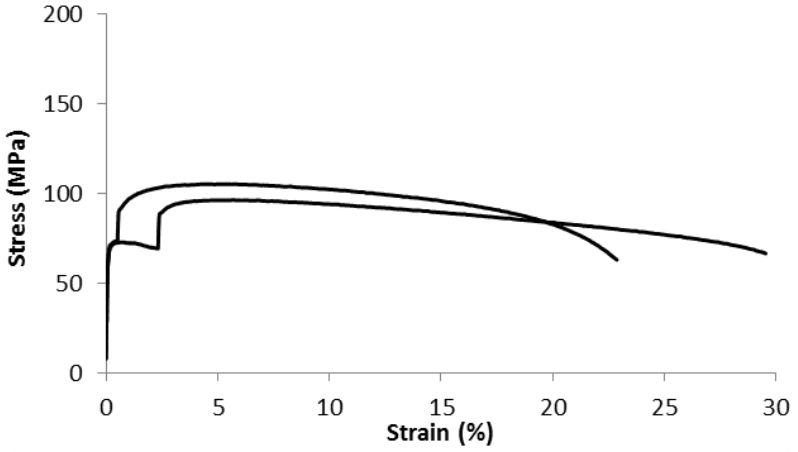

4509-1
T = 750°C

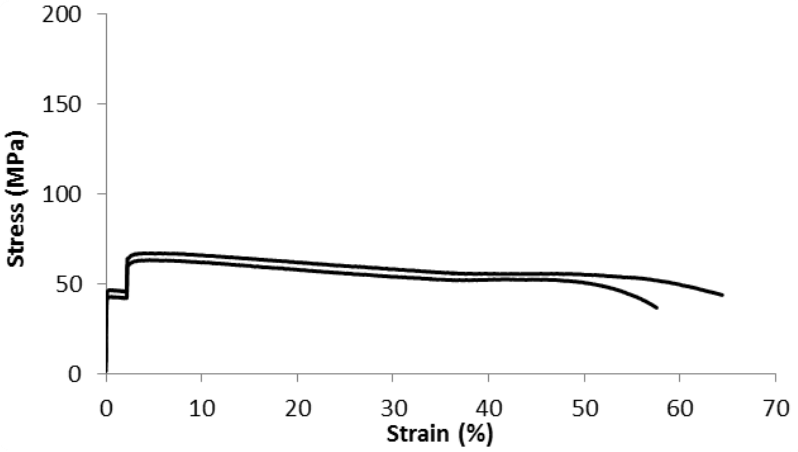

4509-1
T = 800°C

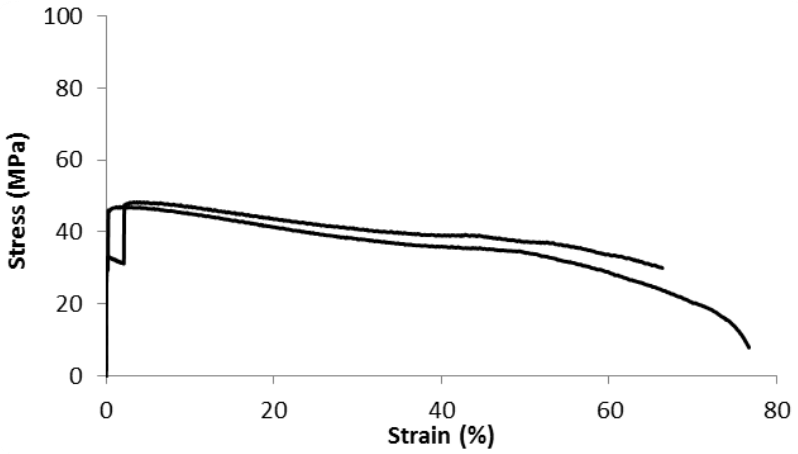

4509-1
T = 850°C

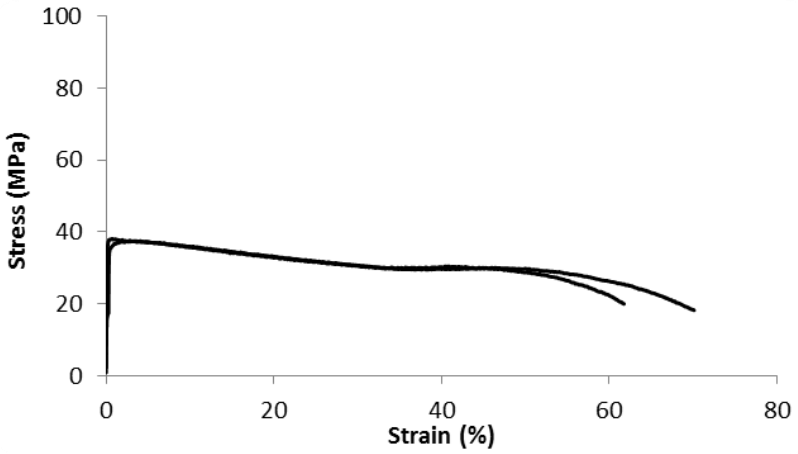

4509-1
T = 900°C

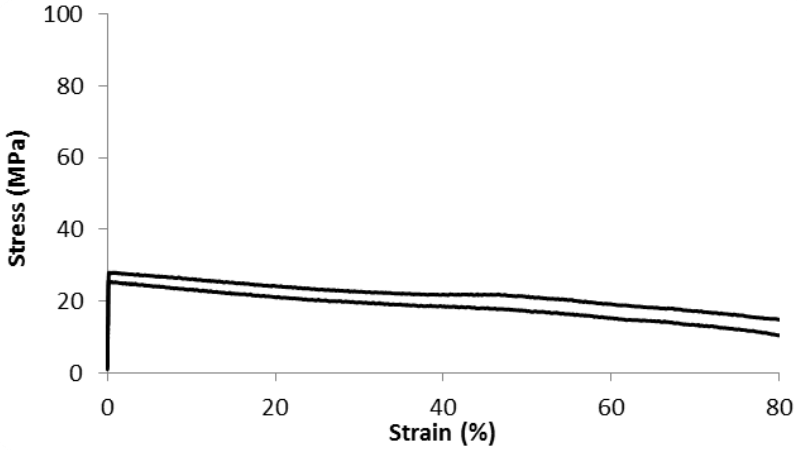

4509-1
T = 950°C

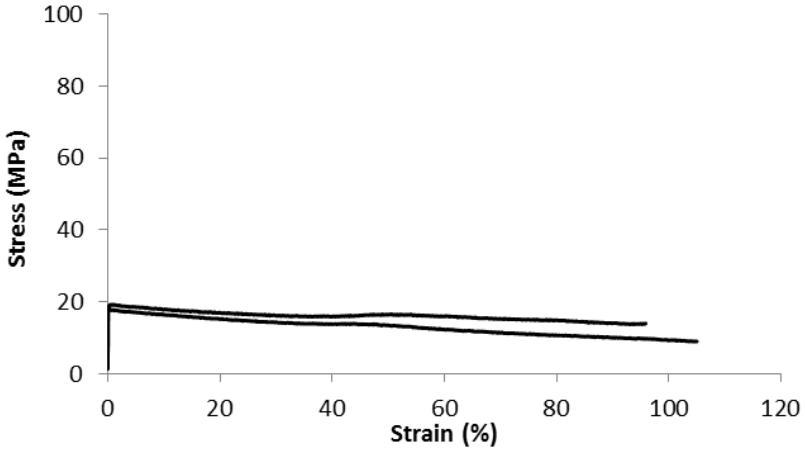

4509-1
T = 1000°C

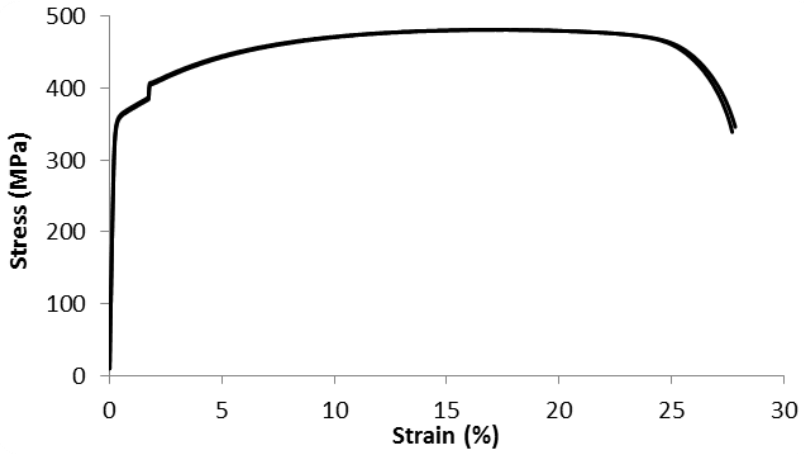

4509-2
T = 25°C

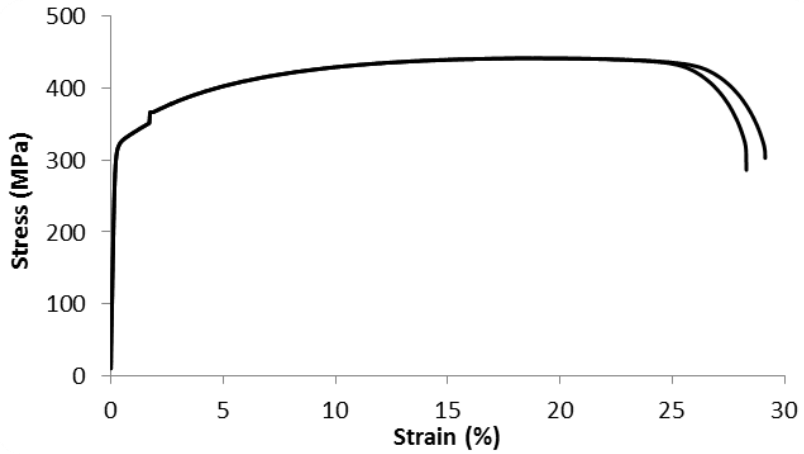

4509-2
T = 100°C

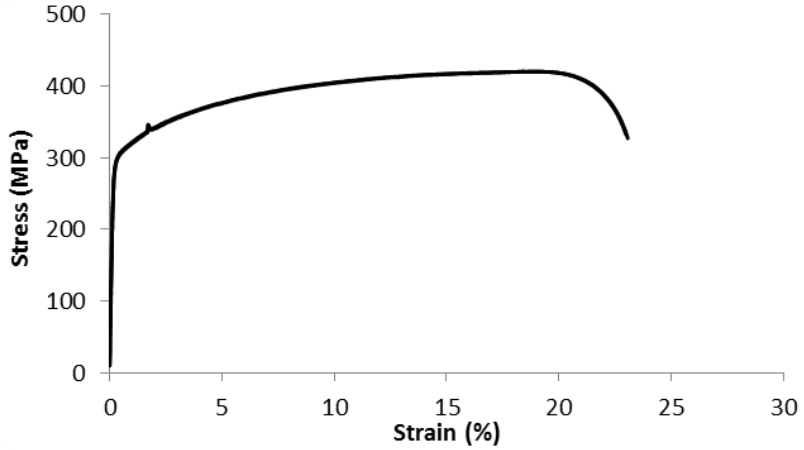

4509-2
T = 200°C

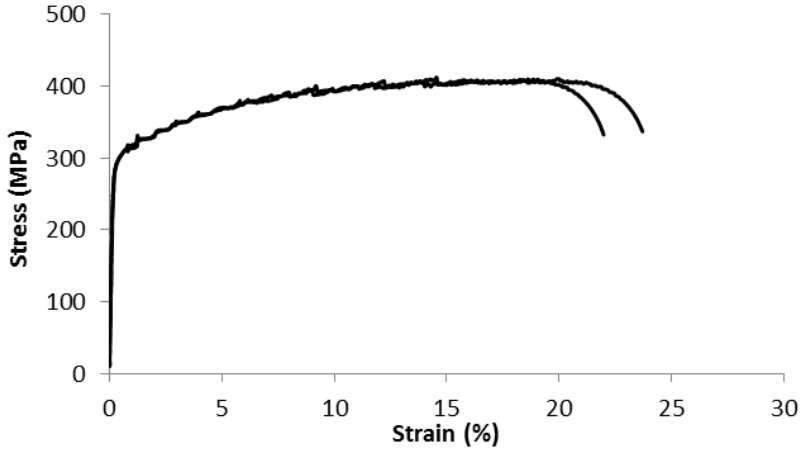

4509-2
T = 300°C

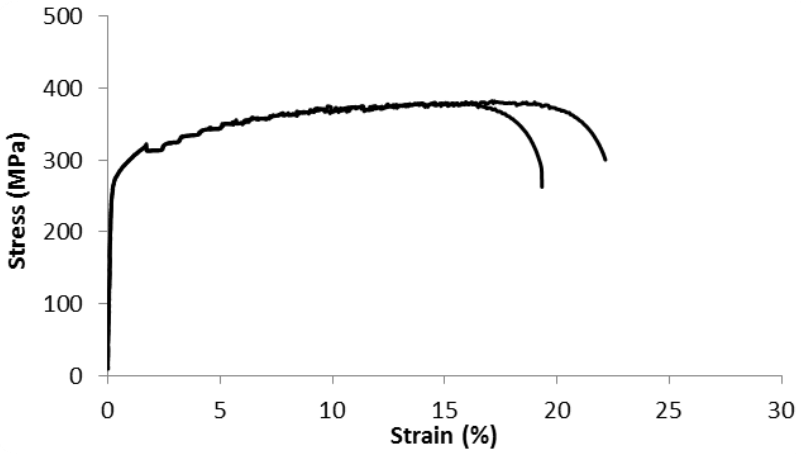

4509-2
T = 400°C

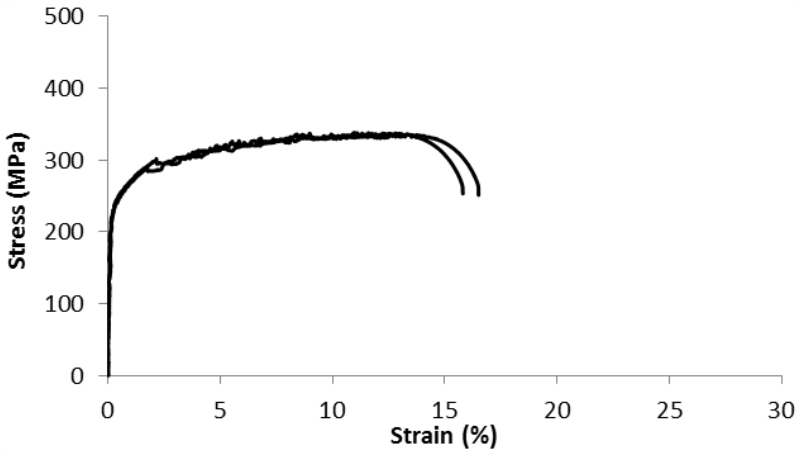

4509-2
T = 500°C

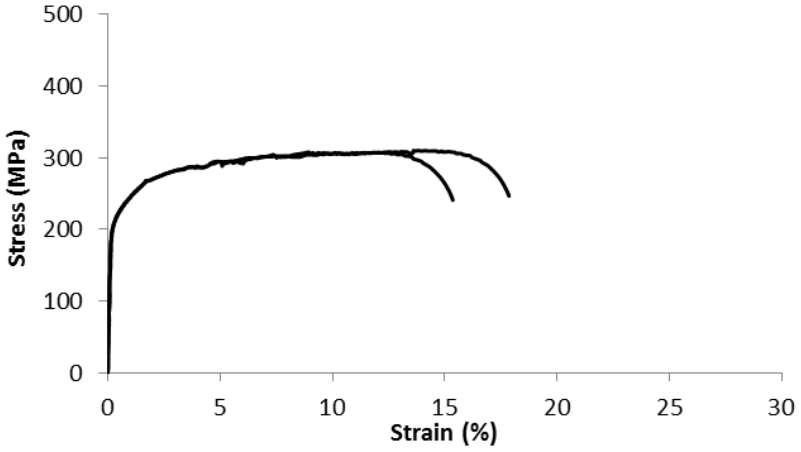

4509-2
T = 550°C

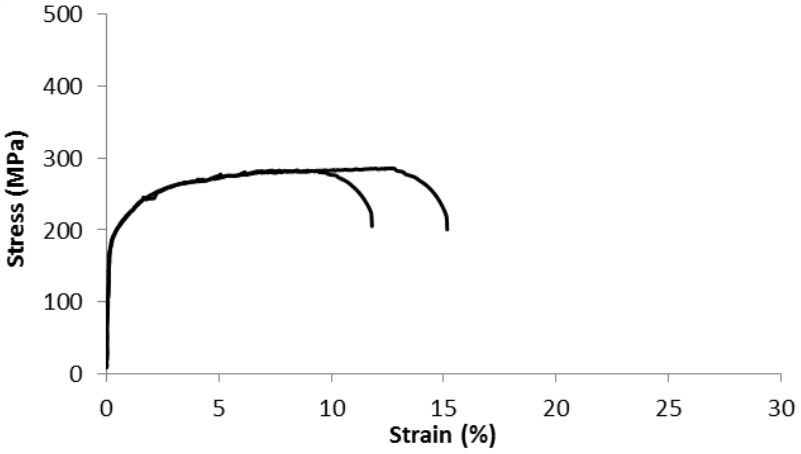

4509-2
T = 600°C

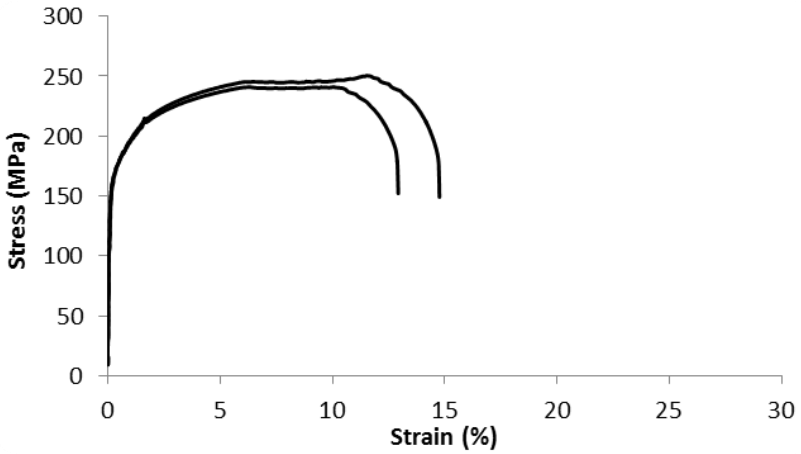

4509-2
T = 650°C

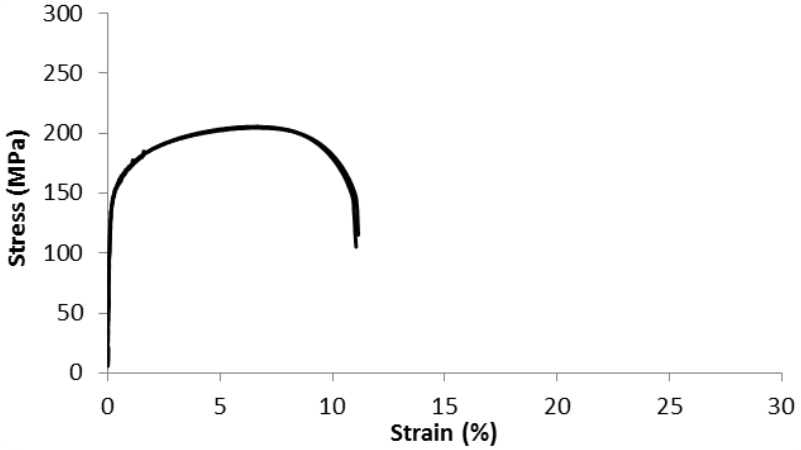

4509-2
T = 700°C

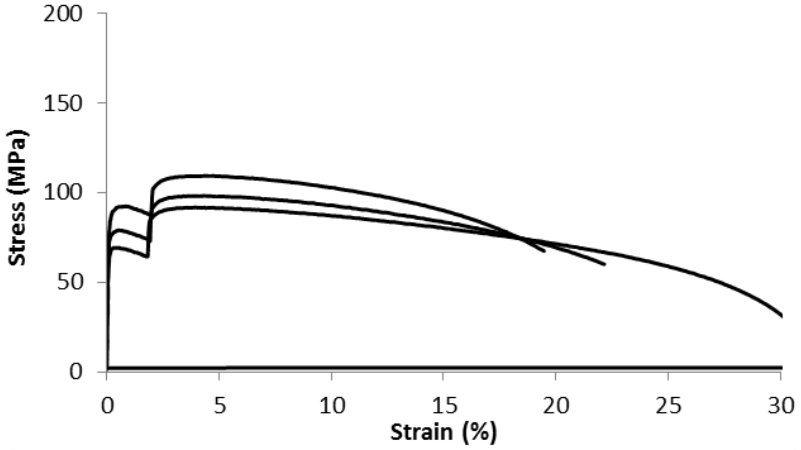

4509-2
T = 750°C

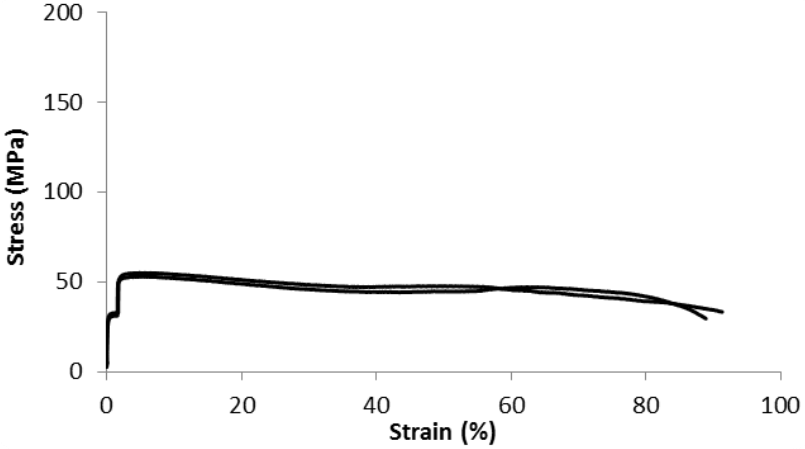

4509-2
T = 800°C

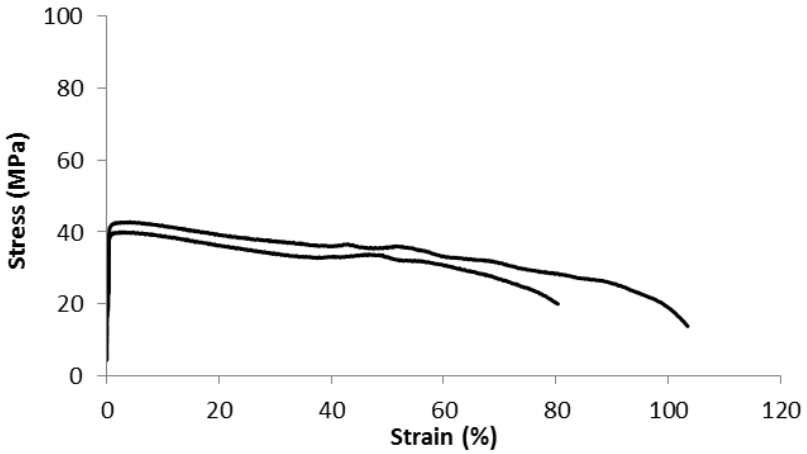

4509-2
T = 850°C

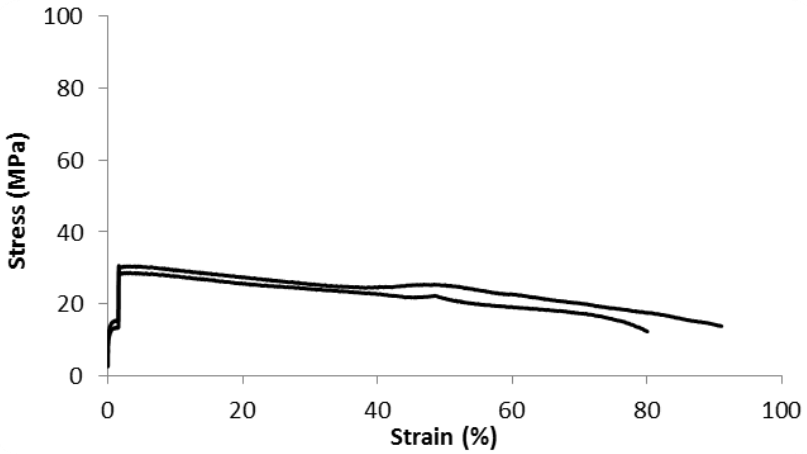

4509-2
T = 900°C

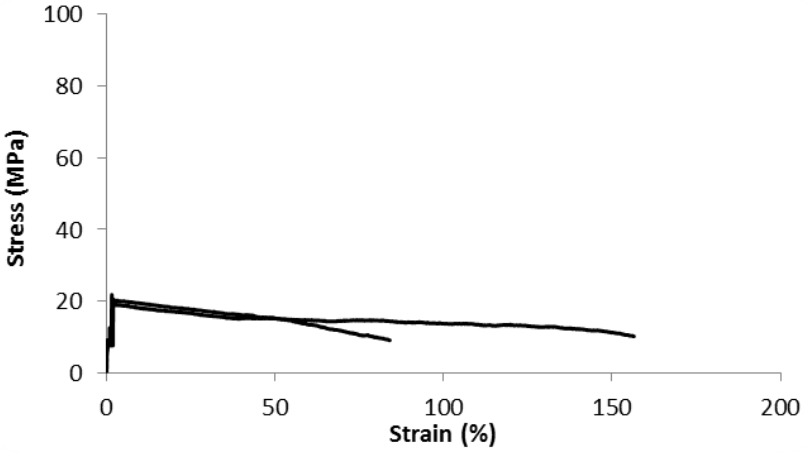

4509-2
T = 950°C

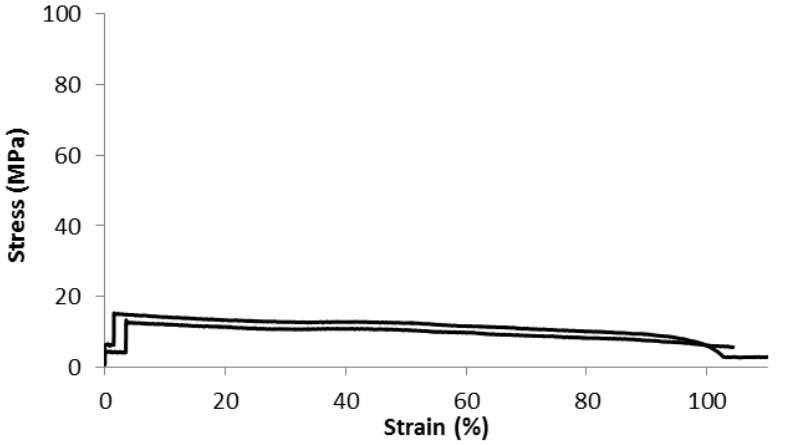

4509-2
T = 1000°C

Isothermal stress-strain curves for the steels 4521-1 and 4521-2.

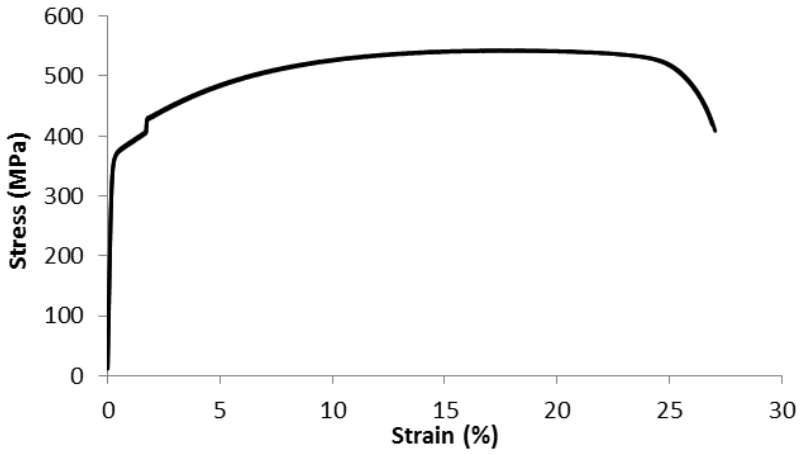

4521-1
T = 25°C

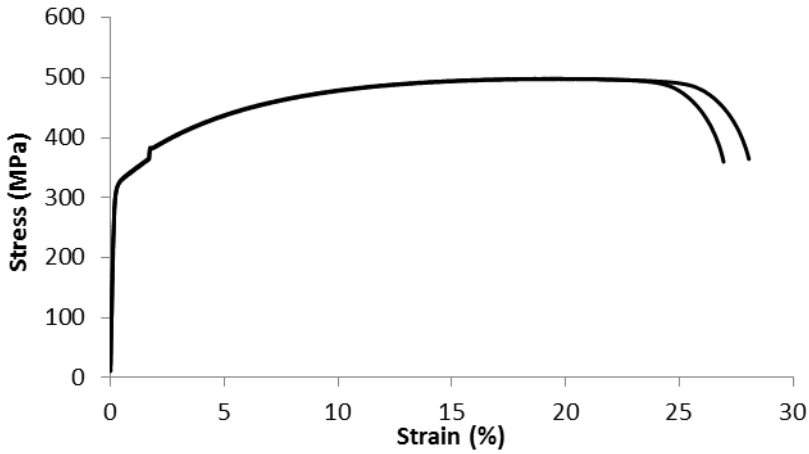

4521-1
T = 100°C

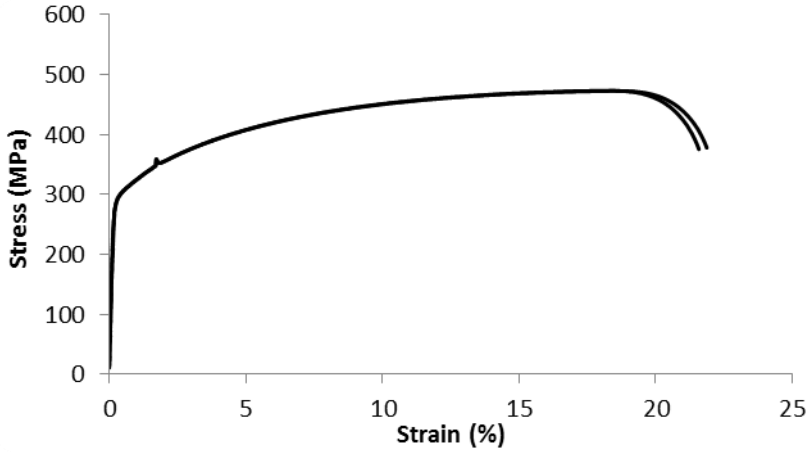

4521-1
T = 200°C

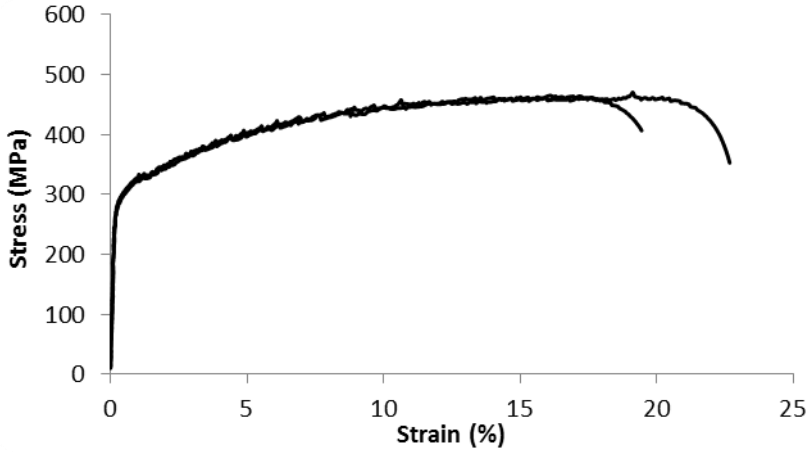

4521-1
T = 300°C

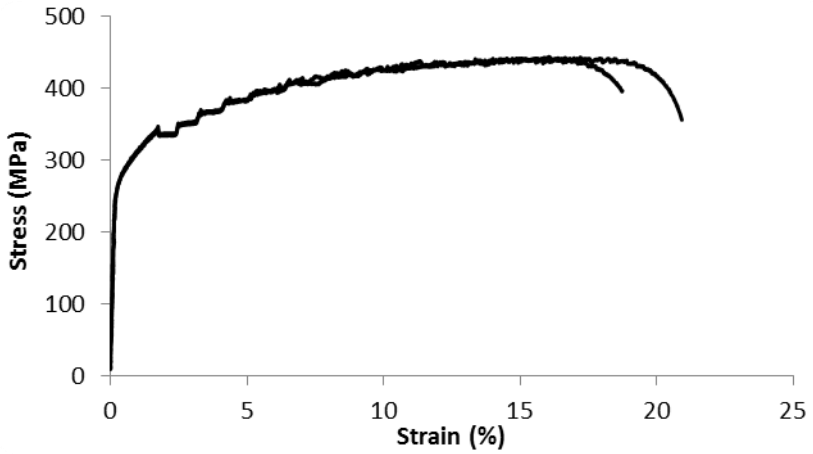

4521-1
T = 400°C

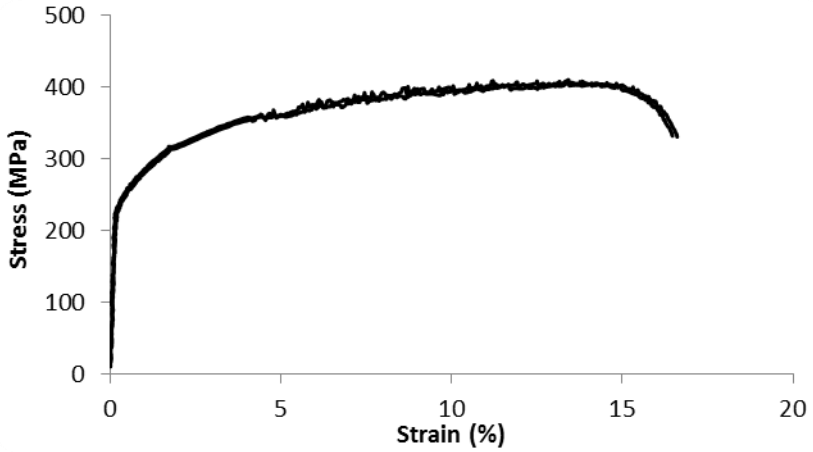

4521-1
T = 500°C

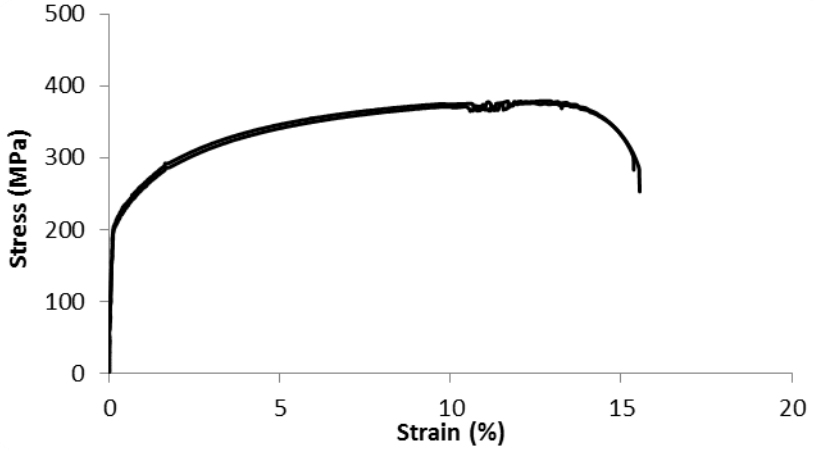

4521-1
T = 550°C

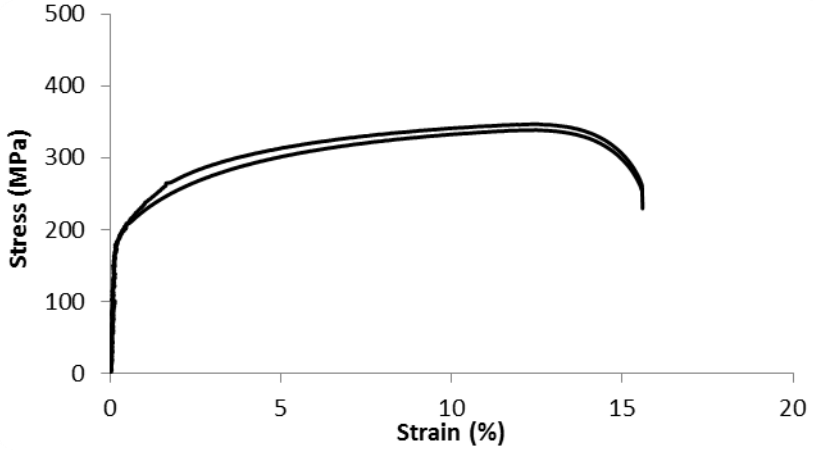

4521-1
T = 600°C

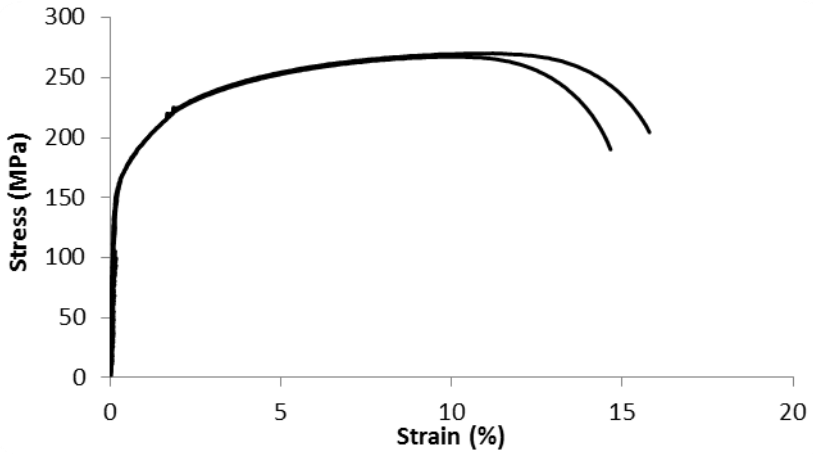

4521-1
T = 650°C

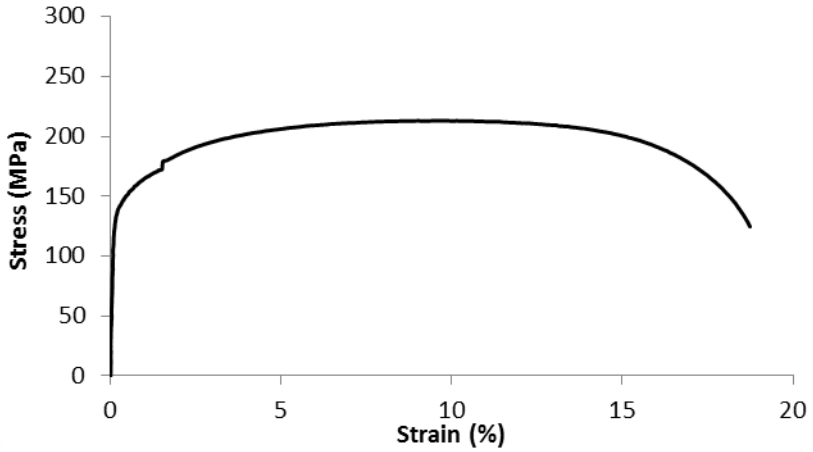

4521-1
T = 700°C

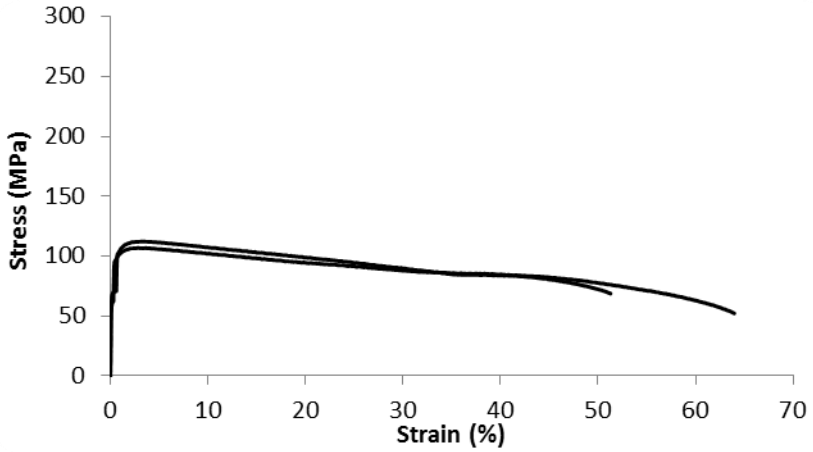

4521-1
T = 750°C

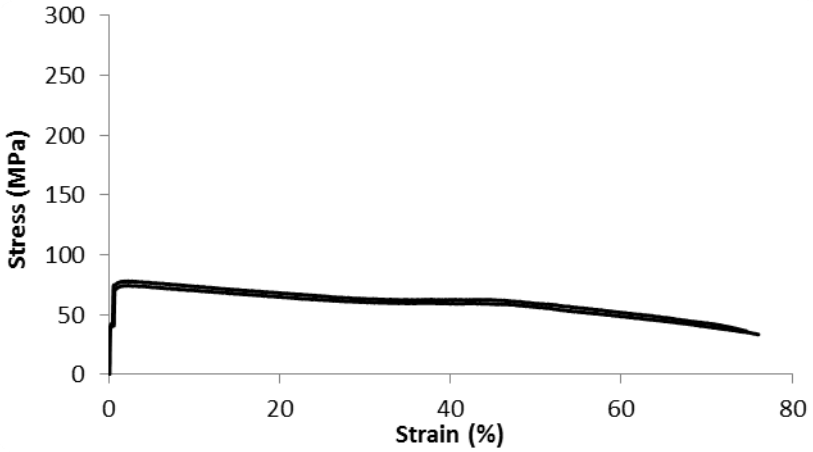

4521-1
T = 800°C

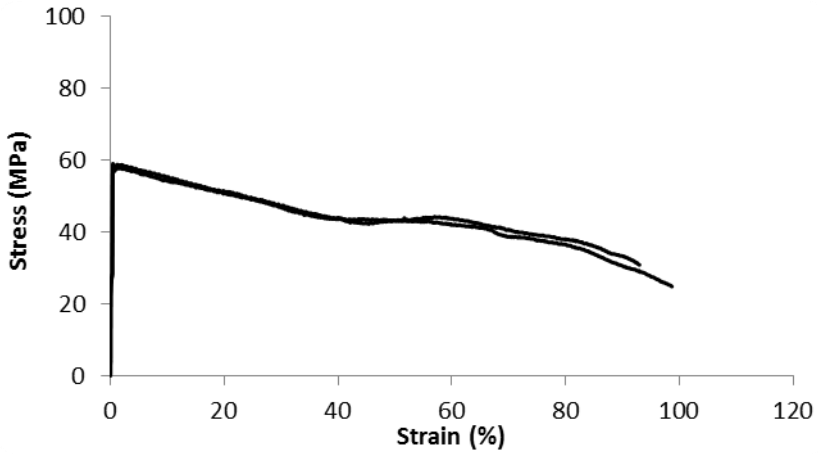

4521-1
T = 850°C

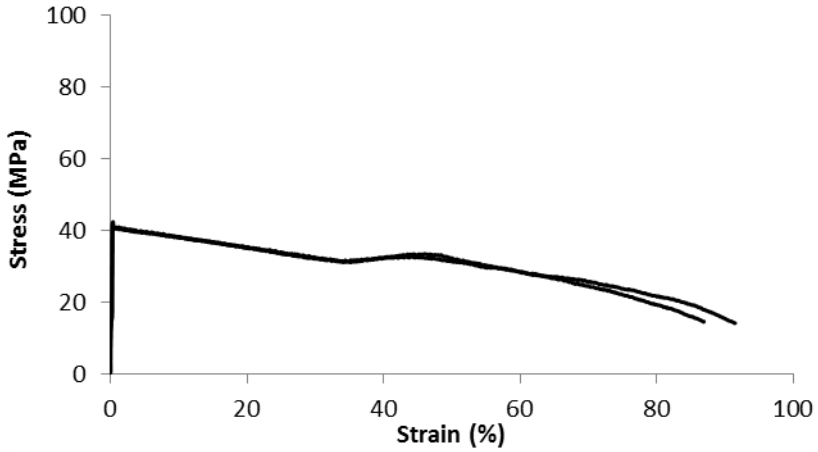

4521-1
T = 900°C

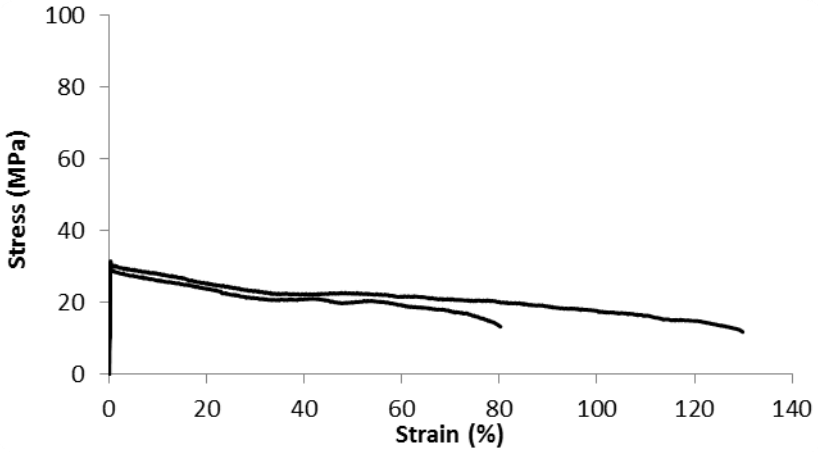

4521-1
T = 950°C

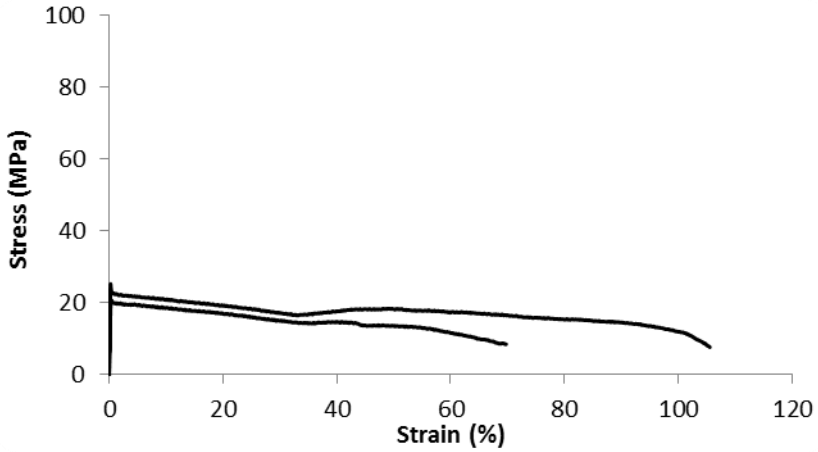

4521-1
T = 1000°C

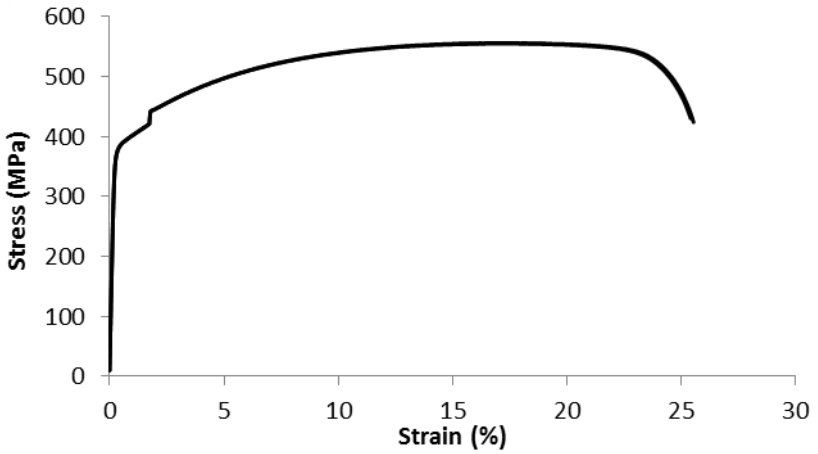

4521-2
T = 25°C

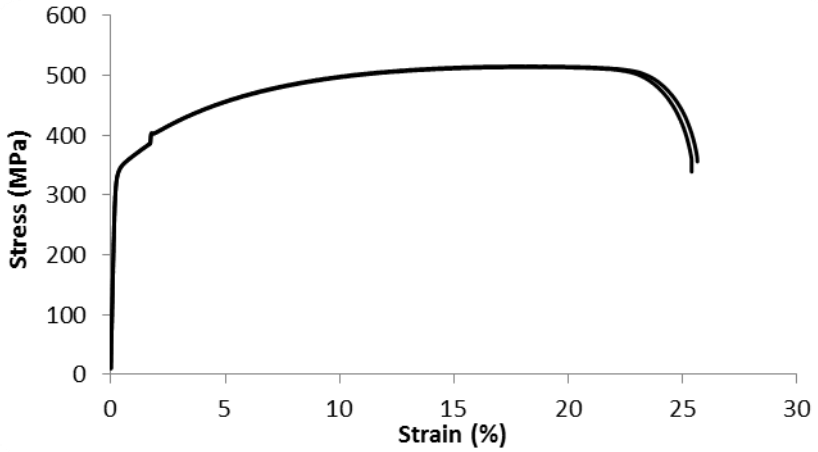

4521-2
T = 100°C

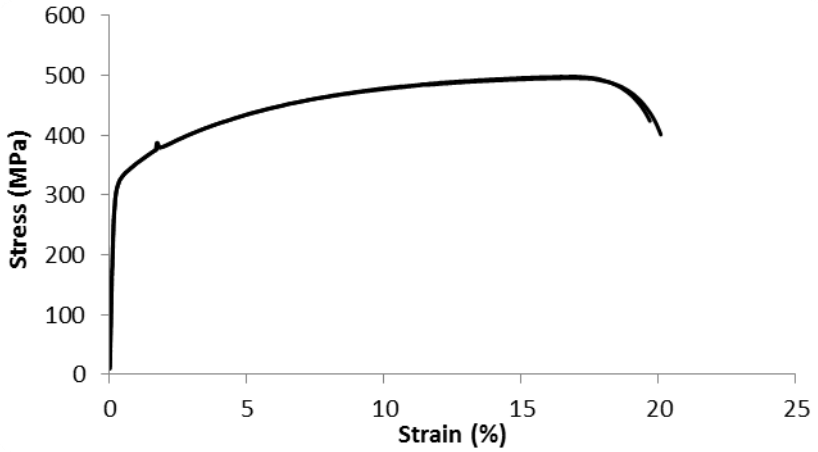

4521-2
T = 200°C

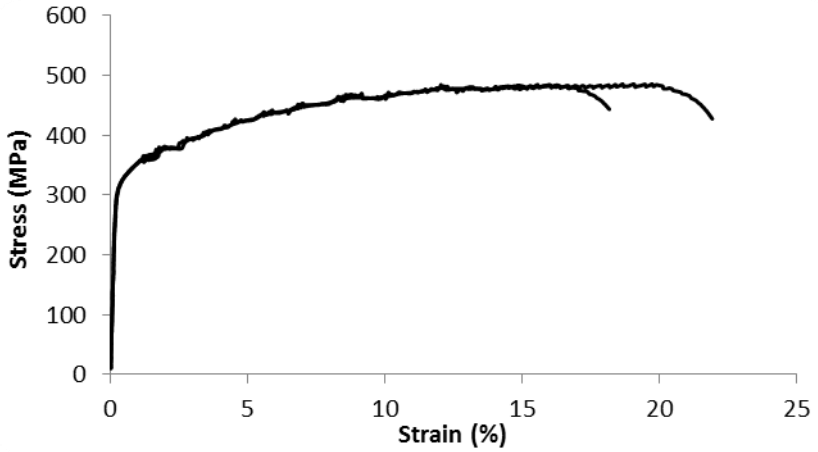

4521-2
T = 300°C

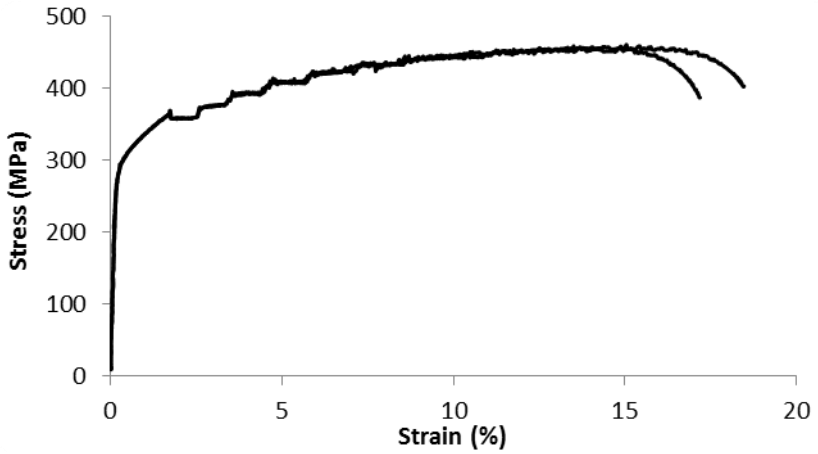

4521-2
T = 400°C

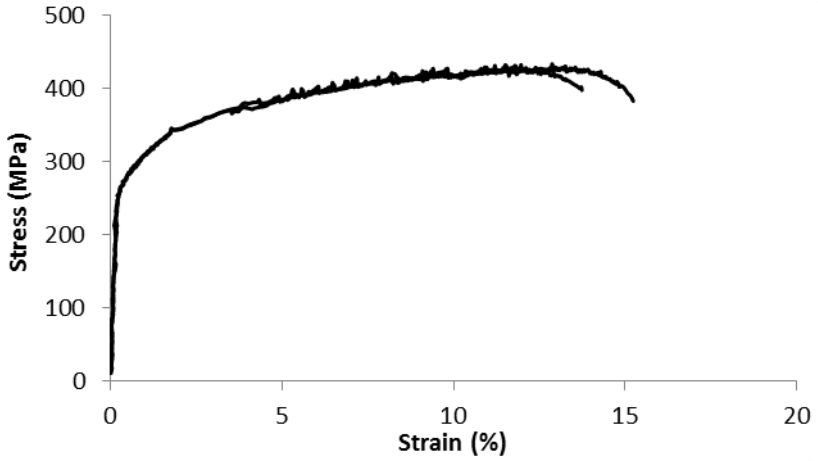

4521-2
T = 500°C

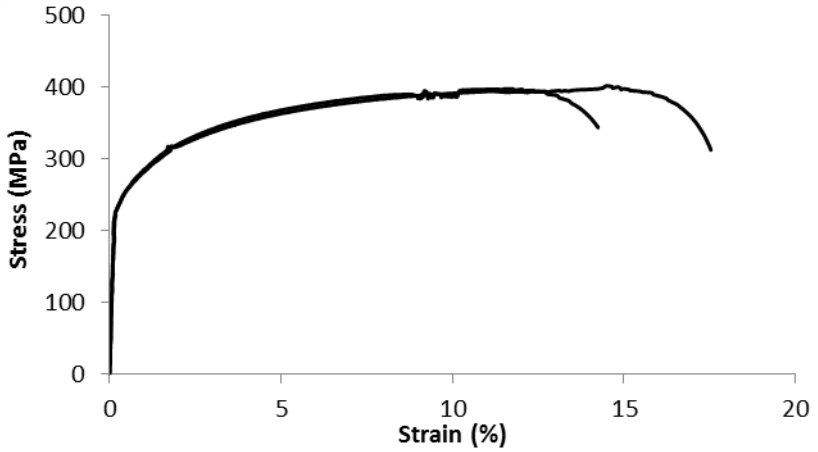

4521-2
T = 550°C

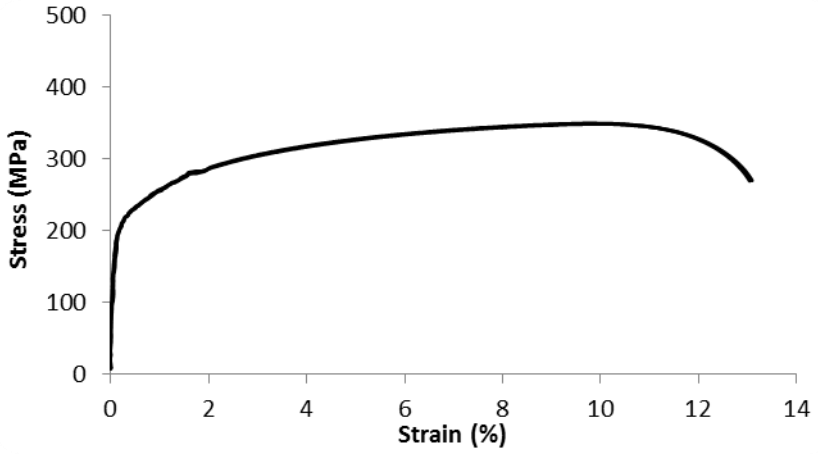

4521-2
T = 600°C

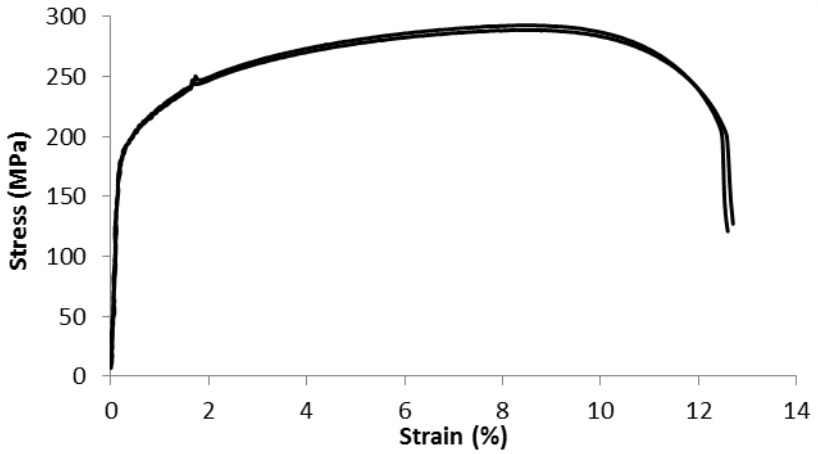

4521-2
T = 650°C

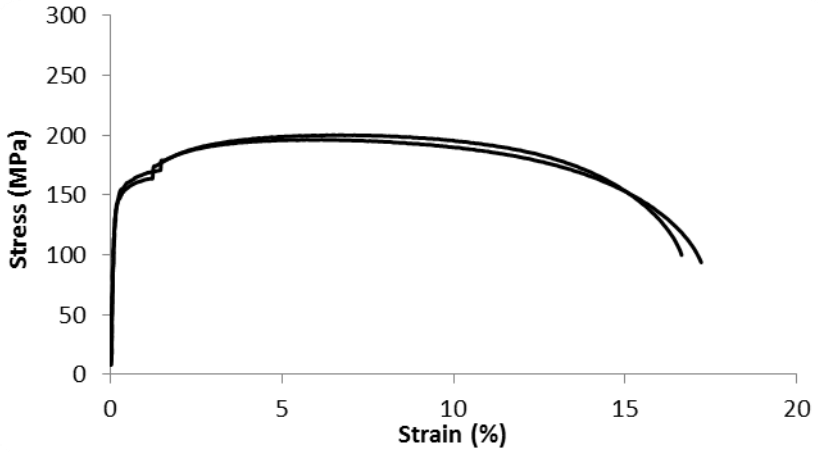

4521-2
T = 700°C

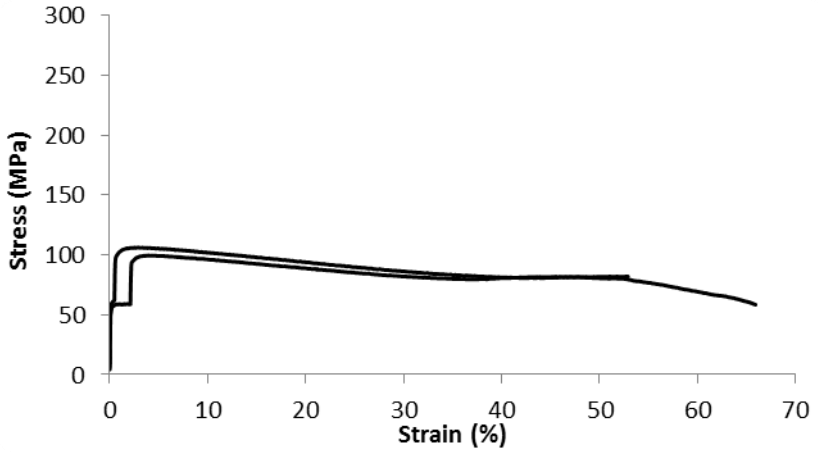

4521-2
T = 750°C

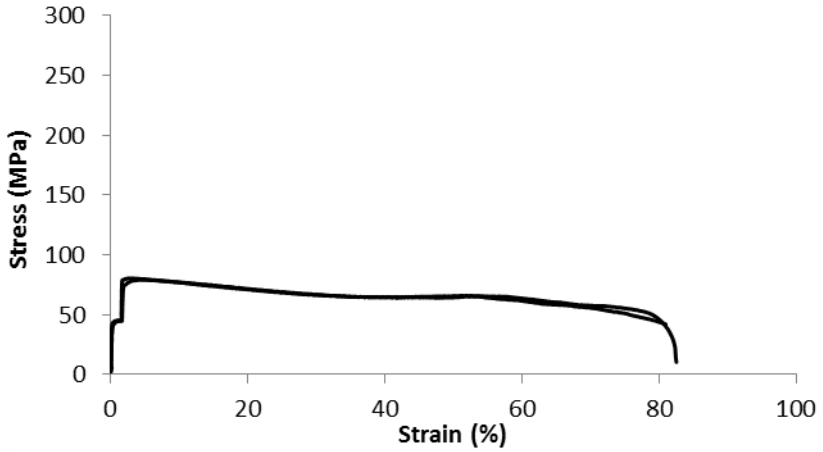

4521-2
T = 800°C

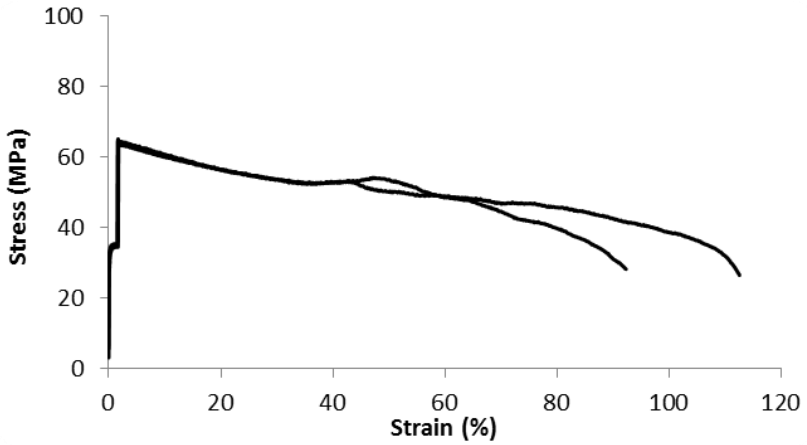

4521-2
T = 850°C

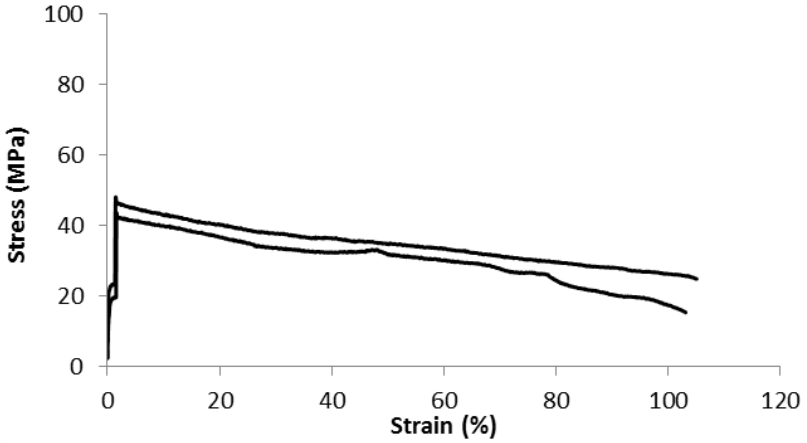

4521-2
T = 900°C

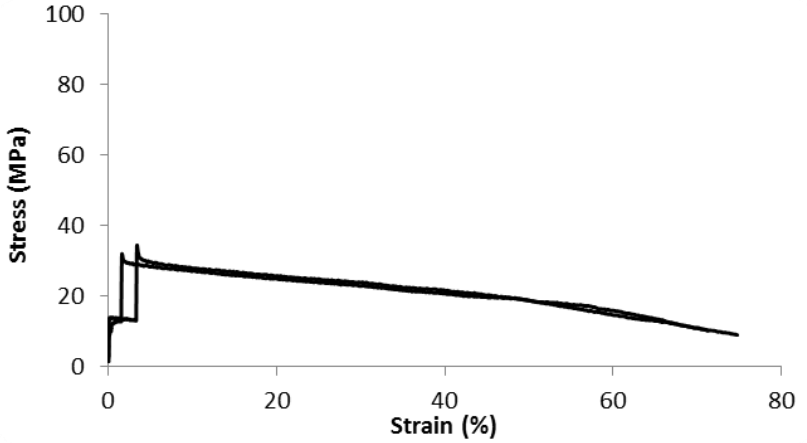

4521-2
T = 950°C

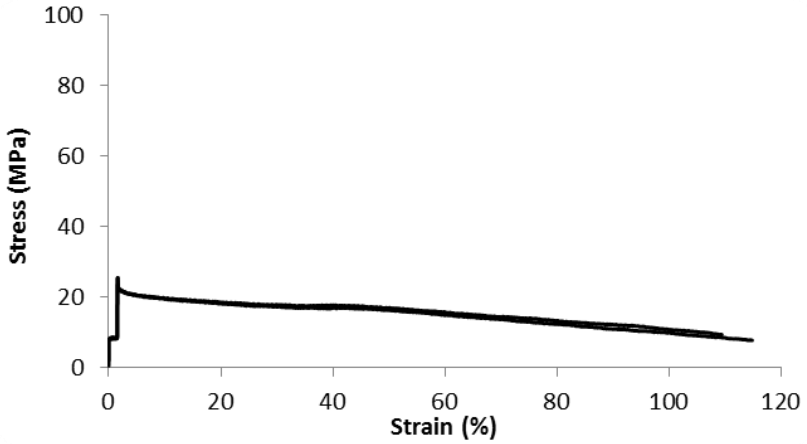

4521-2
T = 1000°C

Isothermal stress-strain curves for the steel 4621-1.

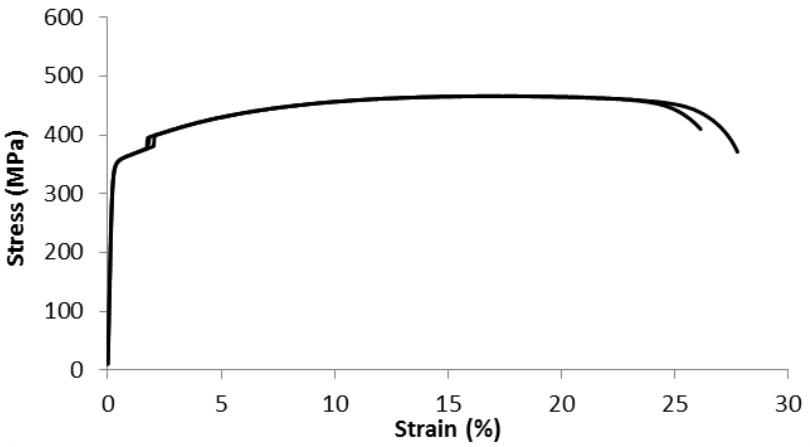

4621-1
T = 25°C

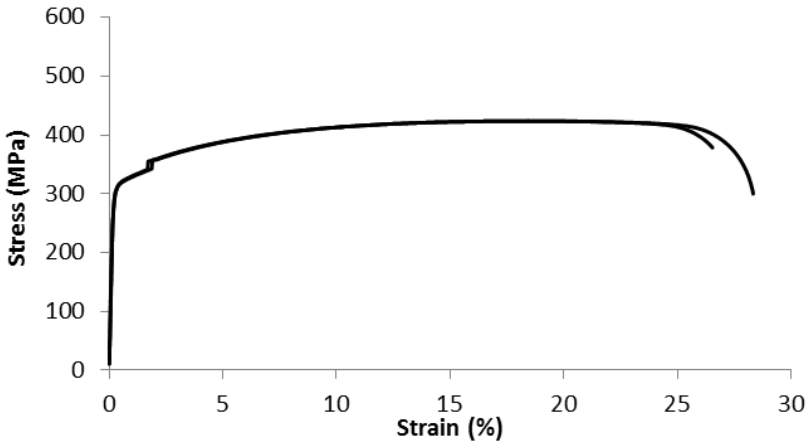

4621-1
T = 100°C

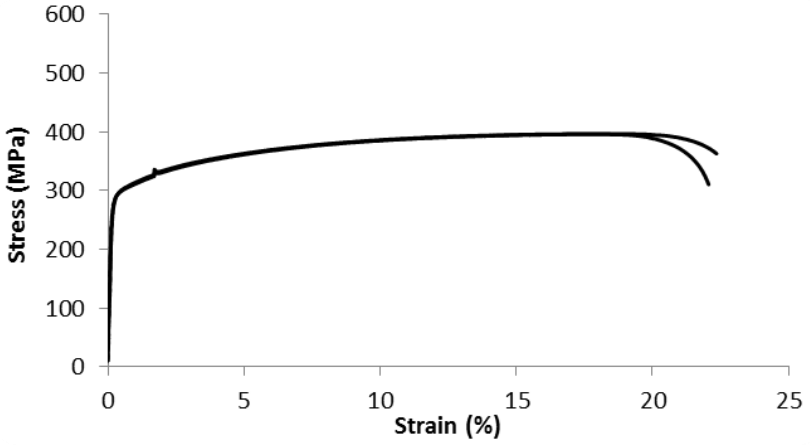

4621-1
T = 200°C

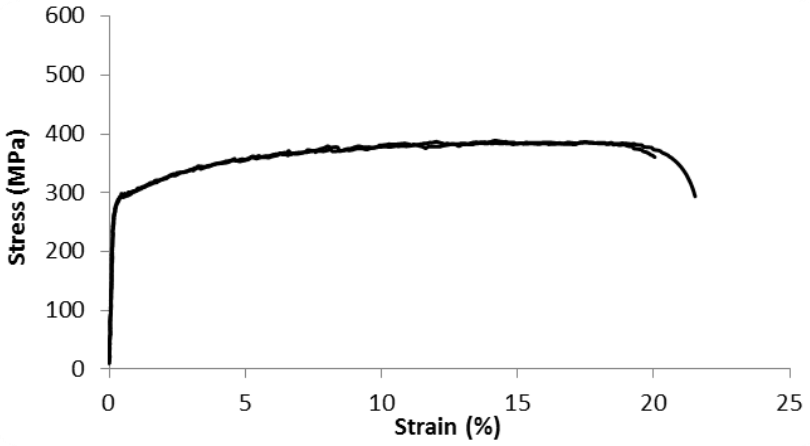

4621-1
T = 300°C

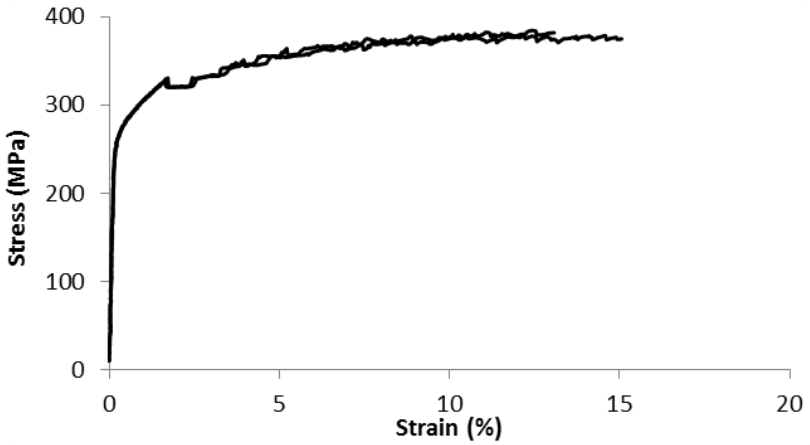

4621-1
T = 400°C

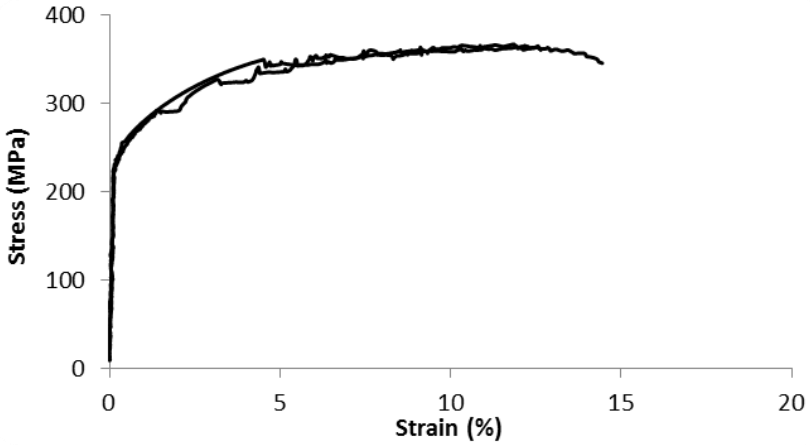

4621-1
T = 500°C

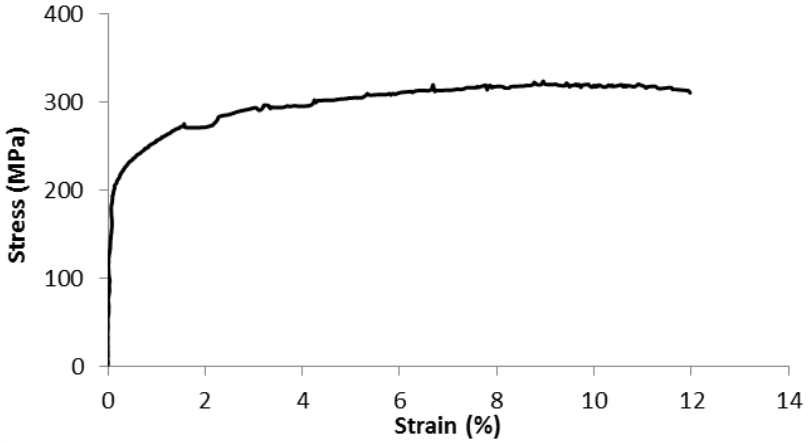

4621-1
T = 550°C

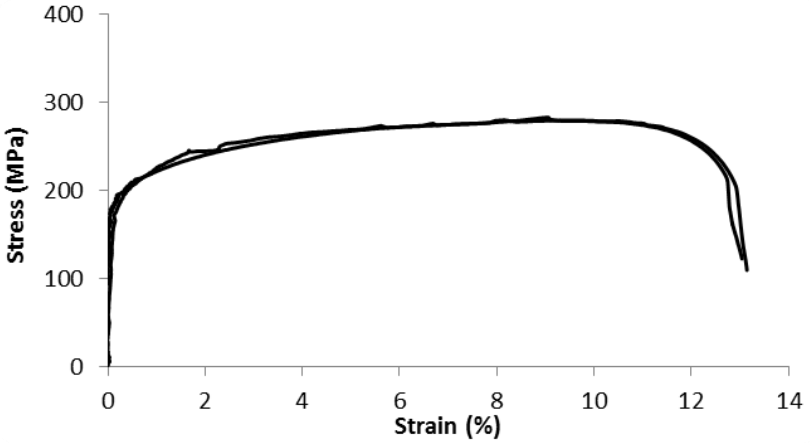

4621-1
T = 600°C

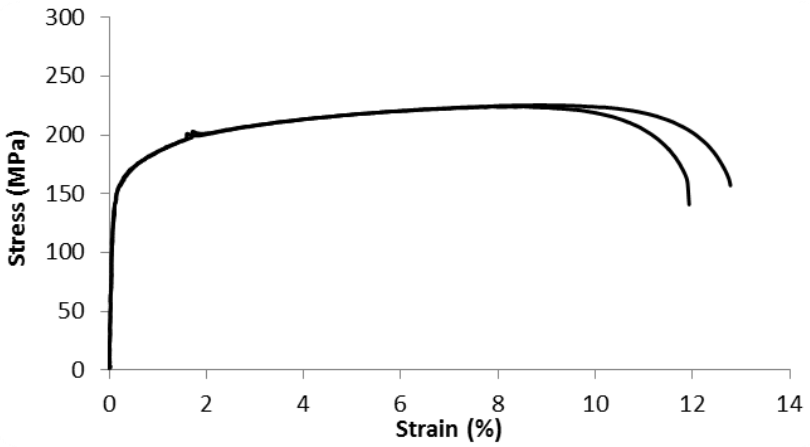

4621-1
T = 650°C

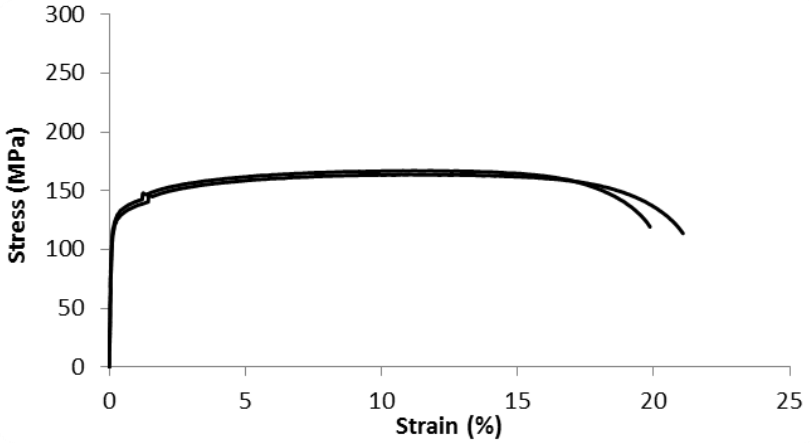

4621-1
T = 700°C

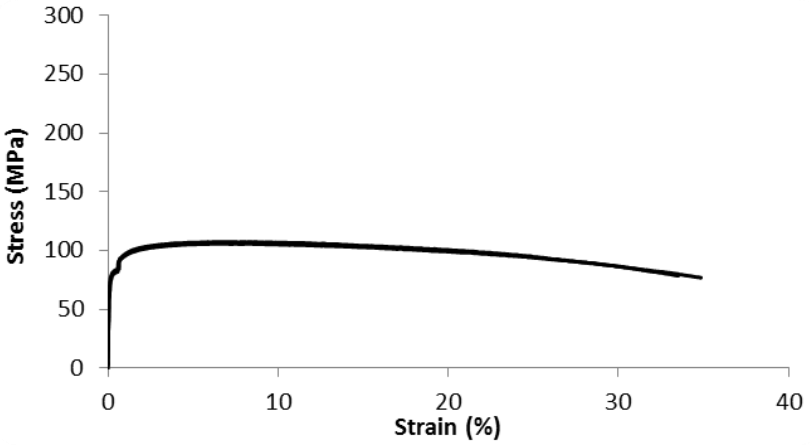

4621-1
T = 750°C

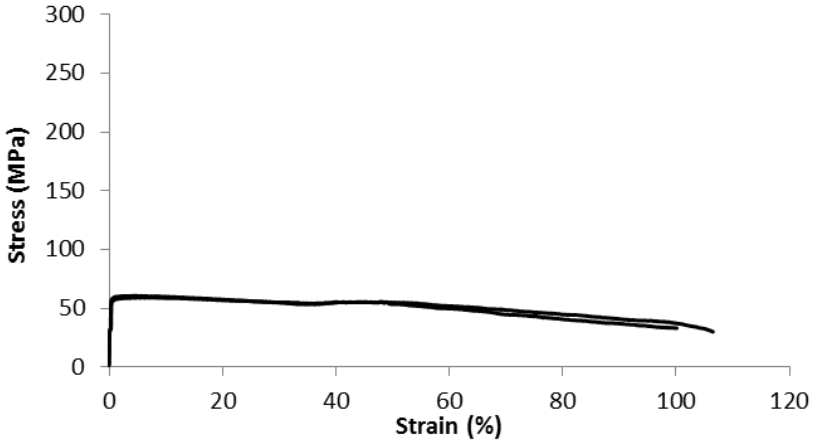

4621-1
T = 800°C

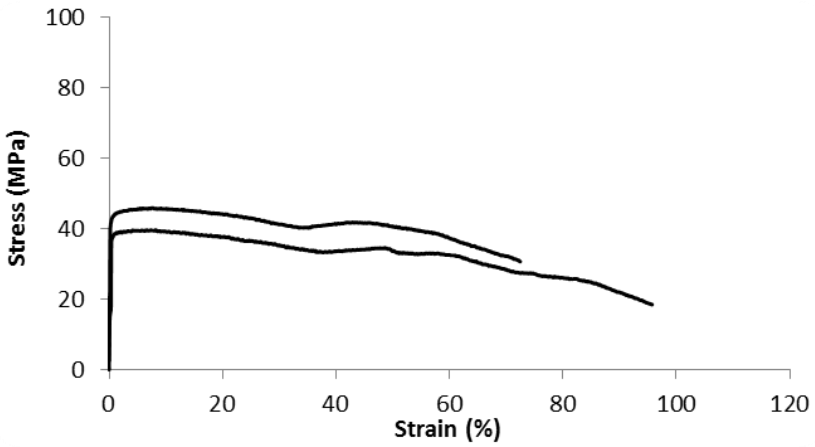

4621-1
T = 850°C

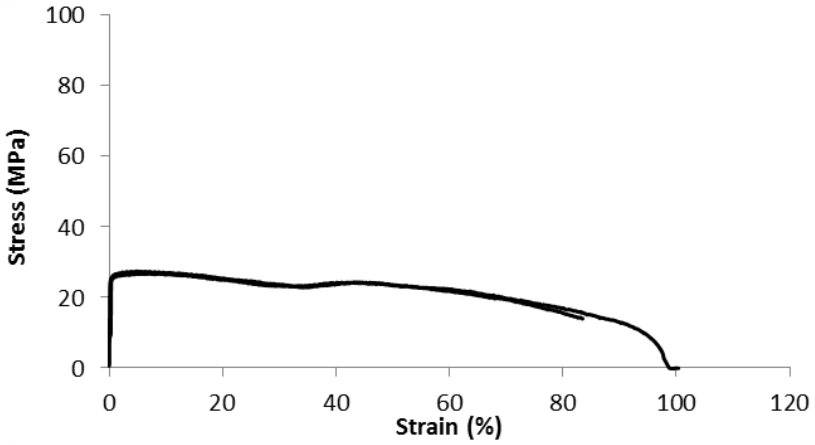

4621-1
T = 900°C

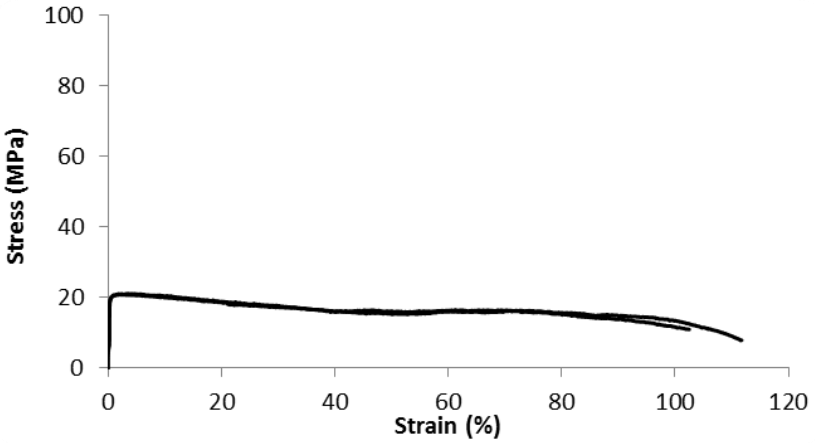

4621-1
T = 950°C

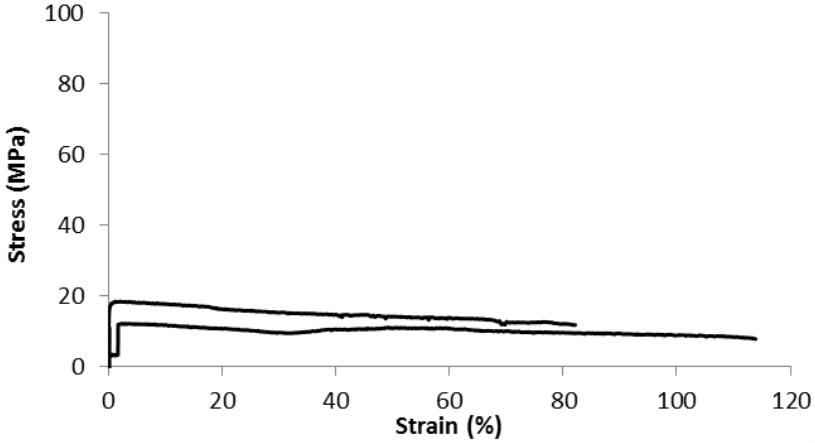

4621-1
T = 1000°C

Table 1. Steady state test results for the steel 4003-1.

Temperature °C	E-Modulus GPa	Rp 0,01 N/mm²	Rp 0,1 N/mm²	Rp 0,2 N/mm²	Rp 1,0 N/mm²	Rm N/mm²	Ag %	A50 %	A5 %	n -
25	159.7	240	315	328	354	484	17.4	32	42	9.6
25	151.7	252	316	328	355	485	17.7	32	43	11.4
100	146.8	228	287	299	326	445	18.9	33	42	11.1
100	144.8	238	287	298	324	442	18.7	33	43	13.3
200	154.9	203	270	282	312	420	19.2	28	36	9.1
200	150.4	212	269	281	311	417	18.4	27	35	10.6
300	193.2	229	285	295	318	410	13.7	20	27	11.8
300	181.3	205	285	298	320	410	17.8	23	31	8.0
400	180	176	274	285	330	412	12.6	17	24	6.2
400	175.4	213	275	286	332	413	11.3	17	23	10.2
500	125.3	198	233	244	283	379	12.4	23	31	14.3
500	150.3	174	231	245	286	384	12.6	22	30	8.8
550	105.6	166	198	206	229	296	9	25	38	13.9
550	124.8	159	185	201	223	274	8.6	26	41	12.8
550	144.2	142	180	187	198	265	10.6	34	49	10.9
550	183.6	142	184	192	206	274	10.7	41	57	9.9
600	148.3	108	137	143	148	196	9.9	42	62	10.7
600	73.3	96	146	147	147	200	9.1	43	64	7.0
650	97.2	66	90	93	95	142	9.1	56	80	8.7
650	64.9	66	90	93	94	141	7.5	54	80	8.7
700	73.3	40	53	57	59	96	6.3	74	105	8.5
700	85.1	38	54	57	58	92	9.1	67	95	7.4
750	21.8	25	31	33	36	62	9.4	98	132	10.8
750	38.4	26	33	34	37	64	10.4	81	101	11.2
800	364.3	19	36	45	50	109	23.4	63	87	3.5
800	32.1	44	48	50	53	113	26.7	64	88	23.4
850	17.3	11	38	39	43	100	27.1	72	101	2.4
850	612.1	17	37	39	43	100	25.5	71	98	3.6
900	38.8	23	26	27	31	78	24	58	72	18.7
900	27.2	19	23	24	28	76	26.2	51	63	12.8
950	46.4	15	19	19	24	66	28.9	52	66	12.7
950	6.2	18	19	20	23	65	27.6	97	147	28.4
1000	22.9	16	17	18	21	56	25.4	58	74	25.4
1000	28.1	12	14	15	18	53	25.7	57	69	13.4

Table 2. Steady state test results for the steel 4016-1.

Temperature °C	E-Modulus GPa	Rp 0,01 N/mm²	Rp 0,1 N/mm²	Rp 0,2 N/mm²	Rp 1,0 N/mm²	Rm N/mm²	Ag %	A50 %	A5 %	n -
25	178.1	295	334	345	370	496	16.7	29	38	19.1
25	185.4	280	323	334	365	504	15.6	27	37	17.0
100	160.2	263	299	311	338	457	17.4	26	34	17.9
100	188.9	250	294	307	339	467	16.3	26	35	14.6
200	207.2	212	285	295	323	429	18	27	34	9.1
200	175.8	254	287	296	325	433	16.1	23	30	19.6
300	166.9	250	282	295	319	410	14.7	21	28	18.1
300	155.3	263	282	295	316	408	15.7	23	28	26.1
400	145	221	257	271	320	400	11.1	16	23	14.7
400	159.1	159	259	272	321	404	10.5	17	22	5.6
500	210	145	213	231	271	362	11.9	24	32	6.4
500	203.4	160	220	232	273	364	11.8	23	30	8.1
550	155.6	131	181	189	207	276	9.9	32	46	8.2
550	186.4	150	182	192	212	283	10.3	30	44	12.1
600	145.9	105	134	136	140	199	9.6	46	65	11.6
600	102.9	104	131	132	132	189	9.4	49	68	12.6
650	54.4	81	83	84	80	126	11.1	61	86	82.4
650	72.7	74	84	86	86	135	9.3	76	111	19.9
700	83.9	47	56	56	56	92	8.8	81	105	17.1
700	209.2	46	49	48	48	82	12	80	104	70.4
750	112.1	29	34	34	34	60	15.6	81	110	18.8
750	37.4	30	36	36	35	62	11.7	71	102	16.4
800	28.9	10	19	25	44	46	9.9	107	146	3.3
800	10.1	20	38	38	39	41	8.4	80	112	4.7
850	38.2	12	16	17	31	32	9.3	88	127	8.6
850	72.2	13	15	29	31	31	8.4	80	139	3.7
900	29.5	15	16	17	17	30	8.7	78	113	23.9
900	38.4	11	12	12	25	25	4.9	95	143	34.4
950	34.2	8	17	22	23	23	0.5	98	147	3.0
950	22.9	4	10	10	10	22	1.7	69	122	3.3
1000	14.5	8	21	21	20	22	0.2	70	98	3.1
1000	28.7	17	21	21	20	21	0.1	74	104	14.2

Table 3. Steady state test results for the steel 4016-2.

Temperature °C	E-Modulus GPa	Rp 0,01 N/mm²	Rp 0,1 N/mm²	Rp 0,2 N/mm²	Rp 1,0 N/mm²	Rm N/mm²	Ag %	A50 %	A5 %	n -
25	141.2	239	300	311	332	455	18.9	33	43	11.4
25	145.8	246	305	314	333	455	18.7	34	45	12.3
100	137.8	202	272	283	304	416	20.6	35	44	8.9
100	142.7	210	273	284	305	417	20.6	38	46	9.9
200	165.9	212	264	273	297	395	17.8	27	37	11.8
200	171.7	208	266	275	299	396	18.8	27	36	10.7
300	148.9	176	274	276	291	386	12.5	20	25	6.7
300	143.3	214	272	276	295	383	10.9	17	25	11.8
400	136.6	154	266	274	319	417	12.6	20	27	5.2
400	136	167	268	275	310	418	14.1	21	28	6.0
500	145.9	200	227	234	279	404	10.5	15	21	19.1
500	119.3	198	226	234	278	401	10.2	15	22	17.9
550	157.1	156	178	186	207	275	9.5	29	43	17.0
550	118.4	166	183	189	212	282	9.2	29	43	23.1
600	67.9	129	134	135	138	193	9.1	41	63	65.9
600	99.1	112	127	132	135	191	8.8	44	66	18.2
650	57.5	73	78	80	82	129	9.8	60	90	32.7
650	66.4	63	73	76	79	129	8.4	60	88	16.0
700	70.3	29	35	39	41	76	9.8	91	114	10.1
700	145.4	27	36	39	42	77	7.4	98	146	8.1
750	29.4	21	29	29	30	57	10.6	121	170	9.3
750	21.1	24	28	30	32	56	12.2	96	127	13.4
800	15.8	21	23	24	25	45	10.4	95	136	22.4
800	40.4	12	17	18	20	39	10.1	142	202	7.4
800	1.8	11	12	15	24	43	55.7	103	149	9.7
850	15.2	13	14	14	15	30	7.6	131	207	40.4
850	7.4	26	28	28	15	31	6.6	115	185	40.4
900	14	8	9	10	10	25	12	86	105	13.4
900	30.1	9	10	11	12	27	9	72	102	14.9
950	2.7	9	10	10	11	23	6.3	125	187	28.4
950	3.1	7	9	10	11	23	5	133	202	8.4
1000	3.3	5	7	8	8	19	1.3	54	79	6.4
1000	5.2	4	6	7	7	19	1.5	80	104	5.4

Table 4. Steady state test results for the steel 4509-1.

Temperature °C	E-Modulus GPa	Rp 0,01 N/mm²	Rp 0,1 N/mm²	Rp 0,2 N/mm²	Rp 1,0 N/mm²	Rm N/mm²	Ag %	A50 %	A5 %	n -
25	189.3	278	337	349	373	495	16.7	33	42	13.2
25	179.8	275	335	347	373	489	16.8	33	40	12.9
100	183.2	242	290	305	337	449	17.6	32	43	12.9
100	186	239	293	307	337	450	18.4	30	40	12.0
200	171.2	230	271	282	314	422	17.3	25	35	14.7
200	186.5	231	270	282	313	421	17.8	27	36	15.0
300	213.9	141	258	274	312	411	14.4	24	34	4.5
300	182.1	138	261	278	313	417	12.8	22	31	4.3
400	157.9	205	245	263	306	392	15.6	23	29	12.0
400	148.2	211	248	263	305	394	15.5	24	31	13.6
500	187.9	149	210	225	273	358	12.7	19	28	7.3
500	200.6	138	207	224	272	358	13	21	30	6.2
550	155.8	164	183	187	234	329	12.1	17	25	22.8
550	142	102	197	212	259	336	10.3	15	22	4.1
600	99	157	183	190	237	315	10.1	17	24	15.7
600	101.4	158	177	191	234	313	9.5	16	22	15.8
650	187	121	159	169	208	275	7.6	17	23	9.0
650	120.2	122	152	166	207	277	8.7	17	25	9.7
700	98.2	114	131	139	164	212	8.8	22	34	15.1
700	72.9	120	135	141	164	209	9	23	35	18.6
750	62.2	60	70	72	72	96	5.5	46	64	16.4
750	51.5	65	72	72	98	105	4.5	38	61	29.3
800	41.3	44	46	46	46	67	5.3	95	140	67.4
800	193.2	36	42	43	43	63	4.5	78	111	16.9
850	43.9	26	29	46	47	47	1.5	99	146	5.3
850	137.3	30	33	33	32	48	3.6	100	144	31.4
900	17.2	15	17	17	37	38	2.7	85	128	23.9
900	25.2	16	37	38	38	38	0.6	95	142	3.5
950	24.5	9	25	25	25	26	0	102	157	2.9
950	43.6	12	28	28	28	28	0.1	119	189	3.5
1000	22.7	7	18	18	18	19	0	136	219	3.2
1000	7.4	5	19	19	19	19	0.7	119	167	2.2

Table 5. Steady state test results for the steel 4509-2.

Temperature °C	E-Modulus GPa	Rp 0,01 N/mm²	Rp 0,1 N/mm²	Rp 0,2 N/mm²	Rp 1,0 N/mm²	Rm N/mm²	Ag %	A50 %	A5 %	n -
25	161.6	293	351	360	378	481	16.8	33	45	14.5
25	157.6	286	348	357	375	481	17.3	33	44	13.5
100	154.7	253	314	322	342	442	18.9	34	44	12.4
100	165.1	249	313	322	342	441	18.7	33	43	11.7
200	163.6	233	292	302	326	420	18.5	27	36	11.5
200	181.3	227	288	300	324	420	18.8	26	34	10.7
300	163.2	194	287	296	317	412	14.3	23	32	7.1
300	186.6	183	285	295	317	410	19.8	25	35	6.3
400	160.7	204	264	276	307	380	16.1	23	32	9.9
400	157.8	156	267	276	307	382	16.9	25	34	5.3
500	135.3	177	229	238	274	336	12.4	20	28	10.1
500	152.3	185	223	240	274	338	10.8	19	26	11.5
550	165.6	87	202	213	250	310	13.4	20	27	3.3
550	123.7	187	207	217	253	307	11.8	19	27	20.1
600	198.6	137	178	193	227	286	12.4	18	25	8.7
600	111.9	115	183	194	228	283	8.2	15	23	5.7
650	339.1	103	152	166	197	241	10	19	28	6.3
650	209.4	106	156	167	200	250	11.4	21	28	6.6
700	117.3	121	144	153	177	206	6.4	16	26	12.8
700	102.8	108	142	152	174	205	6.5	16	26	8.8
750	69.5	80	88	90	92	110	4.3	33	60	25.4
750	70.8	50	67	69	68	92	3.9	45	79	9.3
750	151	52	74	77	78	98	4.3	38	69	7.6
800	29.1	17	26	29	31	53	4.8	106	142	5.6
800	12.3	28	31	32	33	55	4.5	114	161	22.4
850	6.9	17	18	19	21	40	2.6	105	155	26.9
850	28.6	20	22	23	25	43	4.1	123	185	21.4
900	12.6	9	10	11	13	29	1.5	98	129	14.9
900	24.4	9	12	13	15	31	1.5	124	198	8.1
950	2.7	5	7	7	8	20	1.3	172	285	8.9
950	-15.2*	6	9	9	9	22	1.7	109	178	7.4
1000	12.1	4	4	4	4	13	3.5	135	211	35.9
1000	-138.6*	5	6	6	6	15	1.5	>120	>120	16.4

*) Elastic deformations are small compared to the inherent noise in the measurement signals. Consequently, unphysical negative value was obtained for the elastic modulus. The negative value was used for calculation of the proof stress values. However, since the material behaves in a rigid, ideal plastic manner in this temperature range, the value of the elastic modulus does not have a notable influence the proof stress values.

Table 6. Steady state test results for the steel 4521-1.

Temperature °C	E-Modulus GPa	Rp 0,01 N/mm²	Rp 0,1 N/mm²	Rp 0,2 N/mm²	Rp 1,0 N/mm²	Rm N/mm²	Ag %	A50 %	A5 %	n -
25	199.2	265	356	368	392	542	17.1	37	32	9.1
25	181	302	361	372	395	543	17.2	36	32	14.4
100	173.4	262	315	324	350	498	19.4	37	32	14.1
100	186.3	228	313	325	352	498	19.2	34	30	8.5
200	176.3	198	286	298	331	473	18.1	25	25	7.3
200	173.2	200	287	298	331	473	17.9	25	25	7.5
300	162.9	243	279	292	328	470	18.8	26	23	16.3
300	169.9	160	282	294	331	465	15.9	23	22	4.9
400	137.7	133	265	278	324	444	15.8	21	23	4.1
400	148.7	232	263	276	320	443	16.9	25	24	17.3
500	145.9	127	232	243	289	410	13.1	19	19	4.6
500	146.6	144	235	247	294	409	11.0	22	20	5.6
550	220.3	130	211	222	269	380	12.7	18	18	5.6
550	202.9	160	207	216	264	377	12.3	20	19	10.0
600	163.3	137	184	197	243	348	12.3	19	18	8.2
600	217.9	110	181	193	232	339	12.3	19	18	5.3
650	67.9	100	168	175	207	270	10.8	22	22	5.4
650	153.7	100	157	167	202	268	9.5	20	19	5.8
700	123.5	118	138	144	167	213	8.9	29	25	15.0
750	64.2	55	61	62	103	107	2.7	126	81	25.0
750	68.2	62	68	70	107	112	3.0	100	65	24.7
800	59	37	41	42	77	78	1.7	150	93	23.6
800	49.7	34	39	40	73	75	2.1	150	101	18.4
850	22.6	23	27	28	58	58	1.4	198	127	15.2
850	62.2	23	27	28	59	59	0.3	187	115	15.2
900	19.6	9	15	42	41	43	0.2	185	115	1.9
900	-603.4*	9	14	21	41	42	0.3	176	114	3.5
950	38.5	8	11	32	30	32	0.2	263	153	2.2
950	28.9	7	10	31	29	31	0.2	163	0	2.0
1000	7.9	6	21	21	20	21	0.2	141	74	2.4
1000	12.9	7	25	23	22	25	0.2	214	89	2.5

*) Elastic deformations are small compared to the inherent noise in the measurement signals. Consequently, unphysical negative value was obtained for the elastic modulus. The negative value was used for calculation of the proof stress values. However, since the material behaves in a rigid, ideal plastic manner in this temperature range, the value of the elastic modulus does not have a notable influence the proof stress values.

Table 7. Steady state test results for the steel 4521-2.

Temperature °C	E-Modulus GPa	Rp 0,01 N/mm²	Rp 0,1 N/mm²	Rp 0,2 N/mm²	Rp 1,0 N/mm²	Rm N/mm²	Ag %	A50 %	A5 %	n -
25	171.9	296	371	382	408	556	16.7	29	39	11.7
25	173.6	309	372	382	408	555	16.5	30	39	14.1
100	168.1	275	333	344	372	514	17.6	29	36	13.4
100	170.8	268	333	344	372	515	17.8	29	38	12.0
200	189.1	234	311	325	360	495	16.8	22	30	9.1
200	184.2	258	312	325	360	498	16.7	21	29	13.0
300	179	143	309	321	365	484	15.3	21	27	3.7
300	183.2	232	305	320	362	486	19.5	23	29	9.3
400	185.1	207	289	300	344	461	14.8	21	27	8.1
400	236.4	192	282	299	343	459	15.2	21	27	6.8
500	148.9	197	265	273	317	434	12.6	18	23	9.2
500	124.8	191	265	275	321	431	11.5	17	23	8.2
550	136.1	183	235	247	291	402	14.2	20	27	10.0
550	172.4	219	234	244	293	398	11.5	17	25	27.7
600	178.5	143	203	219	262	350	9.6	17	25	7.0
600	290.3	145	197	214	259	349	9.7	17	24	7.7
650	128.7	149	185	195	228	289	8.1	17	25	11.1
650	96.3	167	191	197	232	293	8.1	17	27	18.1
700	126	115	145	150	163	196	5.6	26	43	11.3
700	155.1	94	146	155	169	200	6.6	25	40	6.0
750	73.5	51	55	57	59	100	3.8	87	123	26.9
750	72.7	43	60	60	63	106	2.4	103	143	9.0
800	57.2	16	37	41	45	79	4.7	80	102	3.2
800	364	21	39	43	45	81	2.9	100	135	4.2
850	30	28	31	33	35	64	1.6	131	180	18.2
850	56.7	28	33	34	35	65	1.6	116	170	15.4
900	44.1	6	7	14	20	44	1.6	92	197	3.5
900	20.2	13	20	21	24	48	1.3	82	132	6.2
950	-67.3*	6	9	10	13	32	1.6	98	159	5.9
950	13.1	13	14	14	14	35	3.1	105	171	40.4
1000	30.3	8	8	8	8	26	1.5	148	196	-
1000	21.6	8	8	8	9	26	1.5	125	211	-

*) Elastic deformations are small compared to the inherent noise in the measurement signals. Consequently, unphysical negative value was obtained for the elastic modulus. The negative value was used for calculation of the proof stress values. However, since the material behaves in a rigid, ideal plastic manner in this temperature range, the value of the elastic modulus does not have a notable influence the proof stress values.

Table 8. Steady state test results for the steel 4621-3.

Temperature °C	E-Modulus GPa	Rp 0,01 N/mm²	Rp 0,1 N/mm²	Rp 0,2 N/mm²	Rp 1,0 N/mm²	Rm N/mm²	Ag %	A50 %	A5 %	n -
25	170.4	280	342	353	370	466	16.7	33	44	12.9
25	159.1	292	344	354	370	466	16.3	32	41	15.6
100	186.7	198	300	313	333	424	18.2	32	40	6.5
100	166.7	229	302	312	332	424	17.9	33	42	9.7
200	154.9	257	285	294	318	396	17.9	26	34	22.3
200	149.6	250	287	295	315	396	17.7	26	36	18.1
300	163.9	244	280	290	307	387	11.8	23	29	17.3
300	179.2	138	278	290	309	389	14	23	30	4.0
400	217.8	136	254	269	311	385	12.2	17	24	4.4
400	138.4	245	264	276	313	380	11.7	19	26	25.1
500	133.5	136	237	246	284	365	12.3	19	25	5.1
500	230.5	135	237	247	284	367	11.7	16	22	5.0
550	406.3	129	206	216	258	324	8.9	17	24	5.8
600	252.8	110	181	193	223	280	8.1	16	23	5.3
600	140.2	155	183	195	230	283	8.9	16	23	13.0
650	212.7	113	153	160	188	224	7.8	16	25	8.6
650	155.4	124	156	164	188	225	8.7	16	26	10.7
700	103.3	113	125	130	142	167	11.1	29	43	21.4
700	135.4	98	118	126	138	164	10.7	29	44	11.9
750	87.7	61	79	82	98	108	7.8	49	79	10.1
750	73.2	62	76	80	97	106	6.9	52	80	11.8
800	31.1	25	32	33	60	61	4.3	127	196	10.8
800	165.4	23	31	32	58	59	5.7	134	207	9.1
850	14.8	13	16	17	39	40	7.9	113	180	11.2
850	23.4	16	41	42	44	46	7.3	95	-	3.1
900	22.4	8	24	25	27	27	4.7	108	166	2.6
900	26.9	7	9	9	26	27	7	108	169	11.9
950	8.6	4	6	6	21	21	3.3	133	188	7.4
950	26.8	4	6	18	21	21	1.9	124	188	2.0
1000	8.6	2	3	1	3	12	2.2	-	-	-
1000	12.5	6	16	17	18	19	1.2	93	126	2.9

Factor $k_{2\%,\theta}$ determined using the steady state test results

The factor $k_{2\%,\theta}$ determines the elevated temperature strength at 2% total strain by means of the 0.2% proof strength and the ultimate tensile strength. From experimental point of view, the factor $k_{2\%,\theta}$ can be determined using steady state test results measured at temperature θ.

$$k_{2\%,\theta} = \frac{R_{t2,0}(\theta) - R_{p0,2}(\theta)}{R_m(\theta) - R_{p0,2}(\theta)} \qquad \text{(G1)}$$

In elevated tensile testing it is a common practice to increase the loading rate after the proof stress values have been determined. For the present purpose, it is important that the $R_{p0,2}$ and the $R_{t2,0}$ values are measured using the same loading rate. Therefore, the effect of changes in testing speed has been corrected when necessary; the values of $R_{p0,2}$ and the $R_{t2,0}$ given below correspond to the same slow testing speed at which the $R_{p0,2}$ values were measured

Additional room temperature tensile tests were carried out on steel 4003-1 to study the influence of loading rate speed on the of $k_{2\%,\theta}$ factor. The results summarized in Table 1 show that the $k_{2\%,\theta}$ factor increases from of $k_{2\%,\theta} = 0.28$ to $k_{2\%,\theta} = 0.38$ if the loading rate is changed before recording the $R_{t2,0}$ value.

Table 1. Influence of loading rate on tensile test results at room temperature for steel 4003-1. The test method refers to the standard EN ISO 6892-1 and defines the loading rates used.

Test Method	Change of loading rate at	Rp0,2 N/mm²	Rt2,0 N/mm²	Rm N/mm²	$k_{2\%,\theta}$ -
A222	-	333	379	483	0.31
A222	-	333	379	482	0.31
A224	ε = 1.5%	332	392	491	0.38
A224	ε = 1.5%	333	393	493	0.38
A224	ε = 3.0%	334	380	495	0.29
A224	ε = 3.0%	334	380	496	0.28

The factor $k_{2\%,\theta}$ cannot be determined throughout the whole temperature range using the steady state tensile testing results. After the critical temperature for the steady state creep, the work-hardening ceases. Consequently, the stress strain curve becomes completely flat, and the factor $k_{2\%,\theta}$ given by the equation (G1) becomes indeterminate.

The tables given in this appendix contain the factor $k_{2\%,\theta}$ determined using the steady state test method. The values are reported up to the critical temperature for the steady state creep deformation.

Table 2. Factor $k_{2\%,\theta}$ for the steel 4003-1.

Temperature °C	$R_{p0,2}$ N/mm²	$R_{t2,0}$ N/mm²	R_m N/mm²	$k_{2\%,\theta}$ -
25	328	370	484	0.27
25	328	370	485	0.27
100	299	339	445	0.28
100	298	337	442	0.27
200	282	325	420	0.31
200	281	326	417	0.33
300	295	332	410	0.32
300	298	334	410	0.32
400	285	336	412	0.40
400	286	343	413	0.45
500	244	301	379	0.43
500	245	304	384	0.43
550	186	214	265	0.35
550	201	237	274	0.49

Table 3. Factor $k_{2\%,\theta}$ for the steel 4016-1.

Temperature °C	$R_{p0,2}$ N/mm²	$R_{t2,0}$ N/mm²	R_m N/mm²	$k_{2\%,\theta}$ -
25	311	345	455	0.23
25	314	346	455	0.23
100	283	316	416	0.25
100	284	317	417	0.25
200	273	314	395	0.33
200	275	314	396	0.32
300	276	312	386	0.33
300	276	310	383	0.32
400	274	332	417	0.41
400	275	328	418	0.37
500	234	307	404	0.43
500	234	302	401	0.41
550	186	226	275	0.45
550	189	231	282	0.45

Table 4. Factor $k_{2\%,\theta}$ for the steel 4016-2.

Temperature °C	$R_{p0,2}$ N/mm²	$R_{t2,0}$ N/mm²	R_m N/mm²	$k_{2\%,\theta}$ -
25	345	385	496	0.27
25	334	384	504	0.29
100	311	357	457	0.31
100	307	361	467	0.34
200	295	343	429	0.36
200	296	346	433	0.36
300	295	337	410	0.37
300	295	338	408	0.38
400	271	333	400	0.48
400	272	334	404	0.47
500	231	292	362	0.46
500	232	299	364	0.51
550	189	224	276	0.40
550	192	224	283	0.35

Table 5. Factor $k_{2\%,\theta}$ for the steel 4509-1.

Temperature °C	$R_{p0,2}$ N/mm²	$R_{t2,0}$ N/mm²	R_m N/mm²	$k_{2\%,\theta}$ -
25	349	390	495	0.28
25	347	388	489	0.29
100	305	352	449	0.33
100	307	352	450	0.31
200	282	335	422	0.38
200	282	334	421	0.37
300	274	335	411	0.44
300	278	336	417	0.42
400	263	319	392	0.44
400	263	318	394	0.42
500	225	288	358	0.47
500	224	287	358	0.47
550	187	264	329	0.54
550	212	277	336	0.52
600	190	262	315	0.58
600	191	259	313	0.56
650	169	216	275	0.45
650	166	228	277	0.56
700	139	183	212	0.60
700	141	181	209	0.59

Table 6. Factor $k_{2\%,\theta}$ for the steel 4509-2.

Temperature	$R_{p0,2}$	$R_{t2,0}$	R_m	$k_{2\%,\theta}$
°C	N/mm²	N/mm²	N/mm²	-
25	360	389	481	0.24
25	357	386	481	0.24
100	322	353	442	0.26
100	322	353	441	0.26
200	302	343	420	0.34
200	300	341	420	0.34
300	296	335	412	0.33
300	295	334	410	0.34
400	276	319	380	0.41
400	278	318	382	0.38
500	238	291	336	0.54
500	240	302	338	0.63
550	213	271	310	0.60
550	217	271	307	0.60
600	193	250	286	0.61
600	194	244	283	0.56
650	166	216	241	0.66
650	167	218	250	0.62
700	153	188	206	0.65
700	152	187	205	0.67

Table 7. Factor $k_{2\%,\theta}$ for the steel 4521-1.

Temperature °C	$R_{p0,2}$ N/mm²	$R_{t2,0}$ N/mm²	R_m N/mm²	$k_{2\%,\theta}$ -
25	368	408	542	0.23
25	372	411	543	0.23
100	324	371	498	0.27
100	325	372	498	0.27
200	298	356	473	0.33
200	298	356	473	0.33
300	292	344	470	0.29
300	294	349	465	0.32
400	278	344	444	0.40
400	276	340	443	0.39
500	243	317	410	0.45
500	247	321	409	0.46
550	222	300	380	0.50
550	216	294	377	0.49
600	197	273	348	0.50
600	193	257	339	0.44
650	175	218	270	0.45
650	167	224	268	0.57
700	144	179	213	0.50

Table 8. Factor $k_{2\%,\theta}$ for the steel 4521-2.

Temperature °C	$R_{p0,2}$ N/mm²	$R_{t2,0}$ N/mm²	R_m N/mm²	$k_{2\%,\theta}$ -
25	386	423	556	0.22
25	385	424	555	0.23
100	344	388	514	0.26
100	344	389	515	0.26
200	325	382	495	0.33
200	325	381	498	0.33
300	321	376	484	0.34
300	320	381	486	0.37
400	300	359	461	0.36
400	299	359	459	0.37
500	273	343	434	0.44
500	275	345	431	0.45
550	247	318	402	0.46
550	244	320	398	0.49
600	219	286	350	0.51
600	214	286	349	0.53
650	195	246	289	0.55
650	197	249	293	0.54
700	150	175	196	0.55
700	155	176	200	0.46

Table 9. Factor $k_{2\%,\theta}$ for the steel 4621-1.

Temperature °C	$R_{p0,2}$ N/mm²	$R_{t2,0}$ N/mm²	R_m N/mm²	$k_{2\%,\theta}$ -
25	353	379	466	0.23
25	354	374	466	0.18
100	313	345	424	0.28
100	312	344	424	0.28
200	294	334	396	0.39
200	295	332	396	0.36
300	290	324	387	0.35
300	290	326	389	0.36
400	269	330	385	0.53
400	276	331	380	0.52
500	246	292	365	0.39
500	247	309	367	0.52
550	166	214	248	0.59
550	216	272	324	0.51
600	193	241	280	0.55
600	195	245	283	0.57
650	160	202	224	0.65
650	164	201	225	0.60
700	130	152	167	0.60
700	126	148	164	0.59

Table 1. Room-temperature mechanical properties of 4509-2.

$R_{p0,01}$ N/mm²	$R_{p0,1}$ N/mm²	$R_{p0,2}$ N/mm²	$R_{p1,0}$ N/mm²	$R_{t2,0}$ N/mm²	R_m N/mm²	A_g %	A_{80} %	A_5 %
294	358	367	384	400	488	16.1	34	56

Table 2. Temperature for achieving 0.2% plastic strain in the transient tests carried out at different load levels and the corresponding reduction factors for Rp0,2.

Load MPa	Temperature for $R_{p0,2}$ °C	Reduction factor for $R_{p0,2}$ -
36	803	0.10
55	806	0.15
74	798	0.20
94	764	0.26
94	791	0.26
113	772	0.31
113	773	0.31
132	750	0.36
132	725	0.36
151	667	0.41
170	636	0.46
190	586	0.52
209	531	0.57
228	497	0.62
247	476	0.67
266	435	0.72
286	351	0.78
305	128	0.83
324	73	0.88

Table 3. Temperature for achieving 2% total elongation for in the transient tests carried out at different load levels and the corresponding reduction factors for Rt2,0.

Load MPa	Temperature for $R_{t2,0}$ °C	Reduction factor for $R_{t2,0}$ -
36	822	0.09
55	819	0.14
74	810	0.19
94	799	0.24
94	801	0.24
113	793	0.28
113	788	0.28
132	776	0.33
132	775	0.33
151	760	0.38
170	735	0.43
190	703	0.48
209	669	0.52
228	632	0.57
247	600	0.62
266	564	0.67
286	505	0.72
305	462	0.76
324	406	0.81

Table 4. Temperature for failure in the transient tests carried out at different load levels and the corresponding reduction factors for Rm.

Load MPa	Failure temperature °C	Reduction factor -
36	879	0.07
55	839	0.11
74	822	0.15
94	807	0.19
94	816	0.19
113	798	0.23
113	794	0.23
132	781	0.27
132	788	0.27
151	771	0.31
170	750	0.35
190	729	0.39
209	709	0.43
228	682	0.47
247	666	0.51
266	651	0.55
286	628	0.59
305	599	0.63
324	551	0.66

Table 5. Interpolated strength values in different temperatures and the corresponding factor $k_{2\%,\theta}$.

Temperature (°C)	$R_{p0,2}$ (MPa)	$R_{t2,0}$ (MPa)	R_m (MPa)	$K_{2\%,\theta}$ (-)
555	201	269	323	0.56
560	199	268	321	0.56
570	196	263	317	0.56
580	192	258	313	0.54
590	188	253	309	0.53
600	184	247	305	0.52
610	180	241	298	0.52
620	176	235	291	0.51
630	172	229	285	0.51
640	168	224	276	0.52
650	162	219	267	0.54
660	155	214	255	0.59
670	150	208	242	0.63
680	148	203	230	0.67
690	145	197	222	0.68
700	142	192	215	0.68
710	139	185	208	0.67
720	137	179	198	0.69
730	134	173	189	0.71
740	131	166	179	0.73
750	125	158	170	0.75
760	120	151	161	0.76
770	114	139	152	0.65
780	92	127	135	0.81
790	82	114	126	0.73
800	65	94	109	0.66

Table 1. Room-temperature mechanical properties of 4521-3.

$R_{p0,01}$ N/mm²	$R_{p0,1}$ N/mm²	$R_{p0,2}$ N/mm²	$R_{p1,0}$ N/mm²	$R_{t2,0}$ N/mm²	R_m N/mm²	A_g %	A_{80} %	A_5 %
330	379	391	411	427	532	17.3	28.4	41.9

Table 2. Temperature for achieving 0.2% plastic strain in the transient tests carried out at different load levels and the corresponding reduction factors for Rp0,2.

Load MPa	Temperature for $R_{p0,2}$ °C	Reduction factor for $R_{p0,2}$ -
39	785	0.10
60	775	0.15
80	760	0.20
102	750	0.26
122	745	0.31
143	680	0.37
164	630	0.42
184	585	0.47
206	580	0.53
226	520	0.58
247	465	0.63
268	360	0.69
288	380	0.74
310	200	0.79
330	105	0.84
351	65	0.90

Table 3. Temperature for achieving 2% total elongation for in the transient tests carried out at different load levels and the corresponding reduction factors for Rt2,0.

Load MPa	Temperature for $R_{t2,0}$ °C	Reduction factor for $R_{t2,0}$ -
39	850	0.09
60	795	0.14
80	775	0.19
102	765	0.24
122	755	0.29
143	745	0.33
164	735	0.38
184	715	0.43
206	695	0.48
226	670	0.53
247	635	0.58
268	580	0.63
288	550	0.67
310	510	0.73
330	465	0.77
351	345	0.82

Table 4. Temperature for failure in the transient tests carried out at different load levels and the corresponding reduction factors for Rm.

Load MPa	Failure temperature °C	Reduction factor for Rm -
39	892	0.07
60	853	0.11
80	804	0.15
102	782	0.19
122	770	0.23
143	756	0.27
164	749	0.31
184	731	0.35
206	719	0.39
226	707	0.42
247	697	0.46
268	670	0.50
288	658	0.54
310	624	0.58
330	618	0.62
351	611	0.66

Table 5. Interpolated strength values in different temperatures and the corresponding factor $k_{2\%,\theta}$.

Temperature (°C)	$R_{p0,2}$ (MPa)	$R_{t2,0}$ (MPa)	R_m (MPa)	$K_{2\%,\theta}$ (-)
620	168	253	322	0.55
630	164	249	306	0.60
640	160	244	300	0.60
650	156	238	293	0.60
660	151	232	285	0.60
670	147	226	268	0.65
680	143	218	260	0.64
690	140	210	252	0.62
700	137	201	240	0.62
710	133	190	221	0.64
720	130	179	204	0.66
730	127	169	185	0.72
740	124	154	174	0.60
750	102	133	161	0.52
760	80	112	137	0.56
770	67	91	122	0.44
780	50	75	105	0.46